

NAVAL POSTGRADUATE SCHOOL

Monterey, California



THESIS

**TARGETING AND FIRE CONTROL SYSTEM ANALYSIS
OF THE NEW TURKISH ATTACK HELICOPTER
"THE AH-1Z KINGCOBRA"**

by

Gokhan Lutfu Reyhan

March 2001

Thesis Advisor:
Co-Advisor:

Russ Duren
Alfred W. Cooper

Approved for public release; distribution is unlimited.

**TARGETING AND FIRE CONTROL SYSTEM ANALYSIS OF THE NEW
TURKISH ATTACK HELICOPTER “THE AH-1Z KINGCOBRA”**

Gokhan Lutfu Reyhan-1st Lieutenant, Turkish Army

B.S., Turkish War Academy, 1994

Master of Science in Aeronautical Engineering–March 2001

Advisor: Russ Duren, Department of Aeronautics

Co-Advisor: Alfred W. Cooper, Department of Physics

In May of 1997, the Turkish Military issued a Request for Proposal for the purchase of 145 attack helicopters. Turkey has chosen Bell Helicopter's KingCobra as its attack helicopter. The major difference between the USMC version of AH-1Z and the Turkish version KingCobra is the Targeting and Fire Control System. Bell Helicopter Textron has chosen Lockheed Martin to develop and build a new targeting system, the Target Sight System (TSS). The TSS will contain Lockheed Martin's 3-5 μ m midwave staring array FLIR. On the other hand, The Turkish Secretariat for Defense Industries (SSM) has chosen Aselsan ASELFLIR-300T that contains an 8-12 μ m longwave scanning second-generation FLIR.

A comparison of range performance for these two systems has been made using the TAWS Field Performance Model. Since the physical parameters on these specific FLIRs are proprietary, the FLIR92 Simulation Model is used to generate performance parameters. These parameters are expected to represent the general characteristics of the two systems. The resultant data is used in the TAWS Field Performance Model to predict the range performances.

The results have showed that the staring array midwave FLIR has longer ranges in the scenarios given in this thesis. This may not represent the real performance of the systems.

DoD KEY TECHNOLOGY AREA: air vehicles, sensors, thermal imaging systems

KEYWORDS: Thermal Imaging Systems, Targeting, Fire Control Systems, Forward Looking Infrared, FLIR, TAWS, KingCobra, Attack Helicopter, Infrared

REPORT DOCUMENTATION PAGE			<i>Form Approved OMB No. 0704-0188</i>	
Public reporting burden for this collection of information is estimated to average 1 hour per response, including the time for reviewing instruction, searching existing data sources, gathering and maintaining the data needed, and completing and reviewing the collection of information. Send comments regarding this burden estimate or any other aspect of this collection of information, including suggestions for reducing this burden, to Washington headquarters Services, Directorate for Information Operations and Reports, 1215 Jefferson Davis Highway, Suite 1204, Arlington, VA 22202-4302, and to the Office of Management and Budget, Paperwork Reduction Project (0704-0188) Washington DC 20503.				
1. AGENCY USE ONLY (Leave blank)		2. REPORT DATE March 2001	3. REPORT TYPE AND DATES COVERED Master's Thesis	
4. TITLE AND SUBTITLE: Targeting and Fire Control System Analysis of the New Turkish Attack Helicopter "The Ah-1Z Kingcobra"			5. FUNDING NUMBERS	
6. AUTHOR(S) Gokhan Lutfu Reyhan				
7. PERFORMING ORGANIZATION NAME(S) AND ADDRESS(ES) Naval Postgraduate School Monterey, CA 93943-5000			8. PERFORMING ORGANIZATION REPORT NUMBER	
9. SPONSORING / MONITORING AGENCY NAME(S) AND ADDRESS(ES) N/A			10. SPONSORING / MONITORING AGENCY REPORT NUMBER	
11. SUPPLEMENTARY NOTES The views expressed in this thesis are those of the author and do not reflect the official policy or position of the Department of Defense or the U.S. Government.				
12a. DISTRIBUTION / AVAILABILITY STATEMENT Approved for public release; distribution is unlimited			12b. DISTRIBUTION CODE	
13. ABSTRACT (maximum 200 words) <p>In May of 1997, the Turkish Military issued a Request for Proposal for the purchase of 145 attack helicopters. Turkey has chosen Bell Helicopter's KingCobra as its attack helicopter. The major difference between the USMC version of AH-1Z and the Turkish version KingCobra is the Targeting and Fire Control System. Bell Helicopter Textron has chosen Lockheed Martin to develop and build a new targeting system, the Target Sight System (TSS). The TSS will contain Lockheed Martin's 3-5µm midwave staring array FLIR. On the other hand, The Turkish Secretariat for Defense Industries (SSM) has chosen Aselsan ASELFLIR-300T that contains an 8-12µm longwave scanning second-generation FLIR.</p> <p>A comparison of range performance for these two systems has been made using the TAWS Field Performance Model. Since the physical parameters on these specific FLIRs are proprietary, the FLIR92 Simulation Model is used to generate performance parameters. These parameters are expected to represent the general characteristics of the two systems. The resultant data is used in the TAWS Field Performance Model to predict the range performances.</p> <p>The results have showed that the staring array midwave FLIR has longer ranges in the scenarios given in this thesis. This may not represent the real performance of the systems.</p>				
14. SUBJECT TERMS Thermal Imaging Systems, Targeting, Fire Control Systems, Forward Looking Infrared, FLIR, TAWS, KingCobra, Attack Helicopter, Infrared			15. NUMBER OF PAGES	
			16. PRICE CODE	
17. SECURITY CLASSIFICATION OF REPORT Unclassified	18. SECURITY CLASSIFICATION OF THIS PAGE Unclassified	19. SECURITY CLASSIFICATION OF ABSTRACT Unclassified	20. LIMITATION OF ABSTRACT UL	

THIS PAGE INTENTIONALLY LEFT BLANK

Approved for public release; distribution is unlimited

**TARGETING AND FIRE CONTROL SYSTEM ANALYSIS OF THE NEW
TURKISH ATTACK HELICOPTER**

"THE AH-1Z KINGCOBRA"

Gokhan Lutfu REYHAN
1st Lieutenant, Turkish Army
B.S., Turkish War Academy, 1994

Submitted in partial fulfillment of the
requirements for the degree of

MASTER OF SCIENCE IN AERONAUTICAL ENGINEERING

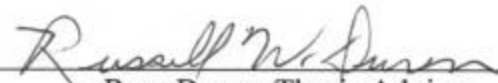
from the

**NAVAL POSTGRADUATE SCHOOL
March 2001**


Author:


Gokhan Lutfu Reyhan

Approved by:


Russ Duren, Thesis Advisor


Alfred W. Cooper, Co-Advisor


Max Platzer, Chairman

Department of Aeronautical and Astronautical Engineering

THIS PAGE INTENTIONALLY LEFT BLANK

ABSTRACT

In May of 1997, the Turkish Military issued a Request for Proposal for the purchase of 145 attack helicopters. Turkey has chosen Bell Helicopter's KingCobra as its attack helicopter. The major difference between the USMC version of AH-1Z and the Turkish version KingCobra is the Targeting and Fire Control System. Bell Helicopter Textron has chosen Lockheed Martin to develop and build a new targeting system, the Target Sight System (TSS). The TSS will contain Lockheed Martin's 3-5 μ m midwave staring array FLIR. On the other hand, The Turkish Secretariat for Defense Industries (SSM) has chosen Aselsan ASELFLIR-300T that contains an 8-12 μ m longwave scanning second-generation FLIR.

A comparison of range performance for these two systems has been made using the TAWS Field Performance Model. Since the physical parameters on specific FLIRs are proprietary, the FLIR92 Simulation Model is used to generate performance parameters. These generic parameters are expected to represent the characteristics of the two systems. The resultant data is used in the TAWS Field Performance Model to predict the range performances.

The results have showed that the staring array midwave FLIR has longer ranges in the scenarios given in this thesis. This may not represent the real performance of the systems.

THIS PAGE INTENTIONALLY LEFT BLANK

TABLE OF CONTENTS

I.	INTRODUCTION	1
II.	TURKISH GOVERNMENT’S RFP	5
A.	CONOPS	5
B.	RELEVANT AVIONICS REQUIREMENTS	7
C.	ARMAMENT AND WEAPON SYSTEMS	10
D.	FIRE CONTROL SYSTEM.....	16
III.	MISSION AVIONICS	19
A.	AH-1Z MISSION AVIONICS	19
B.	KINGCOBRA MISSION AVIONICS CONFIGURATION	21
C.	TSS VERSUS ASELFIR-300T.....	23
D.	FEDERATED AND INTEGRATED AVIONICS ARCHITECTURES..	26
1.	Federated Architectures.....	26
2.	Integrated Architectures	27
3.	KingCobra Architecture	27
IV.	TARGETING AND FIRE CONTROL SYSTEMS.....	29
A.	MILLIMETER WAVE RADAR.....	30
1.	Background on MMW	31
2.	Operational Considerations	33
a.	<i>Advantages.....</i>	<i>34</i>
b.	<i>Limitations.....</i>	<i>36</i>
3.	Millimeter Wave Radar Characteristics.....	37
a.	<i>Narrow Antenna Beamwidth With Small Antenna</i>	<i>38</i>
b.	<i>Wide Frequency Spectrum Availability.....</i>	<i>40</i>
c.	<i>Low Scatter From Terrain</i>	<i>40</i>
d.	<i>High Absorption Around Transmission Windows</i>	<i>41</i>
e.	<i>Doppler Frequency Shift.....</i>	<i>41</i>
f.	<i>Atmospheric Effects</i>	<i>41</i>
g.	<i>Increased Detection Capability of Small Objects</i>	<i>42</i>
4.	Air-to-Ground Millimeter Wave Characteristics.....	42
5.	Target Acquisition Millimeter Wave Characteristics	42
6.	Millimeter Wave Applications	45
a.	<i>Radar</i>	<i>45</i>
b.	<i>Radiometry.....</i>	<i>46</i>
B.	AN/APG-78 FIRE CONTROL RADAR	47
1.	Hellfire Delivery Modes	54
2.	Types of Hellfire Missiles	55
C.	INFRARED AND ELECTRO-OPTICAL SYSTEMS	57
1.	Electromagnetic and IR Spectrum.....	57
2.	Thermal Radiation Laws.....	59
a.	<i>Planck’s Radiation Law</i>	<i>60</i>

	b.	<i>Stefan-Boltzmann Law</i>	60
	c.	<i>Wien's Displacement Law</i>	61
	3.	Target Thermal Signature	61
	4.	Atmospheric Transmission	63
D.		THE CONCEPT OF FLIR	67
E.		FLIR SYSTEM PERFORMANCE PARAMETERS	71
	1.	Physical Parameters	71
	a.	<i>Field of View (FOV)</i>	71
	b.	<i>Detector Angular Subtense (DAS)</i>	72
	c.	<i>Instantaneous Field of View (IFOV)</i>	72
	d.	<i>Modulation Transfer Function (MTF)</i>	72
	2.	Noise Equivalent Temperature Difference (NETD)	73
	3.	Minimum Detectable Temperature Difference (MDTD)	74
	4.	Minimum Resolvable Temperature Difference (MRTD).....	75
F.		GENERAL CHARACTERISTICS OF FLIR SYSTEMS.....	78
	1.	Generations of FLIR Systems	78
	2.	Scanning versus Staring Systems	79
	a.	<i>Staring Systems</i>	80
	b.	<i>Scanning Systems</i>	80
	c.	<i>Scanning Versus Staring Performance</i>	82
	3.	Wavelength Issues	84
	a.	<i>Target Consideration</i>	85
	b.	<i>Atmospheric Consideration</i>	85
	c.	<i>Detectivity Considerations</i>	86
	d.	<i>Integration Time Consideration</i>	86
V.		PERFORMANCE MODELS.....	89
	A.	TACTICAL DECISION AIDS (TDAS).....	89
	B.	FLIR92 THERMAL IMAGING SYSTEM PERFORMANCE MODEL.....	90
	C.	TARGET ACQUISITION AND WEATHER SOFTWARE (TAWS)....	93
	1.	Target Model	94
	2.	Transmittance Model	95
	3.	Sensor Performance Model.....	96
	4.	Output Files	97
VI.		COMPUTATIONS AND RESULTS	99
	A.	SCENARIO INPUT PARAMETERS	99
	B.	FLIR92 MODEL OUTPUTS.....	100
	C.	TAWS MODEL INPUTS	100
	1.	Target Model	100
	2.	Transmittance Model	101
	3.	Sensor Model	102
	D.	TAWS MODEL OUTPUTS	103
VII.		CONCLUSIONS AND RECOMMENDATIONS	105
	A.	CONCLUSIONS	105

B. RECOMMENDATIONS FOR FURTHER RESEARCH	108
APPENDIX A. FLIR92 MODEL OUTPUTS FOR SCANNING SENSOR (WFOV)..	111
APPENDIX B. FLIR92 MODEL OUTPUTS FOR SCANNING SENSOR (MFOV) .	117
APPENDIX C. FLIR92 MODEL OUTPUTS FOR SCANNING SENSOR (NFOV)..	123
APPENDIX D. FLIR92 MODEL OUTPUTS FOR STARING SENSOR (WFOV)....	129
APPENDIX E. FLIR92 MODEL OUTPUTS FOR STARING SENSOR (MFOV)	135
APPENDIX F. FLIR92 MODEL OUTPUTS FOR STARING SENSOR (NFOV)	141
APPENDIX G. FLIR92 MODEL OUTPUTS FOR STARING SENSOR (VNFOV)..	147
APPENDIX H. TAWS OUTPUTS FOR DESERT ENVIRONMENTAL CONDITIONS WITH CONSTANT TOT (1800) FOR DIFFERENT VIEWING ANGLES	153
APPENDIX I. TAWS OUTPUTS FOR URBAN ENVIRONMENTAL CONDITIONS WITH CONSTANT TOT (2100) FOR DIFFERENT VIEWING ANGLES	157
APPENDIX J. TAWS TIME HISTORY PLOTS FOR DESERT ENVIRONMENTAL CONDITIONS	159
APPENDIX K. TAWS TIME HISTORY PLOTS FOR URBAN ENVIRONMENTAL CONDITIONS	161
LIST OF REFERENCES.....	165
INITIAL DISTRIBUTION LIST	169

THIS PAGE INTENTIONALLY LEFT BLANK

LIST OF FIGURES

Figure 3.1.	Mission Avionics System and Subsystem Architecture “From Ref. 10”	20
Figure 3.2.	Hawkeye Design Overview “From Ref. 4”	24
Figure 4.1.	AH-64D Apache Longbow Nose Section “From Ref. 16”	51
Figure 4.2.	Hellfire Missile “From Ref. 19”	55
Figure 4.3.	Hellfire II vs. Longbow Hellfire “From Ref. 17”	57
Figure 4.4.	Electromagnetic Spectral Range Designations “From Ref. 20”	58
Figure 4.5.	Spectral Radiant Emittance of a Blackbody at Various Temperatures “From Ref. 22”	62
Figure 4.6.	Differential Temperature Geometry “From Ref. 21”	62
Figure 4.7.	Apparent Delta T, ΔT_{app} “From Ref. 21”	63
Figure 4.8.	Typical Atmospheric Transmission for a 1-km path length “From Ref. 21”	67
Figure 4.9.	Simple FLIR Block Diagram “After Ref. 20”	68
Figure 4.10.	Typical MRT Curve “From Ref. 21”	76
Figure 4.11.	Serial Scanning “From Ref. 21”	81
Figure 4.12.	Parallel Scan Configurations (a) Bidirectional interlaced scan; (b) bidirectional interlaced scan with TDI; (c) unidirectional scan with TDI “From Ref. 21”	82
Figure H.1.	Scanning Sensor WFOV	153
Figure H.2.	Staring Sensor WFOV	153
Figure H.3.	Scanning Sensor MFOV	154
Figure H.4.	Staring Sensor MFOV	154
Figure H.5.	Scanning Sensor NFOV	155
Figure H.6.	Staring Sensor NFOV	155
Figure H.7.	Staring Sensor VNFOV	156
Figure J.1.	Scanning Sensor NFOV Max. Range Time History Plot at 0 Degrees.	159
Figure J.2.	Staring Sensor NFOV Max. Range Time History Plot at 0 Degrees	159
Figure J.3.	Staring Sensor WFOV Min Range Time History Plot at 180 Degrees	160
Figure J.4.	Staring Sensor WFOV Min Range Time History Plot at 180 Degrees	160
Figure K.1.	Scanning Sensor NFOV Max. Range Time History Plot at 0 degrees with 2mm/hour Rain Rate.	161
Figure K.2.	Staring Sensor NFOV Max. Range Time History Plot at 0 degrees with 2mm/hour Rain Rate.	161
Figure K.3.	Scanning Sensor WFOV Min Range Time History Plot at 90 degrees with 2mm/hour Rain Rate.	162
Figure K.4.	Staring Sensor WFOV Min Range Time History Plot at 180 degrees with 2mm/hour Rain Rate.	162
Figure K.5.	Scanning Sensor NFOV Max. Range Time History Plot at 0 degrees with 1mm/hour Rain Rate.	163
Figure K.6.	Staring Sensor NFOV Max. Range Time History Plot at 0 degrees with 1mm/hour Rain Rate.	163

Figure K.7.	Scanning Sensor WFOV Min. Range Time History Plot at 90 degrees with 1mm/hour Rain Rate.	164
Figure K.8.	Staring Sensor WFOV Min. Range Time History Plot at 180 degrees with 1mm/hour Rain Rate.	164

LIST OF TABLES

Table 3.1.	KingCobra Configuration “From Ref. 2”	22
Table 3.2.	Summary of Main Differences of TSS and ASELFLIR-300T.....	25
Table 4.1.	Millimeter Wave Radar System Trade-Off Considerations “From Ref. 12”..	35
Table 4.2.	Radar System Performance Comparison “From Ref. 12”	44
Table 4.3.	Longbow System Specifications “From Ref. 16”.....	49
Table 4.4.	Distinction Between the FLIR Generations “From Ref. 28”.	79
Table 4.5.	Detector Array Configurations “From Ref. 21”.	80
Table 4.6.	Summary of the Scanning and Staring System Differences “From Ref. 21”.....	83
Table 6.1.	Scenario Input Parameters.....	102
Table 6.2.	Detection Range Comparison Table.	104

THIS PAGE INTENTIONALLY LEFT BLANK

ACKNOWLEDGMENTS

First of all, I owe many thanks to my advisor, Professor Russ Duren for his patience, knowledge, and consultation. The success of this project is largely due to his support. I will always be grateful to him for his generosity, support, and most of all for his friendship.

My special thanks to Professor Alfred Cooper for his patience and support for this work. I would like to thank the professors in Department of Aeronautics who helped me a lot during my time here at Naval Postgraduate School.

I would like to thank Turkish Land Forces Command for giving me the opportunity to attend the Naval Postgraduate School, study for this degree, and to serve my country.

I also would like to thank Hezarfen ORUC, from ASELSAN, Mark Gibson, from Bell TEXTRON, Joe Elmer, from Lockheed Martin, John Dowell, from Litton Guidance Systems and Dr. Andreas Goroch from NRL, Monterey for providing me with the data.

Most important, I wish to thank my beloved wife Emel who always inspired and motivated me for success showing a great patience, time and understanding.

Finally, I dedicate this thesis to my wife for her support and to my parents, who were back in Turkey while I was here.

THIS PAGE INTENTIONALLY LEFT BLANK

I. INTRODUCTION

This thesis will examine the targeting and fire control system of the new Turkish attack helicopter. Turkey has chosen Bell Helicopter's KingCobra, a version of AH-1Z, which is under development for the US Marine Corps, as its attack helicopter. The AH-1Z KingCobra was selected over the Franco-German Eurocopter's Tiger, IAI Kamov's Ka-50-2 Erdogan, which is a variant of the Ka-50 Shark, and Agusta's A129-I Mangusta after Boeing's Apache Longbow had been eliminated earlier in the competition.

One of the chief selection criteria for the program was technology transfer to Turkey. Most of the components will be built in Turkey by Turkish Aerospace Industries (TAI), which currently assembles Black Hawks and Cougars for the Turkish Armed Forces, with Bell acting as principal subcontractor. The number of subsystems on which Turkish and foreign companies can collaborate is approximately 140. Besides manufacture and assembly, TAI will create an Instrument Landing System (ILS) structure and manage subcontracts with the intent to maximize technology transfer to Turkey.

The principal subcontractor for avionics is Aselsan, a Turkish military electronics company, whose ASELFLIR-300T is the targeting system selected for the KingCobra. Aselsan also makes Night Vision Goggles (NVGs) and will supply MDF 268E multifunction Liquid Crystal Displays (LCDs), licensed from Rockwell Collins. The navigation system will combine GPS and INS in the IN 100G units, built by Aselsan under license from Litton Guidance and Control Systems.

The Secretariat for Defense Industries (SSM), which is in overall charge of the program, will acquire the other systems including weapons, electronic warfare and IFF

equipment. Turkish companies such as Netas, Rocketsan and MKEK will also benefit. SSM wants to have the turreted guns, air-to-air (ATA) and air-to-ground (ATG) missiles, rockets and launchers made locally. In terms of basic technology, Turkey wishes to make and test critical components such as gearboxes, gears, rotor, and other dynamic components, including the landing gear.

The major difference between the USMC version of the AH-1Z and the Turkish version KingCobra, in terms of avionics, is the Fire Control System, which is the main interest of this thesis.

Bell Helicopter Textron has chosen Lockheed Martin Electronics and Missiles to develop and build a new targeting system, the Target Sight System (TSS), for the US Marine Corps AH-1Z attack helicopter H-1 Upgrade Program. The TSS will combine Lockheed Martin's Sniper 3-5 μm band staring array FLIR and commercially developed imaging technology from WESCAM. The complete system is named the HAWKEYE AN/AAQ-30 Target Sight System (TSS). On the other hand SSM has chosen Aselsan's ASELFLIR-300T turret that contains an 8-12 μm scanning focal plane array second-generation thermal imager developed jointly with Raytheon.

The common disadvantage of both targeting systems is the lack of the ability to engage more than one target at a time. I will present the other advantages and disadvantages of these two targeting system as this thesis develops. At this point this common disadvantage of AH-1Z targeting systems brings the AH-64D Apache Longbow into the picture. With its Millimeter-Wave Radar, mounted on its main rotor, it can detect moving targets at ranges up to 8km while the detection range for static targets is reduced to 6km. The Longbow Radar System can display, classify and track up to 128 targets

simultaneously, prioritize the 16 most dangerous targets, transmit the information to other aircraft, and initiate a precision attack, all in 30 seconds or less. It can use either its Target Acquisition Designation Sight or Fire Control Radar as a targeting sight.

To compare the KingCobra and the Apache Longbow in every aspect is beyond the scope of this thesis. The objectives of this thesis are to present the mission capabilities and tactical use of these two helicopters at the highest operational level and then to discuss the underlying principles and major differences of their targeting systems. Finally, the main goal will be to compare the performances of the FLIRs of USMC's AH-1Z and Turkish AH-1Z KingCobra in different meteorological conditions for a given scenario. Since it is not possible to get specific proprietary data on specific FLIR systems, generic data will be used to represent the general characteristics of these two FLIR systems. We will start Chapter II by presenting the Turkish Government's RFP that will discuss the required avionics for the requested attack helicopter. This will be followed by the presentation of AH-1Z Avionics for both US Marine Corps' AH-1Z and KingCobra in Chapter III. Then the analysis of targeting systems will be presented in Chapter IV. The next two chapters will discuss the FLIR92 Thermal Imaging Systems Performance Model and Target Acquisition and Weather Software (TAWS) Field Performance Model. These two models will be used to obtain performance parameters for these two specific FLIR systems and get a rough estimate of their respective performance. The results from these two models will be presented in Chapter VI. Finally Chapter VII will summarize and draw conclusions from the results of simulation models and make necessary recommendations for further research.

THIS PAGE INTENTIONALLY LEFT BLANK

II. TURKISH GOVERNMENT’S RFP

In May of 1997, the Turkish Military issued an RFP (Request for Proposal) for the purchase of 145 attack helicopters. The \$3.5-\$4.5 billion deal brought bids from the five companies below:

- Boeing (USA)_____ AH-64D “Apache Longbow”
- Bell-Textron (USA)_____ AH-1Z “KingCobra”
- Kamov (Russia) _____ Ka-50-2 “Erdogan”
- Agusta (Italy) _____ A129-I “Mangusta”
- Eurocopter (France-Germany) _____ UHU-HAS “Tiger”

In July of 2000, Turkey announced its decision to buy the AH-1Z “KingCobra”.

The purpose of this Chapter is to give a short summary of the Turkish Government’s RFP and present the avionics requirements associated with the Fire Control System. Only those requirements that relate to the objectives of this thesis will be presented. The RFP establishes functional and performance requirements for the Turkish Attack/Reconnaissance Helicopter, its mission, equipment, armament, and system integration. For ease of understanding of the requirements, the related parts of the RFP will be presented AS IS (direct quotes).

A. CONOPS

The concept of operations is given in Turkish Attack and Reconnaissance Helicopter Program Volume-V (System Performance Specification) as [Ref. 1]:

3.1.1. GENERAL DESCRIPTION

Turkish Army needs fully integrated, low Life Cycle Cost advanced technology multi-role Attack and Reconnaissance helicopter system to provide enhanced mission effectiveness by increased lethality, flexibility, growth capability, mobility, supportability, availability, maintainability, reliability and survivability with increased operator and

maintainer efficiency. Turkish Attack and Reconnaissance Helicopter is designated as ATAK (Turkish Attack and Reconnaissance Helicopter).

ATAK shall perform both attack and reconnaissance missions and shall have both Air-to-Air and Air-to-Ground combat capability comprised in one platform. Configuration change is desired to be accomplished at Aviation Unit Level. ATAK shall have limited capability (landing, take-off, refueling, re-supply) for operations from ships. Air vehicle shall have twin engines, multi-bladed rotor, two tandem flight stations, be single pilot operable from either crew station. Sufficient endurance and range to accomplish mission profiles with internal fuel is required. Low altitude, high-speed flight, Nap-Of-Earth (NOE) flight and autonomous search and target acquisition capability is desired. Mission areas are:

- Attack
- Armed Reconnaissance and Observation
- Aerial Fire Support (Ground Support)
- Air-to-Air Combat
- Escort to all airborne and assault aviation units

3.1.2. MISSIONS

3.1.2.1. TYPE MISSIONS

3.1.2.1.1. Primary Missions: The A/C shall perform the following mission in deep, close and rear operations at day/night and adverse/extreme weather conditions.

3.1.2.1.1.1. The A/C shall destroy massed and mechanized armored enemy forces

3.1.2.1.1.2. Armed Reconnaissance and Observation

3.1.2.1.2. Secondary Missions: In addition to its primary mission, the A/C shall perform the following missions at the same operational and environmental conditions defined in primary missions:

3.1.2.1.2.1. Close Air Support

3.1.2.1.2.2. Air-to-Air (ATA) combat

3.1.2.1.2.3. Escort to all airborne and air assault units

3.1.2.1.3. Special Missions:

3.1.2.1.3.1. Off Shore and Naval Aerial Fire Support

3.1.2.1.3.2. Joint Operations (JAAT)

3.1.2.2. ADDITIONAL MISSIONS

3.1.2.2.1. Training: The A/C shall provide training requirements of pilots and crews.

3.1.2.2.2. Assistance to SAR (Search and Rescue): A/C shall provide assistance to SAR teams.

3.1.3. OPERATIONAL CONCEPT

ATAK will be located in attack battalions and training fleet. Total number of attack battalions is 5. In each attack battalion, there will be 27 helicopters. In training fleet the number of helicopters located is 10. ATAK shall provide attack battalions with highly mobile and lethal attack capability against personnel, ground and air targets. Mission shall be conducted during day/night extreme/adverse weather partially in NBC (Nuclear, Biological and Chemical) environment

B. RELEVANT AVIONICS REQUIREMENTS

Avionics requirements are defined in Ref. 1 as:

3.2.12. NAVIGATION/GUIDANCE:

3.2.12.1. General:

The navigation system shall improve the situational awareness of crewmembers and reduce the pilot workload on navigation function in day/night and adverse/extreme weather while performing missions stated in 3.1.2.

3.2.12.1.1. Navigation system shall have a redundant structure. Any failure shall not cause total disability of navigation function. Redundancy and degradation aspects, for each navigation system, shall be described.

3.2.12.1.2. Navigation function shall be manageable by each crewmember.

3.2.12.1.3. The installed performance for different navigation modes at different weather conditions, at different altitudes shall be specified.

3.2.12.1.4. The embedded INS/GPS is required to be primary navigation equipment. GPS shall have the capability of P (Y) code. Dual INS/GPS configuration is desired.

3.2.12.1.5. Information on navigation modes and associated sensors shall be provided.

3.2.12.1.6. A complete and detailed block diagram of navigation function shall be provided.

3.2.12.2.A/C Position:

The Navigation Function shall perform the processing required to determine and maintain A/C position, air and ground velocity, attitude, altitude, absolute altitude and heading. Navigation System shall provide necessary information such as A/C heading, attitude, present position, velocities, altitude, wind speed and direction, waypoint, target steering, and distance calculation for navigating the A/C. Navigation system shall supply all navigation and air information to be used for armament systems, guidance data calculation, flight display, automatic flight control system, reconnaissance system, data communication system, electronic warfare system and mission management.

3.2.12.3. A/C Guidance:

3.2.12.3.1. The Navigation Function shall perform the processing to provide TACAN guidance, VOR/ILS guidance.

3.2.12.3.2. The Navigation Function shall perform the processing to provide VHF/FM homing and UHF direction finding. Low frequency direction finding processing is desired.

3.2.12.4. Piloting:

3.2.12.4.1. Navigation system shall provide the information to be displayed necessary for piloting the A/C day/night, and adverse weather.

3.2.12.4.2. All the position information shall be displayed and handled on different grid systems (including Lat/Long, UTM, MGS), SID/SIL/Jeppesen plans on fixed and moving map.

3.2.12.4.3. The navigation system shall be able to perform calculations including but not limited to, fixed and moving waypoint, distance, bearing, course, estimated time of enroute/arrival and endurance.

3.2.12.4.4. FLIR navigation capability is required and detailed description shall be provided.

3.2.13. RECONNAISSANCE

3.2.13.1. The reconnaissance system shall allow the crew to detect, recognize, and identify targets in adverse weather battlefield obscuration during night and day in minimal time through use and integration of information from different portions of electromagnetic spectrum from radio to UV. Reconnaissance system shall enable the crew to acquire moving and stationary, emitting and non-emitting targets of military value at sufficient range to support required response in less time than the threat engagement cycle while minimizing detection by the threat.

3.2.13.2. Reconnaissance system is desired to be capable of total search prioritization and supporting continuous/subsequent guided missile delivery to multiple targets.

3.2.13.3. Electro-optical system capability shall allow the crew to detect, recognize and identify rotary wing, tank and a single soldier targets. Installed FLIR performances of detection, recognition and identification for each FLIR on the A/C shall be given for each available Field of View and for the following target and conditions:

- Probability of detection: 50%
- Atmospheric extinction: $\sigma = 0.1, 0.2, 0.3, 0.4, 0.5, 1.0$
- A/C Out of Ground Effect
- Target size: 2.3m X 2.3m (NATO standards)
- Detection Resolution Target: 1 pair line of strips of equal width
- Recognition Resolution Target: 3 pair line of strips of equal width

- Identification Resolution Target: 6 pair line of strips of equal width
- Strip Temperature Difference: 2 °K
- Background Temperature Difference: 5 +/- 2 °K
- Environment Temperature: 300 °K +/- 20 °K

Other constraints shall be specified by the bidder.

3.2.13.4. Sensor field of regard and field of view, which enables the crew to acquire moving and stationary targets throughout the A/C operational envelope, shall be specified.

3.2.13.5. Manual and auto tracking of moving and stationary targets are required.

3.2.13.6. Selectable auto tracking initiation is desired.

3.2.13.7. Simultaneous tracking of multiple targets within field of view (FOV) is desired. Limitations and features of simultaneous multiple target tracking shall be specified.

3.2.13.8. DELETED

3.2.13.9. A/C shall have following reconnaissance system: A targeting FLIR, TV CAMERA, Integrated Image Intensifier, Laser Designator Laser Range Finder and Laser Spot Tracker.

3.2.13.10. A/C reconnaissance system is desired to have millimeter wave radar.

C. ARMAMENT AND WEAPON SYSTEMS

Although the areas of interest of this thesis are Targeting and Fire Control Systems, which includes the missiles and rockets only, the overall Weapon Systems overview will be useful for better understanding. Weapons specifications are given in Reference 1 as:

3.2.7 ARMAMENT SYSTEM

3.2.7.1. General:

3.2.7.1.1. All armament systems shall be capable of concurrent operation and shall collectively provide for short and long-range engagement of moving and stationary ground and air targets.

3.2.7.1.2. The A/C shall be capable of firing all munitions limited only by individual armament system safety and performance constraints.

3.2.7.1.3. The armament system is desired to be operable to the maximum extent from either crew station without degrading the capabilities of munitions. Any limitation shall be specified.

3.2.7.1.4. Armament installation shall be so that frangible rocket pod fairing, missile debris, ejected cartridges, cases, and links shall not endanger or substantially damage the A/C or external stores.

3.2.7.1.5. Safety provisions shall be incorporated to preclude collisions of projectiles in near proximity of the A/C.

3.2.7.1.6. Armament installation shall be so that weapon blast and noise shall have no significant detrimental effect on the crew, A/C, other weapons or performance of the mission.

3.2.7.1.7. Characteristics of weapons and ammunition including but not limited to minimum and maximum effective ranges of the ammunition in different modes of operations shall be specified.

3.2.7.1.8. All of the weapons and ammunition certified on the A/C shall be specified. The undesired effects of incorporating these weapons and ammunition on the A/C shall be specified.

3.2.7.2. Weapons:

Detailed information, including but not limited to followings on Missile Systems shall be given IAW following WBS as applicable. Refer to MIL-STD-881B.

- Air Vehicle
- Propulsion (Propulsion Element, Stages etc.)
- Payload (Warhead, Sub-munitions etc.)
- Airframe (Aerodynamics, mounting surfaces, environmental protection)
- Guidance and Control (Elements, functions including acquiring and tracking targets, guidance intelligence data, interface requirements, seekers, autopilot)
- Airborne Test Equipment
- Airborne Training Equipment
- Auxiliary Equipment (environmental control, safety and protective subsystems etc.)
- Integration, Assembly, Test and Checkout
- Command and Launch (includes equipment required to acquire, command to launch, guidance and control where such capability is not contained aboard the air vehicle)
- Surveillance, Identification and Tracking Sensors (required to support the missile systems where such capability is not self contained aboard the air vehicle)
- Command and Launch Software Interface Requirements

3.2.7.2.1. Working, designation, tracking, guidance and fire control principles, engagement sequence, and safety principles, characteristics [mass, flight time vs. range, warhead (mass, type, destruction power, seeker, autopilot)] shall be specified.

3.2.7.2.2. Performance including but not limited to armor penetration capability, min. and max. effective range, ECCM and/or EOCM (Electro-Optic Countermeasures)

capability shall be specified and explained in detail. CATGM (Captive Air Training Guided Missiles) availability is required.

3.2.7.2.3. Test results, reliability, firing history, hazard tests, constraints and limitations, environmental conditions and considerations and external interface requirements for missiles shall be provided.

3.2.7.2.4. Anti-Tank Guided Missile (ATGM): A/C desired to have capability of firing Fire and Forget type ATGM missiles. Laser and/or wire guided missiles firing capability is required.

3.2.7.2.5. Air-to-Air Missile (ATAM): A/C shall have capability of Fire and Forget ATAM missiles. Stinger ATAM firing capability is required.

3.2.7.2.6. Anti-Radiation Missile: A/C is desired to have capability of firing Anti-Radiation missile.

3.2.7.2.7. Anti-Ship Missile: A/C is desired to have capability of firing Anti-Ship missile.

3.2.7.2.8. Rockets:

3.2.7.2.8.1. Folded Fin Aerial Rockets (FFAR): The A/C shall be capable of firing 2.75 inch (70mm) folded fin aerial rockets including wall-in-space rocketry. Detailed information including but not limited to followings on rocket systems shall be given IAW following WBS as applicable. Refer to MIL-STN-881B.

- Air Vehicle
- Structure (fins, parachutes)
- Payload (Warhead)Availability of High explosive fragmentation, high explosive anti-tank/anti-personnel, high explosive general purpose, flechette, smoke, flare, practice type warheads shall be specified, Sub-munitions etc.)
- Airframe (Aerodynamics, mounting surfaces, environmental protection)

- Guidance and Control (Elements, functions including acquiring and tracking targets, guidance intelligence data interface requirements)
- Airborne Test Equipment
- Fuses
- Safety and arm (mechanical, timer, etc.)
- Integration, Assembly, Test and Checkout
- Launch and Guidance Control
- Command and Launch Software Interface Requirements

3.2.7.2.8.1.1. Working, designation, and fire control principles, engagement sequence and safety principles, characteristics (dispersion vs. air speed and distance, mass, flight time vs. range, warhead (mass, type, destruction power) shall be provided.

3.2.7.2.8.1.2. Test results, reliability, firing history, hazard tests, constraints and limitations, environmental conditions, external interface requirements shall be provided.

3.2.7.2.9. Bombs: If applicable, information shall be provided.

3.2.7.3. Gun and Turret:

A universal turreted gun (minimum 20mm caliber) is required. Following parameters shall be provided for the turreted gun as applicable.

3.2.7.3.1. Modes of operation of the gun shall be described. Selectable firing modes are desired. Burst firing capability and selectable burst rate is desired. Fixed forward mode of operation of the turreted gun is required.

3.2.7.3.2. Azimuth and elevation range limits of the gun shall be specified; a minimum of 80-degree left, 80-degree right and 10 degree up and 30 degree down range is required.

3.2.7.3.3. Gun shall be slaved and synchronized to the pilot's/copilot's sight and targeting systems. High rate of swing of the turret is desired.

3.2.7.3.4. Field adjustable gun firing rate is desired.

3.2.7.3.5. The capability of the gun against targets shall be specified.

3.2.8. WEAPONS DELIVERY

3.2.8.1. General:

3.2.8.1.1 .A/C shall enable installation of wing payloads in different configurations. Combinations, and limitations on configuration shall be specified.

3.2.8.1.2. Two stations on each wing are required. An additional third stations on each wing is desired.

3.2.8.1.3. Each wing shall have jettisoning capability. Complete provisions to carry, launch, and eject or jettison the stores shall be specified. Any limitation related with jettison procedure shall be specified.

3.2.8.1.4. Installation of the launchers and loading of the ammunition shall be performed in minimum time and with minimum personnel requirement. The requirements including but not limited to time, special equipment, and personnel for installation/removal of each launcher and pod shall be specified.

3.2.8.1.5. Boresight with minimum effort is desired. Requirements shall be specified. Automatic boresight capability is desired.

3.2.8.2. Launchers:

3.2.8.2.1. General: NATO STANDARD interface is desired. Types, allowable munition loads, limitations on loading, field of fire, safety interlocks shall be specified. Detailed information for the followings shall be provided:

3.2.8.2.2. Rocket Launcher: The A/C shall be equipped with 2.75-inch rocket launchers.

3.2.8.2.3. Guided Missile Launcher:

3.2.8.2.3.1. Air To Air Missile Launcher

3.2.8.2.3.2. Anti-Tank Missile Launcher

3.2.8.2.3.2.1. Fire and Forget Missile Launchers

3.2.8.2.3.2.2. Laser and/or Wire Guided Missile Launchers

3.2.8.2.3.3. Anti-Radiation Missile Launcher

3.2.8.2.3.4. Anti-Ship Missile Launcher

3.2.8.2.4. Dispense Launcher

3.2.8.2.5. Pods (if applicable)

D. FIRE CONTROL SYSTEM

In today's helicopter industry, there are many Fire Control Systems offered by different companies. It is very difficult to say one is better than the other. It can be said that for a particular mission one might be more suitable than the other. To be able to decide which one is better for a specified mission, it is necessary to look at the requirements. Fire Control System requirements for Turkish Attack Helicopter (ATAK) are specified in Reference 1 as:

3.2.9. FIRE CONTROL SYSTEM

The fire control system shall perform functions for short and long range engagement of moving and stationary ground and air targets and shall be capable of employing munitions against personnel, ground and air targets.

3.2.9.1. The fire control system shall be integrated to reconnaissance, navigation, weapons delivery and other systems.

3.2.9.2. The fire control system shall perform the processing to maintain inventories, manage ordnance and control the launch of weaponry.

3.2.9.3. Any degradation in performance of weapons due to fire control system shall be specified.

3.2.9.4. A master armament power switch, which enables the control of power applied to firing circuitry is required.

3.2.9.5. Detailed description of armament modes of operation management, calculations for precision and non precision ammunition, firing sequence, target designation, safety management, weapon status management functions shall be provided and also detailed block diagram of fire control system including the integration to the other systems shall be provided.

3.2.9.6. DELETED

3.2.9.7. Weapons-aiming capability with different sight systems is required. Target aiming capabilities, respective limitations and firing sequence of each target acquisition system respective to each weapon shall be specified.

3.2.9.8. Simultaneous multiple target aiming with different sight systems is required. Target aiming capabilities, respective limitations of each sight system imposed by simultaneous use of multiple target acquisition systems respective to each weapon shall be specified.

3.2.9.9. Crew task sharing for the different types of firing engagement shall be described in detail.

THIS PAGE INTENTIONALLY LEFT BLANK

III. MISSION AVIONICS

There are some differences between the avionics suites of the AH-1Z and the KingCobra. The purpose of this chapter is to name the mission avionics for both helicopters and present, not to compare, the general overview of their targeting systems. The performance comparison of their targeting systems will be discussed later in Chapter VI.

A. AH-1Z MISSION AVIONICS

The AH-1Z's Mission Avionics includes:

- TAMMAC (Tactical Aircraft Moving Map Capability) Digital Map and Data Loader
- Mission Computers
- Multi-function Display
- Keyboard Unit/Limited Function Display
- Embedded GPS/INS
- Countermeasures
- Laser Warning System
- IR Jammer
- TSS (Target Sight System)

Figure 3.1 shows the Mission Avionics System and Subsystem Architecture.

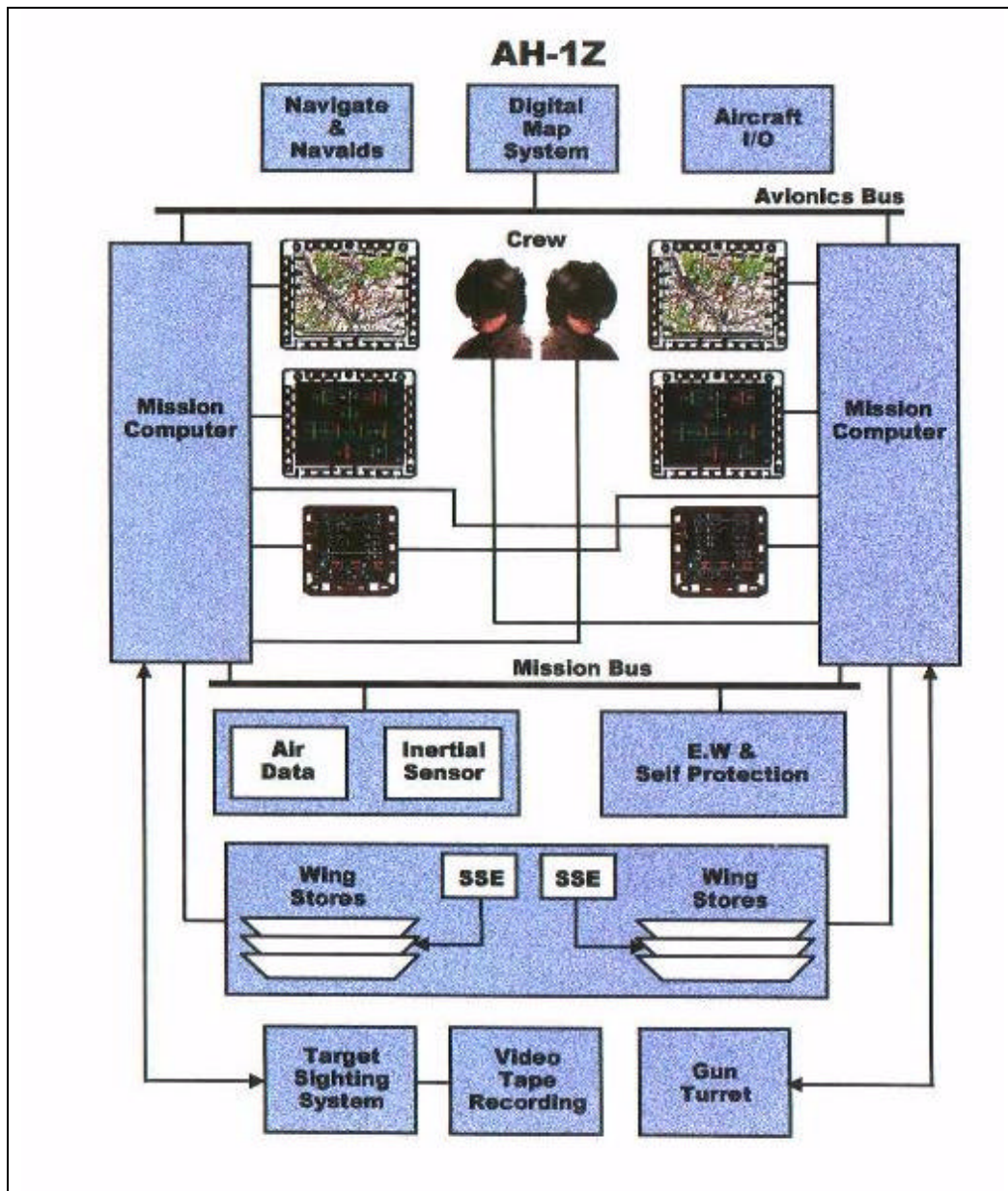


Figure 3.1. Mission Avionics System and Subsystem Architecture "From Ref. 10".

B. KINGCOBRA MISSION AVIONICS CONFIGURATION

Turkish Government requested an alternate proposal that includes a specific avionics/armament suite to be integrated to the A/C. This suite is specified as [Ref. 1]:

CONFIGURATION

3.1.5.1. The Bidder is required to submit alternative proposal, in response to this System Performance Requirements, as defined below:

3.1.5.1.1. The Bidder shall submit a technical proposal taking into consideration the following avionics/armament required to be integrated into the A/C configuration.

- UHF/VHF Radio: Aselsan MXF484. The UHF/VHF radios shall have PRC 9600 hopping compatibility in the band 30MHz-108MHz with ground forces. The radios shall also have national crypto compatibility in the bands 30MHz-108MHz and 146MHz-174MHz with ground forces together with NATO crypto compatibility.
- IFF transponder/Interrogator: NETAS APX 113 including Mode-4 capability.
- INS/GPS: ASELSAN LN100G, dual configuration.
- TARGETING FLIR: ASELSAN (FLIR, Laser Rangefinder and Designator subunits).
- Stinger ATA missile.
- MFD: ASELSAN MFD-268E.
- CDU (Control Display Unit): ASELSAN CDU-900.

3.1.5.2. The bidder shall provide for each avionics/armament equipment in the configuration, a technical specification document in the format provided in Annex-1 of this document.

Based on this request, Bell Helicopter Textron presented the KingCobra Avionics Suite Configuration and its differences from AH-1Z as in Table 3.1 [Ref. 2].

The most important difference for this thesis is the difference between the Targeting Systems of the two helicopters. The Turkish Government replaced the Lockheed Martin's TSS with Aselsan's ASELFLIR-300T.

Bell Helicopter TEXTRON			
KINGCOBRA CONFIGURATION			
Manufacturer	USMC Baseline AH-1Z with the following changes:		
	Added	Replaces	Remove
Aselsan	Three MXF484 VHF/UHF Radio and KY-58	Two Collins RT-1794	
Collins	9087 HF Radio and KY-100		
Aselsan	Targeting FLIR/Laser Rangefinder/Designator/LST/TV Camera	Lockheed Martin TSS	
GEC Marconi	NETAS AN/APX-113 IFF	Allied Signal AN/APX-100 IFF	
Lockheed Martin	Stinger		
	Fuseable 2.75" Rockets		
	Tricycle Wheel Gear	Skid Gear	
	Ice Detection System		
	Space, Weight, and Power Provisions for AN/ALQ-144A IR Jammer		
Symetrics Industries	MD-1295/B IDM (with PRISM Card)		
Rockwell			Rcvr/Xmtr
Tracor			One set of Chaff/Flare Dispensers and sequencer switch
Smith/Harris			Digital Map System Electronics Box
Pacific Scientific	15 KVA AC Generator and GCU (2)	400 Amp DC Generator and GCU (2)	
Bendix or Ieland	350 Amp TRU (2)	Avionic Instruments 1500 VA Inverter (2)	
TBD	100 KVA Generator	Lucas APU Starter Generator and QAD	
TBD	APU Electric Starter		
TBD	Electric Hydraulic Pump	Pad Driven Hydraulic Pump	

Table 3.1. KingCobra Configuration "From Ref. 2".

C. TSS VERSUS ASELFLIR-300T

The United States Marine Corps and Bell selected the Lockheed Martin TSS as the EO/IR fire control system for the new AH-1Z attack helicopter. Lockheed Martin Missiles and Fire Control in Orlando, Florida, has selected Hawkeye XR as the name under which it will market TSS. XR stands for extended range.

Officially designated as the AN/AAQ-30, Hawkeye was selected for the AH-1Z program after a full competition in 1998. The combination of the 8.55-inch aperture with the large format focal plane array, Lockheed Martin proprietary filters and algorithms, and precision stabilization of the WESCAM gimbal provide very high performance. According to the Program Director, Terry Carsten: “This is currently the world’s leading Target Sight System”.

Hawkeye is a multi-sensor EO/IR fire control system. It consists of a large aperture mid-wave FLIR, color TV, laser designator/range finder, laser spot tracker (LST), and on-gimbal inertial measurement unit (IMU). These components are integrated into a highly stabilized turret that mounts to the nose of the aircraft. It has 8.5-inch aperture, four Field-of-VIEWS (FOVs) Mid-Wave Infrared (MWIR) staring FLIR for maximum image resolution and long-range performance. It also has the capability of target detection, recognition and positive ID at and beyond the maximum weapons range. TSS Hawkeye Design Overview is given in Figure 3.2 as:



Figure 3.2. Hawkeye Design Overview “From Ref. 4”.

The Aselsan ASELFLIR-300T Second Generation Thermal Imaging System, on the other hand, is a low-weight multipurpose thermal imaging sensor for pilotage/navigation, surveillance, search-and-rescue (SAR), automatic tracking, target classification and targeting. The ASELFLIR-300T is an open architecture and hardware/software flexible unit that can be adapted to various platforms including rotary wing, fixed wing and unmanned air vehicles (UAVs).

The key features of ASELFLIR-300T include Electronic Image Stabilization (EIS), Local Area Processing (LAP) for image enhancement, Multi-Mode-Tracking (MMT), Analog and Digital video outputs for transmission and/or recording, MIL-STD-1553, ARINC, and other discrete Data Busses to interface with other on-board avionics such as radar, navigation and weapons system. It has three FOVs. Narrow Field-of-View (NFOV) for recognition and identification, Medium Field-of-View (MFOV) for detection and Wide Field-of-View (WFOV) for navigation and pilotage.

The ASELFLIR-300T Second Generation Thermal Imaging System, will have a 2nd generation FLIR, Laser Rangefinder/Designator, Laser Spot Tracker, and a Camera in a stabilized gimbal.

At first look, the main differences of TSS and ASELFLIR-300T are summarized in Table 3.2.

Parameter	TSS	ASELFLIR-300T
Wavelength	3-5 μm	8-12 μm
FOVs	4	3
Array Size	640X480	240 vertical with 4 TDI elements
Sensor	MWIR Staring Focal Plane Array	2 nd generation scanning LWIR array
Filter	Short-Pass and Long-Pass	Spectral Band-Pass

Table 3.2. Summary of Main Differences of TSS and ASELFLIR-300T.

At this point, we assume that the performance of the targeting system is basically determined by the performance of the FLIR. Although it has a fully integrated architecture, it will be assumed that targeting system performance is not affected by the other components of the system. This will limit the main consideration of this thesis to the performance comparison of two FLIR systems. We will discuss this in the next chapter. For ease of understanding the brief discussion of Federated and Integrated Avionics Architecture will be useful.

D. FEDERATED AND INTEGRATED AVIONICS ARCHITECTURES

Avionics architectures describe the form, structure and interrelationships between the avionics system and the aircraft, and amongst the elements of the avionics system itself. The selection of buses, the types of radar and Electro-Optic sensors used, and the switches used on the control panel are all part of “architecture”. Several different types of avionics architecture have evolved over the years. To explain all the avionics architecture types is out of the scope of this thesis. Only two of them will be described in this section.

1. Federated Architectures

In the federated system, overall control and a certain amount of functionality of each avionics subsystem is assigned to a central mission computer. As computer capability increased, so did the percentage of total functionality given to software. Subsystems (radar, navigation, fire control, etc.) talk to each other over a standardized data bus, such as MIL-STD-1553, using a common data format. The data bus might be local (within a subsystem) or global (to all or a major block of aircraft subsystems).

The advantage of the federated system is that it permits better interaction of several avionics subsystems to form a whole. For example targeting and navigation

systems can interact with each other to provide positional updates for the navigational system and better target information for the targeting system.

Federated architecture does not imply that the subsystem does not have any computer processing of its own. The central coordination and control is delegated to the mission computer. FLIR (Forward Looking Infrared), Electro-Optics and radar subsystems might each have very powerful signal processing computers and data computers within the subsystem, but control, display and interactions with other systems are handled by a central mission computer. The F/A-18 is a very good example of advanced federated avionics architecture.

2. Integrated Architectures

In integrated avionics architecture, all, or nearly all, of the electronics elements of the avionics system are packaged in standard modules, and installed in several co-located common racks. Because of the numerous computer resources of a modern avionics suite, the term “integrated” could also mean a system in which the computing elements and supporting modules are co-located in a common rack.

Elements such as RF (Radio Frequency) modules, for use in communications and navigation systems, radar and electronic warfare could also be integrated into a single rack structure. Problems of interface connections and electromagnetic interference (EMI) within the racks must still be solved, however.

3. KingCobra Architecture

The avionics system proposed for the KingCobra has a federated architecture. The two mission computers communicate to other federated subsystems via MIL-STD-1553 busses.

THIS PAGE INTENTIONALLY LEFT BLANK

IV. TARGETING AND FIRE CONTROL SYSTEMS

There are many Targeting and Fire Control Systems on the market that are used for different purposes, depending upon the platform (attack helicopter, ASW helicopter, fixed-wing fighter/attack aircraft, or bomber) and tactical mission. Aircraft companies choose the most appropriate system for the requirements of the aircraft they are building. In this chapter, the Targeting and Fire Control Systems on AH-64D and AH-1Z will be presented. The AH-64D has a millimeter wave radar (Longbow Radar) and the AH-1Z has a FLIR system. It should be noted that the RFP for the ATAK helicopter specified that a MMW radar for the targeting systems is desired, but not required. Although our area of interest is FLIR targeting systems, it will be appropriate, for completeness, to present the principles and applications of the MMW radar system. These two targeting systems are designed for different purposes. The AH-64D is designed to be able to engage multiple targets in a battlefield, especially mass armored vehicles, such as tanks. Longbow radar provides the capability for multi-target engagement. The AH-1Z KingCobra, on the other hand, is designed for long-range search and target acquisition. It can detect targets before entering the battlefield, out of the range of air defense missiles.

First, we will define a basic radar system and focus on the millimeter wave radar. Then information on the Longbow Fire Control Radar will be presented. Next, we will look into FLIR systems in detail and give the performance parameters used in FLIR systems. This will be followed by the presentation of Thermal Radiation Laws, which have a great importance. As mentioned before, USMC version of AH-1Z will have a 3-5 μm staring focal plane array FLIR system in its TSS (Target Sight System) and the

Turkish version will have a 8 - 12 μm scanning focal plane array FLIR in the ASELFLIR-300T. The specifications of these two systems will be presented next. Finally the definitions and specifications of the 2nd generation and 3rd generation FLIR will be discussed at the end of this chapter.

A. MILLIMETER WAVE RADAR

Radar is an electronic instrument used to detect and locate moving or fixed objects. Radar can determine the direction, distance, height, and speed of objects that are much too far away for the human eye to see. It can find objects as small as aircraft or as large as mountains. Radars can even operate effectively at night and in adverse weather conditions.

The ability of radar to do so many tasks makes it useful for a wide variety of purposes, such as aviation, navigation, air defense, missile defense, space surveillance, intelligence gathering, weapon fire control, etc.

Radar works by sending radio waves toward an object and receiving the waves that are reflected from the object. The time for the reflected waves to return indicates the object's range. The direction from which the reflected waves return tells the object's location.

Radar sets vary in size and shape, but they all have the same kind of basic parts. Every radar has a transmitter to produce radio waves and an antenna to send them out. In most types of radar, the same antenna collects the waves bounced back from an object. The reflected waves are amplified by a receiver, processed, and presented on a display. The typical radar display resembles the picture tube of a television set. It shows the echoes as either spots of light, indicating location, or an image of the object observed.

Radar sets operate at different frequencies. Radars that transmit at lower frequencies are more effective than high-frequency radars in penetrating clouds, rain, and fog, and are widely used on planes and ships.

1. Background on MMW

The millimeter wave (MMW) region of the electromagnetic spectrum has received increased interest in recent years due to significant advances in the development of devices and components, and their use in system applications in such fields as radar, remote sensing, missile guidance, radiometry, communications etc. Millimeter waves have been proposed for varied applications and have been subject of countless overviews, survey papers, and forecasts, over the past four decades.

The MMW portion of the electromagnetic spectrum lies between the microwave and far infrared regions. It is defined as the frequency range from 30 to 300 GHz (or wavelengths between 1cm and 1mm). At this intermediate position in the spectrum, waves are not considered to be totally similar to either the microwave or the EO regions. In fact, their importance comes from their unique characteristics.

Millimeter waves have three specific qualities impacting their performance: interactions with atmospheric constituents and gases, a large bandwidth, and a narrow beamwidth for a small antenna aperture. For a given physical antenna size (aperture) the antenna beamwidth is smaller and the antenna gain is higher than at the microwave frequencies used for conventional radars; therefore, to obtain a specific gain or narrow beamwidth, a much smaller antenna may be used. In some applications, where the size and weight of the hardware is important, such as for missile guidance seekers and airborne surveillance sensors, this characteristic is very important.

Atmospheric propagation effects dominate design considerations relating to many MMW radar applications. Propagation throughout the electromagnetic spectrum, ranging from the infrared and radio frequencies to the visible, suffers to some degree from absorption of the electromagnetic energy by atmospheric gases, such as water (H_2O), carbon dioxide (CO_2), oxygen (O_2) etc., and from attenuation by atmospheric aerosols such as fog, clouds, rain and haze. This attenuation is sometimes so severe that propagation becomes impossible, especially when using the electro-optic region of the spectrum.

The absorption caused by the atmospheric gases is a minimum at certain frequencies, and these regions of superior propagation are referred to as “atmospheric windows”. The regions of maximum absorption are referred to as the “absorption bands”.

The atmospheric windows for the IR, RF and visible regions are IR 3 to 5 μm and 8 to 12 μm ; RF-10 and 3 cm (main microwave bands); and visible 0.4 to 0.7 μm . The main millimeter wave windows are 8.5, 3.2, 2.1 and 1.4 mm corresponding to frequencies of 35, 94, 140 and 220 GHz. respectively.

The electromagnetic energy tends to interact much more with the atmospheric particles at the millimetric region than at the lower microwave region. The RF portion can be considered as a continuous window up to 18 GHz. At higher frequencies, however, it has been found that a frequency selective absorption and scattering of the energy takes place and that this is caused by resonances of the atmospheric gases. The millimeter wavelengths are comparable in size to the rain and fog particles. So similar electrical resonances are caused, without exciting molecular resonance. This results in

scattering and absorption of the energy. Since this effect is much less evident at the millimeter wave window, most applications are concentrated around these frequencies.

Millimeter waves do not have the same all-weather capability as microwaves, but they have higher resolution. The component size is related to wavelength, and so millimeter wave systems are also much smaller. Although they do not have the extremely high resolution of their EO counterparts, they have superior penetration through smoke, fog and rain. Thus millimeter waves represent a region where the disadvantageous effects are minimized and most of the advantageous characteristics of the microwave and EO regions are available.

2. Operational Considerations

The understanding of the operational characteristics of MMW radar requires the knowledge and the appreciation for the location of the MMW band within the electromagnetic spectrum and the resulting effects of the propagation of MMW energy. There have been discussions about exactly what region constitutes millimeter waves. One definition for millimeter wave region is between 1mm (300 GHz) and 10mm (30 GHz). However, IEEE Standard defines it as the region between 40 and 300GHz, which excludes the operationally important and very active region around 35 GHz. Operation around 35 GHz. has to be considered in discussions of general MMW radar system performance and characteristics.

Most applications of radar involve achieving a long detection range. Consequently, radar research and development has been concentrated in the areas of lower attenuation at the MMW window frequencies. These frequencies are 35, 95, 140 and 220 GHz. Over 220 GHz., there has not been much radar development. Abnormally

large absorption regions, provided by water vapor and oxygen molecule electromagnetic resonances, cause the relative peaks to occur at approximately 60, 120, and 180 GHz. To take advantage of the covertness provided by the high atmospheric absorption, radars have also been developed at these frequencies. These frequencies also give the opportunity to operate in exo-atmospheric space where atmospheric absorption does not exist.

Table 4.1 provides some important MMW radar trade-offs and compares the relative advantages and disadvantages or current limitations of MMW relative to microwave radar. Activities in the MMW area continue to increase and lead to production and large scale manufacture and standardization of MMW components. Therefore the importance of the first two limitations is considerably decreased.

a. Advantages

(1) Small Size. The shorter wavelengths relative to microwave make it possible to reduce the size of components considerably and so build smaller systems. For the applications where size and weight restrictions apply, as in missile and aircraft, the MMW systems are an area of considerable interest.

(2) High Bandwidth. At each MMW window, extremely large bandwidths are available. For example, in the previous section the main windows are stated as 35, 94, 140, 220GHz. The available bandwidths for these windows are 16, 23, 26, and 70GHz. respectively. The advantages are considerable. It makes jamming more difficult, unless the exact frequency to be jammed is known. In radar, the range resolution can be increased. The large bandwidths also make radars more sensitive to Doppler frequency shift measurements, since these are much greater.

Advantages	Limitations
Physically Small Equipment Low Atmospheric Loss ^a High Resolution Angular Doppler Imaging Quality Classification Small Beamwidths High Accuracy Reduced ECM Vulnerability Low Multipath and Clutter High Antenna Gain Large Bandwidth High Range Resolution Spread Spectrum Doppler Processing	Component Cost High Component Reliability and Availability Low Short Range (10-20km) Weather Propagation ^b
^a Compared to IR and visual Wavelengths ^b Compared to Microwave Frequencies	

Table 4.1. Millimeter Wave Radar System Trade-Off Considerations “From Ref. 12”.

(3) Low Beamwidth. For a given antenna size, smaller radiated beamwidths are possible, which provides higher resolution and better precision. This is very important in target tracking where the smaller beamwidths can pick out more details and can discriminate better against small targets. They also minimize losses caused by side-lobe returns, which is a major problem in microwave radars. These

narrow beams are very difficult to detect and monitor, and so jamming them is an extremely difficult problem. Interference from friendly transmissions is also reduced.

“Small beamwidths are obtained with comparatively small sized antennas” [Ref. 11].

(4) Atmosphere Losses. Atmospheric absorption and attenuation losses, compared to the problem faced by laser or IR transmission in fog, smoke or rain, are relatively low in the transmission windows. It may be said that millimeter wave sensors are more effective than EO ones in adverse weather or battlefield smoke/dust conditions. The high attenuation encountered in the absorption bands limits the range so much; only short-range point-to-point secure communications are possible within these bands [Ref. 11].

b. Limitations

Although the millimeter wave region has its limitations, for some applications these are not considered as being considerably restrictive factors.

Because of the atmospheric absorption and attenuation, even in good weather conditions, the range of the millimeter wave radar is limited to 10-20 km. This range is further reduced in the presence of rain and fog. Therefore, major applications involve airborne fire control radars and weapon terminal guidance systems. Atmospheric losses increase with higher frequencies, but at the same time beamwidths get narrower and as a result component sizes get smaller. Compromise solutions must be found. At 100 GHz, the atmospheric attenuation is an order of magnitude greater than at 10 GHz. For an average atmosphere condition containing 7.5 gr of water per cubic meter, this attenuation is approximately 0.06, 0.14, 0.8 and 1 dB/km for the frequencies 10, 35, 94, and 140 GHz. respectively.

The small size of antenna reduces the sensitivity of the system, since it collects less energy. If more system gain is required and it is not possible to increase the antenna aperture, then the system should operate at the highest frequency possible to obtain maximum gain for that aperture size. Similar to this, range can be increased by increasing the aperture size, but this also reduces some of the inherent advantages of millimeter waves. The narrow beamwidths make millimeter wave systems unsuitable for search and target acquisition. Thus, most applications are for target tracking and homing.

Large bandwidths allow better Doppler shift measurements to be made, but in ground to space communications, on the other hand, this shift can be so large as to go beyond the band limits of the transmission window. Therefore, the maximum shift to be expected must be known in advance. A major limitation in development was the lack of suitable components. This has been overcome up to the 94 GHz window. Above this frequency, readily available devices are rare and users have to develop their own. Moreover, high power sources still pose a problem at all millimeter wave frequencies.

Advantages or disadvantages of MMW relative to microwave apply equally to IR compared to MMW.

3. Millimeter Wave Radar Characteristics

As shown in Table 4.1 MMW radar offers significant operational advantages when compared to microwave radar, especially in the area of high angular resolution, resulting from smaller antenna beamwidths for a fixed antenna aperture size.

Antenna half power (3 dB) beamwidth, θ , is related to the operating wavelength by the following expression for a diffraction limited antenna [Ref. 12]:

$$\theta = k\lambda/l \quad (\text{radians}) \quad (4.1)$$

where:

k = constant ($4/\Pi$ for -25 dB side lobes)

λ = wavelength

l = aperture dimension

It can be easily seen that θ is inversely proportional to frequency ($\theta \propto 1/f$). Therefore, for a fixed antenna aperture, a radar operating at 95 GHz. would radiate an antenna beam ten times smaller than a radar operating at 9.5 GHz (X band). :

$$\theta_{9.5} = \theta_{95} * 10 \quad (4.2)$$

The use of very short wavelengths and very narrow antenna beamwidths in radar designs in a number of desirable features for Army weapons system applications. The most important of these are:

a. *Narrow Antenna Beamwidth With Small Antenna*

(1) High antenna gain with small aperture. The gain, G , of an antenna relative to an isotropic radiator is:

$$G = 4 * \Pi * A_e / \lambda^2 \quad (4.3)$$

where:

A_e = effective area of antenna aperture.

For a fixed aperture, the antenna gain increases in proportion to the frequency of operation squared. Antenna gain is one of the most important radar parameters determining target detection performance.

(2) High Angular Tracking and Guidance Accuracy. A radar's angular tracking accuracy is directly related to its antenna beamwidth, θ . For a thermal noise limited case it is represented as:

$$\sigma_t = (k_t * \theta) / [(S/N) * n]^{1/2} \quad (4.4)$$

where:

σ_t = root mean square (rms) angle tracking error

k_t = constant depending on type of tracking

(S/N) = signal-to-noise ratio at the receiver output

n = number of pulses integrated

If all the other things are assumed equal, a MMW radar can be expected to achieve a reduction in tracking errors when compared to a lower frequency radar as a direct result of smaller antenna beamwidth.

(3) Capability of tracking down to very low elevation angle before ground multipath and ground clutter becomes appreciable.

(4) High angular resolution for area mapping and target surveillance.

(5) Capability of detecting and locating small objects such as wires, poles and projectiles.

(6) Good resolution of closely spaced targets.

(7) High immunity to jamming. Narrow beamwidth makes jamming through the main beam difficult), which provides reduced Electronic Countermeasures (ECM) Vulnerability: Smaller radar antenna beamwidths provide less opportunity for a jammer to inject energy to the radar's main beam and thus reduce the radar's susceptibility to jamming. Also, as mentioned before, higher antenna gains reduce vulnerability to jamming through the antenna side lobes. The basic cross-range resolution of a radar, d_x , is defined in terms of half-power beamwidth of antenna and range to the target cell as follows:

$$d_x = \theta_x * R \quad (4.5)$$

where:

d_x = cross-range resolution

θ_x = half-power beamwidth

R = range to target cell

The higher angular resolution available with MMW radar allows spatial isolation of a target in a volume clutter background such as might be present in a chaff cloud or rain background. This isolation provides higher target-to-noise-plus-clutter ratios and improved detection performance.

b. Wide Frequency Spectrum Availability

(1) High information rate capability for obtaining fine structure detail of target signature with narrow pulses or wideband, FM.

(2) As mentioned before, wideband spread-spectrum capability for reduced multipath and clutter at low elevation angles: A MMW radar with small beamwidth typically has less ground intercept than a lower frequency radar with larger beamwidths. Since ground intercept is reduced, multipath propagation conditions and ground clutter effects are correspondingly reduced.

(3) High immunity to jamming.

(4) Multiple adjacent radar operation without interference.

(5) Very high range resolution capability for precision tracking and target identification. A radar's ability to separate multiple, closely spaced targets and provide information for target identification is closely coupled to its resolution. Thus, MMW has inherent advantages in these areas.

c. Low Scatter From Terrain

(1) Reduced multipath interference

(2) Reduced terrain clutter

d. High Absorption Around Transmission Windows

- (1) Difficulty of long-range jamming
- (2) Secure operation, by selecting a frequency with higher

absorption (when required)

e. Doppler Frequency Shift

Doppler frequency shift is high from low radial velocity, which provides good detection and recognition capability against slowly moving or vibrating targets. Any target motion in the radar's beam causes a shift in the received signal frequency as follows:

$$f_d = 2 * V_r / \lambda \quad (4.6)$$

where:

f_d = shift in transmitted frequency

V_r = radial target velocity

λ = wavelength of transmitted signal

For a target having a 30m/s radial velocity with respect to the radar, a radar operating at 9.5 GHz. would experience a 1.9 kHz. frequency shift, where a radar operating at 95 GHz. that observes the target, would experience a 19 kHz. frequency shift.

These large Doppler shifts obtained from relatively small targets provide the capability for increased target detection and maybe recognition of such target features as second and higher order velocity signatures. These features may be used in the automatic classification of target using radar signatures.

f. Atmospheric Effects

Penetration of dry contaminants in atmosphere, which provides good operation under limited visibility conditions of dust, dry snow and smoke.

g. Increased Detection Capability of Small Objects

Small targets become an important part of a wavelength, which provides a good capability of detecting, wires, poles, birds and insects.

4. Air-to-Ground Millimeter Wave Characteristics

Airborne radars operating against ground targets generally suffer from target acquisition problems and ground clutter. Radars, with narrow antenna beams, operating at millimeter wavelengths will give high ground target resolution. Using a narrow antenna beamwidth will also reduce the target clutter, but dense foliage obscuration will not be helped. However, because of the high resolution of angle and range, the target might be seen where the foliage is not dense.

At millimeter wavelengths ground mapping and target acquisition can be done exceptionally well. A millimeter wave air-to-ground system should provide excellent gun aiming accuracy or weapon delivery guidance and terminal homing, given that the target is acquired and designated.

The use of millimeter wavelengths for Instrument Landing System (ILS) applications offers advantages such as very high resolution and accuracy with acceptable aircraft.

5. Target Acquisition Millimeter Wave Characteristics

The use of millimeter wave sensors for target acquisition is highly complicated. It holds a promise for performing all the functions, such as the volume search, detection of presence of a target, discrimination of a target from clutter and background, categorization, location, automatic target tracking for determination of range, azimuth and elevation angles and radial velocity, target-to-weapon assignment for engagement,

and assessment of the damage by the indication of lack of movement or absence of signal return, that are involved in acquisition [Ref. 11].

A millimeter wave radar acquisition system has its own limitations, which are discussed earlier, such as reduced performance in rain, foliage obscuration, clutter, terrain masking and false target returns. Since it searches a large volume with a narrow beamwidth, it is also limited by the problem of a longer search time or more rapid scan rate requirement. Search radars used against low-flying aircraft, require only limited elevation search, primarily at the horizon. These search systems reduce the search volume and make the use of a narrow beamwidth search radar feasible.

A millimeter wave target acquisition sensor would have advantages and possibilities, such as [Ref. 11]:

- Since the small targets are appreciable part of a wavelength, they can be detected.
- The performance is not affected by the dry contaminants in the atmosphere.
- Detection and jamming by the enemy gets difficult at long ranges, because of the absorption in the atmosphere and the narrow beams.
- Effective separation of the desired target from nearby scatterers is made available for effective target discrimination from natural and man-made objects.
- Wideband spread-spectrum operation provides good target-to-clutter enhancement by averaging out the clutter.
- If there is some vibration or rotary motion of a component that is a millimeter wave reflector, then stationary and moving targets have unique detectable signatures. It is possible to detect very small (millimeter) movements of reflectors since such movements are an appreciable part of a wavelength and cause a large change in the phase of the reflected signal.
- Extremely high range resolution techniques make the identification or recognition of spatial features of targets available.
- A millimeter wave radar used in conjunction with an acoustic sensing system, which has a good capability to detect and identify audio and

noise-emitting targets, would provide accurate target location and tracking information. The acoustic signature of the desired target would serve to help the radar in acquiring the target by matching the spectrum of the acoustic signal with that of rotation/vibration Doppler modulation on the radar signal.

- To be able to detect slowly moving targets hidden in clutter, the design of a very effective MTI system is necessary. If narrow beam and narrow transmitted pulse are combined, then the target-to-clutter ratio is improved which allows design of an effective MTI system. At millimeter wavelengths, the doppler frequencies resulting from small radial velocities are in the audio frequency range and are convenient to process.

Even with the advantages given in the Table 4.1 and presented above, a MMW radar should not be considered a remedy for all surveillance and tracking problems. MMW radar is basically a short-range, high-resolution sensor, which may be severely limited in some adverse weather conditions, for terrestrial applications. However, for many other applications, it represents an excellent model that carries the performance characteristics of optical infrared sensors operating at higher frequencies on one hand, and microwave and lower frequencies on the other. Table 4.2, which is adapted from Currie and Brown, compares the relative performance of MMW radar with its optical and microwave counterparts for several operating characteristics. MMW radar performance usually falls between the extremes of the optical sensors and microwave.

Radar Characteristics	Microwave	Millimeter Waves	Optical
Tracking Accuracy	Fair	Fair	Good
Classification & Identification	Poor	Fair	Good
Coverttness	Poor	Fair	Good
Volume Search	Good	Fair	Poor
Adverse Weather Performance	Good	Fair	Poor
Performance in Smoke & Dust	Good	Good	Poor

Table 4.2. Radar System Performance Comparison “From Ref. 12”.

6. Millimeter Wave Applications

The three main military applications for millimeter wave technology are the fields of radar, radiometry and communications. Since our area of interest is radar and radiometry, communications applications will not be mentioned.

a. Radar

The microwave region has been used for a number of applications, not least of them being radar. However, most of these radars can easily be countered by Electronic Counter Measures (ECM), and have some disadvantages that can cause errors or ambiguities. Because of the wide beamwidths they have, it is possible that they receive false returns due to multi-path propagation and side-lobe echoes. For aircraft and missile applications, they can be very heavy. Millimeter wave techniques provide the ability to eliminate or minimize such problems.

Since the millimeter wave radars are smaller in size and have a greater accuracy, the short ranges they provide do not necessarily present a major disadvantage. For many aircraft, the short ranges are adequate, and the high angular resolutions, obtained with smaller apertures, are far more important.

In ground-based radars, the range limitation is overcome by using microwave frequencies for the long-range search and target acquisition. When the target is within the range of the millimeter wave radar, it is handed over for more accurate tracking. Millimeter wavelengths also provide better target detail for small targets such as aircraft, boats and land vehicles. Thus, millimeter wave tracking radars are very useful in low-level air defense systems.

There are many advantages of MMW radars such as small size, high accuracy and reasonable operation in adverse weather conditions, which make them very attractive as active seekers for terminal guidance of missiles and munitions, as well as for fusing. Such seekers could replace EO seekers in high battlefield smoke and dust and in bad weather conditions, when IR/lasers/TV-based sensors are virtually useless [Ref.11].

The MMW system's performance is sufficient to be able to recognize and distinguish individual tanks. Therefore it appears to be most practical solution in certain scenarios for defense against massed armor. On a flat battlefield, armored vehicles have significant radar cross-sections throughout the MMW region and can be distinguished easily. This may be more difficult when the tank is standing next to a building or a tree. However, this is largely a problem of lack of practical experience in the analysis of such target returns. Suitable methods of processing the large amount of fine detail have to be developed and the problem of pattern recognition has to be studied.

Millimeter wave radars also have practical applications at sea. Although a sufficiently broad data base of sea clutter and target information is lacking, they can help the conventional microwave radar to distinguish small ships and other targets from sea clutter and can overcome the multi-path problems of sea-skimming missile tracking.

b. Radiometry

The radiometer is a passive means of detecting the noise temperature as seen by its antenna. This noise, or radiometric temperature, is related to the emissivity of the radiating objects as well as to their reflection temperatures. It need not necessarily be the same as the thermal ambient temperature. In the case of millimeter wave and microwave, this temperature, when viewing the earth, is approximately equal to the

thermal ambient temperature. For metallic targets or the sea surface, the apparent temperature can be much lower than ambient temperature. This results from the low emissivity of such surfaces and also such surfaces reflect the brightness of the cold sky.

Undesired background radiation interferes with the target radiation. A narrow antenna beam, which increases the resolution and target contrast, can minimize this interference. Using millimeter waves, narrow beamwidths can be obtained with small-sized antennas, and wide bandwidth provides greater sensitivity. Therefore MMW are very attractive to prevent background interference. They are ideal for use as passive sensors.

Development of dual mode seekers, such as active/passive MMW, IR/MMW, laser/MMW etc., provides alternate sensor techniques in case the use of one type is limited due to a tactical situation.

B. AN/APG-78 FIRE CONTROL RADAR

The AN/APG-78 Fire Control Radar (FCR), more commonly called as Longbow Radar, is a multi-mode millimeter wave (MMW) sensor, integrated on the Apache Longbow, with the antenna and the transmitter located above the aircraft main rotor head. The Longbow package includes a mast-mounted MMW fire control radar dome, a programmable signal processor and a MMW Hellfire missile.

The design purpose of this system is to provide a rapid automatic search, detection, classification and prioritization of multiple moving and stationary targets on land, air and water to the maximum range of the Longbow missile, in adverse weather and under battlefield obscurants. After this procedure has been done, target coordinates are automatically available to all sensors and weapons, enabling target confirmation,

reducing the probability of killing friendly land and/or air vehicles and permitting rapid launch. Then, the sensor system transfers the targeting data to the Longbow Hellfire missile seeker. Upon selection of the target from the captured target database, the missile will have those coordinates transferred to it and an internal MMW radar seeker head will search and capture the target of choice. When launched it will maintain track to the target without updates from the launching helicopter. Hence it is “Fire-and-Forget”. It is also possible to launch the missile upon transfer of the target coordinates and have the MMW seeker capture the target right after the launching.

Target data is also available through the improved data modem for real-time transfer to other platforms and command posts. Specifications of FCR (AN/APG-78) and Hellfire missile (AGM-114L) are given in Table 4.3 [Ref. 16].

By instantaneously linking data from on-board systems and sensors, both on and off the aircraft, and putting that information directly into the flight crew’s hands, the battle can effectively be won before it is fought, according to Marty Stieglitz, vice president of Apache programs. With the radar, Apache Longbow crews can scan the battlefield in real-time, classify and prioritize multiple threats, and digitally share this battlefield information with other AH-64Ds as well as other friendly forces.

The FCR has four modes:

- The Air Targeting Mode (ATM), which detects, classifies and prioritizes fixed and rotary wing threats.
- The Ground Targeting Mode (GTM), which detects, classifies and prioritizes ground and air targets.
- The Terrain Profiling Mode (TPM), which provides obstacle detection and adverse weather pilotage aids to the Longbow crew.
- The Built in Test (BIT) Mode, monitors radar performance in flight and isolates electronic failures before and during maintenance.

Fire control radar (AN/APG-78)	
Range	8 km
Frequency	Ka band
Modes	Surveillance, targeting, RFI cued, terrain profiling, and air overwatch
Weather	Clear to adverse
Environments	All battlefield obscurants
Missile (AGM-114L)	
Range	0.5 - 8 km
Guidance	Millimeter wave
Compatibility	Launch from multiple platforms
Commonality	Bus and warhead with Hellfire II
Weight	108 lb (49 kg)
Length	69 in (175 cm)
Diameter	7 in (17.8 cm)

Table 4.3. Longbow System Specifications “From Ref. 16”.

The emission of Longbow radar has a very low probability of intercept by the opposing forces, and can sweep up to an arc of 50 square km in front of the aircraft. If the target is moving, the radar can detect at ranges up to 8 km, but for static targets this range is reduced to 6 km. At these ranges the Longbow system can display, classify and track up to 128 targets. These targets can be tracked within the radar and by extension within the fire control computer, and data transfer terminals.

The Longbow FCR incorporates an integrated radar frequency interferometer for passive location and recognition of radar emitting threats. Data from this sensor can be

displayed on a display screen in the cockpit to indicate position and distance of the threat. The advantage of MMW is that it performs under poor visibility conditions and is less sensitive to ground clutter. As mentioned earlier, the short wavelength allows a very narrow beamwidth, which is resistant to countermeasures.

While individual types of vehicles cannot be identified, such as T-72 vs. T-80, the Longbow system can classify a vehicle based on the following criteria: wheeled, tracked, air-defense, airborne. Also, it can indicate to the crew if the target is mobile or stationary. The Longbow FCR is able to accomplish this by using radar waves of very high frequency. This results in a radar with a very fine resolution, which can identify particular features of the target being swept. The results of this process are then compared against a library of threats. If the match is found, then the target can be categorized.

The Apache features a Target Acquisition and Designation System, TADS (AN/ASQ-170) and a Pilot Night Vision System, PNVS (AN/AAQ-11), designed and built by Martin-Marietta (now Lockheed Martin), which enables the crew to navigate and conduct precision attacks in day, night and adverse weather conditions. The PNVS is mounted above the nose structure of the aircraft, while the larger TADS turret occupies the underside of the nose section. Because of their locations, in order to use those sensors, Apache has to completely unmask. Before the Longbow Radar, this was the only method of targeting for the Apache.

The drive mechanism of each turret contains both a “coarse” gimbal for rapid tracking and a “fine” gimbal for precision tracking of targets. Both turrets can be rotated to a rearward facing position when not needed in order to preserve the optics from the wear of flight-path particles.

PNVS consists of a FLIR device that improves the pilot's night vision capability. The FLIR's field of view is 40 degrees horizontal and 30 degrees vertical. The FLIR imagery can be displayed in a 1:1 view, thus representing the true picture outside the aircraft.

The TADS assembly is divided into day (port) and night (starboard) halves, as shown in Figure 4.1 [Ref. 16].

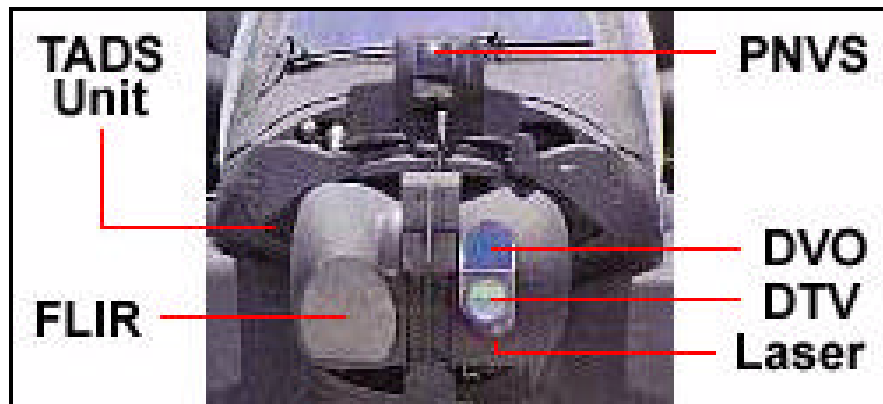


Figure 4.1. AH-64D Apache Longbow Nose Section "From Ref. 16".

On the port side there are three sensors for the detection and tracking of targets when the daylight is present. They are mounted in a vertical column and consist of:

- Direct View Optics (DVO), views real world, full color and magnified images during daylight and dusk conditions.
- Day TV (DTV), views images during day and low light levels, black and white.
- Laser Range Finder/Designator (LRF/D), used to designate for the Hellfire missile system as well as provide range for the Fire Control Computer's calculations of ballistic solutions.

DVO is an optical telescope with two magnifications: x4 magnification at 18 degrees FOV, or x16 magnification at 4 degrees FOV. The DTV optical sensor, on the other hand, offers up to x127 magnification with a corresponding FOV of 0.45 degrees. The laser designator is a neodymium laser with an effective range of 20 km (12 miles). It

has two specific functions. First, it designates targets for either its own missiles or the missiles of another helicopter. Second, the laser acts as a range finder, measuring the precise distance between aircraft and target.

While designating, the laser pulses in a pre-designated pattern rather than operating in a continuous beam. This “codes” that particular laser to distinguish it from others. This unique code ensures that missiles intended for that target are guided to the correct target, since they are instructed to seek that unique code.

The starboard component of the TADS system contains a FLIR sensor that views thermal images, real world and magnified, during day and night and adverse weather conditions. This FLIR sensor provides variable FOVs, ranging between 50, 10, 3.1, and 1.6 degrees. Positive target identification through FLIR is extremely difficult. FLIR provides good visual identification up to the ID range limit due to the resolution and contrast. FLIR detects the difference in the emission of heat from objects; on a hot day, ground clutter highly affects its performance. The ground may emit or reflect more heat than the target. In such case, the target will be “cool” and the environment will be “hot”. When the emissions of heat from both target and the surrounding environment are equal, IR crossover occurs, most often when the environment is wet. This is because the humidity of the air creates a buffer in the emissivity of objects. This limitation is present in most of the systems that use FLIR for target acquisition. To be able to overcome this limitation partially, the TADS unit can be switched between “white hot”, on a hot day, and “black hot”, at night when crossover occurs, in order to provide better contrast against the surrounding terrain for increased target discrimination.

The Longbow RF missile and the Longbow Hellfire Launcher (LHML) are referred to as the Longbow Hellfire Modular Missile System (LBHMMS). The system incorporates a fire-and-forget missile that accepts primary and/or secondary targeting information from the FCR and single targeting information from TADS or another aircraft to acquire and engage targets. The RF missile, similar to the FCR, provides the capability to engage threats in adverse weather and through battlefield obscurants.

There are two acquisition modes, lock-on-before-launch (LOBL) and lock-on-after-launch (LOAL) that allow engagement of ground and rotary wing threats at extended ranges. In LOBL mode, the missile will acquire and track moving or short-range stationary targets prior to leaving the launch platform. In the LOAL mode, on the other hand, it will acquire long-range stationary targets shortly after leaving the launch platform.

With the integration of the FCR, the Apache Longbow aircraft enhances battlefield awareness by providing coverage of the battle area at extended ranges and increasing the operational independence of weather and battlefield conditions.

The FCR and TADS are completely independent target acquisition sensors that may be operated independently by either crewmember or combined to provide a high degree of multi-sensor accuracy. When they are operated independently, the pilot can use the FCR to search for air targets in the ATM while the copilot/gunner searches for ground targets using TADS.

By using both TADS and the FCR together, the advantages of each sight are combined. The FCR's rapid search, detection, classification and prioritization of targets can be used to direct the optics of TADS for positive identification. Once the targets are

prioritized, then the center view can be focused on the location of the highest priority target and the CPG (Copilot/Gunner), at the touch of a switch, can view either display. Alternatively, the FCR centerline can be cued to the TADS so that a rapid and narrow search could be made of a suspected target area.

An integral part of the Longbow FCR is the Radar Frequency Interferometer (RFI). It has sensitivity over a broad RF spectrum for passive location and recognition of radar emitting threats when the threat radar is in search and acquisition mode and also when the threat emitter is looking directly at and tracking the Longbow system. It also has a programmable threat emitter library to allow additional threat signatures to be stored and updated.

The AH-64D Longbow is armed with the Lockheed Martin AGM-114L Longbow Hellfire air-to-surface missile. Longbow Hellfire incorporates a millimeter wave radar seeker on a Hellfire II aft section, which allows the missile to perform in full fire-and-forget, also called launch-and-leave, mode. The primary advantages of the Longbow missile include adverse weather capability (fog, smoke, rain, snow, battlefield obscurants); fire-and-forget guidance, which allows the Apache Longbow to launch and then remask, thus minimizing exposure to enemy fire; MMW countermeasures; survivability; an advanced warhead that is capable of defeating reactive armor configurations; and reprogrammability to adapt to changing threats and mission requirements.

1. Hellfire Delivery Modes

As mentioned before, there are four delivery modes that aircrews can utilize when firing the hellfire missile. These are driven by three important factors: distance to the

target, the weather (primarily cloud ceiling and visibility), and terrain conditions. The four delivery modes are:

- **Lock-on Before Launch (LOBL):** In this mode, the missile seeker acquires and locks-on to the coded laser energy reflected from the target prior to launch. When the missile is fired in this mode, aircrew is assured that the missile has already positively locked on to the target prior to launch. In this mode, the farther the target, the higher the missile trajectory is.
- **Lock-on After Launch-Direct (LOAL-DIR):** This mode has the lowest of all trajectories. In this mode, the aircraft launches the missile toward the direction of the target before the target is designated by a laser. Initially missile flies blind. It will climb slightly, still relatively low, until the laser is activated. Once it acquires the reflected laser energy, it pitches up to achieve an optimum dive angle at the target.
- **Lock-on After Launch-High (LOAL-HI):** This mode allows the missile to clear a 1000 feet high terrain feature to the front of the aircraft, provided that the aircraft is 1500 meters behind the peak of the terrain. Effective range for this mode is 8 km.
- **Lock-on After Launch-Low (LOAL-LOW):** In this mode the terrain mask that the missile is able to clear is reduced to 260 feet to the front of the aircraft, provided that the aircraft is 600 meter behind the peak of the terrain. Although the maximum range is the same with the previous mode, this mode has a lower trajectory.

The last two delivery modes are unique in that they allow the aircraft to remain masked behind terrain to increase aircraft survivability.

2. Types of Hellfire Missiles

There are six different models of Hellfire missiles with different design features and capabilities. The basic subcomponents of a Hellfire missile are shown in Figure 4.2:

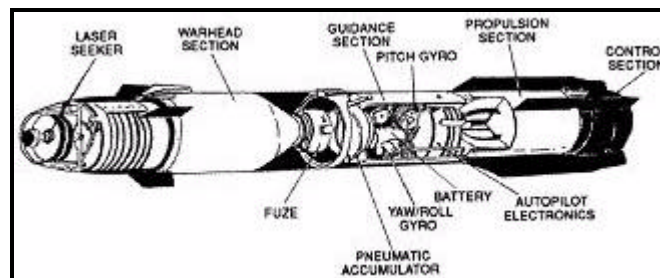


Figure 4.2. Hellfire Missile “From Ref. 19”.

The six models of Hellfire missiles include:

- AGM-114A: This missile is the original design Hellfire missile. It has a low-smoke rocket motor and basic subcomponents. It fires the highest trajectory of all six models.
- AGM-114B: This model has an improved low visibility (ILV) capability and minimum-smoke rocket motor. It flies lower trajectories than the A model. The Safe and Arm Device (SAD) that it has provides mechanical and electrical blockage in the rocket motor firing.
- AGM-114C and AGM-114F: These two missiles are the same in terms of their improved low visibility capabilities as the AGM-114B. The only difference is that they do not have a Safe and Arm Device (SAD) capability.
- AGM-114K (Hellfire II): This model has a unique capability that the other models above do not have. It is that, if the missile flies into low clouds, it has the highest probability of re-acquiring the target. It has an internal guidance algorithm. If the missile, somehow, loses the laser lock after its initial acquisition, the seeker continues to point at the target. It stops climbing and does not fly a normal profile. It is programmed to turn and point in the same direction as the seeker, which causes the missile to fly down (out of the cloud) toward the target and maximize the probability of re-acquiring.
- AGM-114L (Longbow Hellfire): This is the latest development of the Hellfire family and based on the AGM-114K missile. The solid-rocket motor and tandem warheads are the same in both missiles. The difference between the missiles is that while the AGM-114K uses a laser seeker to find its target, the AGM-114L, on the other hand, is a Millimeter Wave Imaging (MMWI) model and has inertial midcourse guidance. The nose section of the AGM-114L has the glass dome of the Hellfire II laser seeker replaced by a dome-shaped radome and is slightly longer and heavier.

The two missiles are shown in profile in Figure 4.3 [Ref. 17]. The AGM-114L uses its MMWI radar seeker to detect, acquire and home in on a targeted threat. This means that, after the missile is launched, the missile and the Longbow FCR take over the control and guide the rocket to its target.

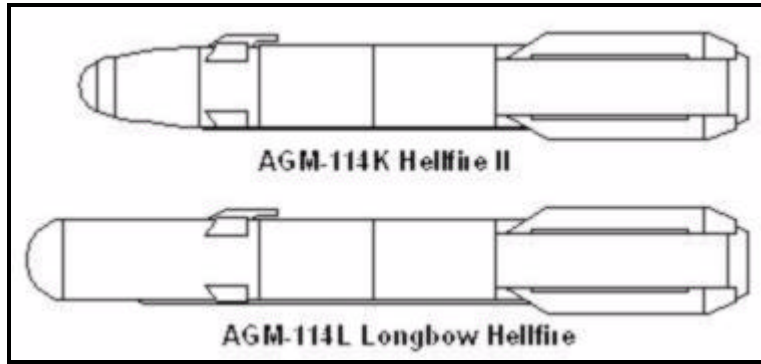


Figure 4.3. Hellfire II vs. Longbow Hellfire “From Ref. 17”.

The weapon can be fired LOBL, or for maximum range fired in LOAL mode, with the launch aircraft masked behind terrain, flying under inertial guidance to a preprogrammed footprint where the target is acquired. In either LOBL or LOAL mode, after launch no operator input is required to guide the missile.

The AGM-114F and AGM-114K models have an additional warhead for improved performance against reactive armor.

C. INFRARED AND ELECTRO-OPTICAL SYSTEMS

1. Electromagnetic and IR Spectrum

The electromagnetic spectrum covers a very large range of frequencies and wavelengths and can be described in terms of propagating electric and magnetic fields. The propagating wave fields are characterized by frequency and amplitude. The standard range designations of the electromagnetic spectrum are shown in Figure 4.4 [Ref. 24].

There are no sharp boundaries between these regions. They are distinguished by their methods of detection and production, atmospheric transmission, etc.

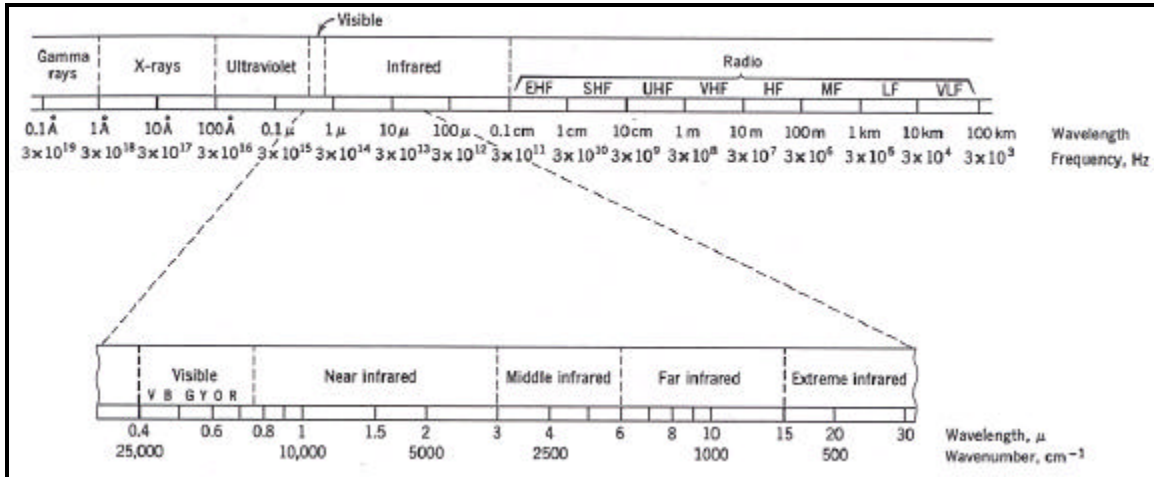


Figure 4.4. Electromagnetic Spectral Range Designations “From Ref. 20”.

The optical spectrum may be defined as a subset of the electromagnetic spectrum, which covers the optical wavelengths. These sub-regions are shown in Figure 4.4 in detail.

Systems that operate in the region of 0.4-0.7 micrometer wavelengths, the visible band, are found to the short-wavelength side of the infrared region and are described as “visible” sensors. Those using radiation in the spectral region from 0.7 to 14 micrometer wavelength are called “infrared” sensors. On the long-wavelength side the infrared region is bounded by the microwave region. The infrared spectrum is further divided into three sub-regions, the near or short-wave infrared (SWIR) region (from 0.7 to 2 micrometers), the mid-wave infrared (MWIR) region (from 3 to 5 micrometers), and the long-wave infrared (LWIR) region (from 8 to 14 micrometers) [Ref. 21].

Electro-optical systems utilize wavelengths within the 0.4 to 2 micrometer region comprising the visible and SWIR regions. Electro-optical (EO) sensors collect the light that was reflected by the objects. The mid-wave (3-5 μm) and long-wave (8-14 μm) band imagers are infrared sensors and called Thermal Imaging Sensors (TIS) including FLIR

(Forward Looking Infrared) systems or I²R (Imaging Infrared) sensors. Unlike EO sensors, I²R sensors collect the radiation that is emitted by the objects. For the EO and I²R sensors, the analytical techniques are similar, but the performance parameters are different. Usually EO systems are described in terms of radiant contrast, while I²R parameters are described in terms of differential temperature.

Thermal devices basically collect the thermal energy emitted by the objects in the infrared region to detect or identify the objects.

2. Thermal Radiation Laws

It is necessary to develop a vocabulary of clearly and consistently defined terms to clarify the basic laws of thermal radiation. The definitions below are taken from Cooper [Ref. 24] and Seyrafi [Ref. 22].

- Blackbody: defined as an ideal body or surface that absorbs all radiant energy, incident upon it at any wavelength and at any angle of incidence, so that none of the radiant energy is reflected or transmitted.
- Emissivity (ϵ): the ratio of the emitted radiant power from a surface to that emitted from a blackbody (perfect emitter) at the same temperature. The emissivity of a blackbody is equal to 1 ($\epsilon = 1$).
- Absorptivity (α): the ratio of the absorbed radiant power to the incident radiant power. Both α and ϵ are spectral functions, i.e. functions of wavelength.
- Reflectivity (ρ): the ratio of the reflected radiant power to the incident radiant power.
- Transmissivity (τ): the ratio of the transmitted radiant power to the incident radiant power.

The definitions of the last three quantities involve the ratio of absorbed, reflected or transmitted energy to the incident energy. Conservation of energy dictates that [Ref. 21]:

$$\alpha(\lambda) + \rho(\lambda) + \tau(\lambda) = 1 \quad (4.7)$$

For materials that are opaque ($\tau(\lambda) = 0$):

$$\alpha(\lambda) + \rho(\lambda) = 1 \quad (4.8)$$

For a target at thermal equilibrium (neither gaining nor losing heat), the absorptivity and emissivity are identical [Ref.21], which is:

$$\varepsilon(\lambda) = \alpha(\lambda) \quad (4.9)$$

Then Eq. 4.8 becomes:

$$\varepsilon(\lambda) + \rho(\lambda) = 1 \quad (4.10)$$

Eq. 4.10 indicates that a highly emissive target has a low reflectivity.

a. Planck's Radiation Law

This law gives the spectral distribution of radiant emittance of a blackbody and can be formulated as [Ref. 21]:

$$M_\lambda(T) = 2\pi c^2 h / [\lambda^5 (e^{hc/k\lambda T} - 1)] \quad (4.11)$$

where:

$M_\lambda(T)$ = blackbody spectral radiant exitance at wavelength λ (Watts/cm³)

h = Planck's constant, (6.6256×10^{-34} W-sec²)

k = Boltzman's constant, (1.38054×10^{-23} W-sec/K)

T = absolute temperature of the blackbody (K)

λ = wavelength (m)

b. Stefan-Boltzmann Law

This law gives the total radiant exitance from a blackbody surface in terms of temperature, and can be derived by integrating M_λ over all wavelengths. The result is [Ref. 20]:

$$M(T) = \varepsilon_e \sigma T^4 \quad (4.12)$$

where:

M = total radiant emittance of a non-blackbody source

ϵ_e = effective emissivity

σ = the Stefan-Boltzmann's constant (5.6697×10^{-12} Watts/cm²-K⁴)

c. *Wien's Displacement Law*

This law gives the wavelength of the maximum emission for a given blackbody temperature (T), which is found to be inversely proportional to T, by [Ref. 20]:

$$\lambda_{\max} T = 2897.8 \quad [\mu\text{m-K}] \quad (4.13)$$

where:

λ_{\max} = wavelength where the peak of the radiation occurs (micrometers)

T = temperature (Kelvin)

In Figure 4.5, it can be easily seen that the total radiant emittance (the area under the curve) increases rapidly with temperature and the peak of the curve shifts to shorter wavelengths as the temperature rises [Ref. 20]. The dashed curve represents Eq. 4.13.

3. Target Thermal Signature

Real targets differ in radiance from real backgrounds due to more factors than just the temperature difference. The target-to-background contrast is represented in the infrared by the equivalent temperature difference, or “delta T” (ΔT). Although it appears to be a thermal quantity, it really is a radiometric quantity. It is the temperature difference of two blackbody sources (referenced at 300 °K), required to provide the actual target and actual background radiance difference. The visual geometry of differential temperature is given in Figure 4.6. This can be used to obtain ΔT for extended targets.

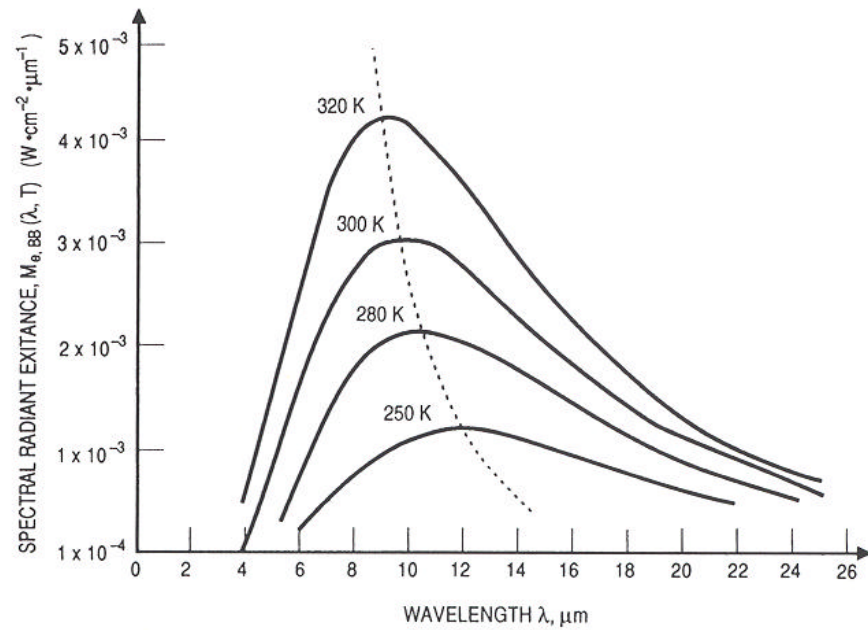


Figure 4.5. Spectral Radiant Emittance of a Blackbody at Various Temperatures “From Ref. 22”.

A more important quantity than ΔT is the apparent ΔT (ΔT_{app}), which is the equivalent blackbody differential temperature that would produce the same sensor output voltage difference as the real target and background seen through some atmospheric path.

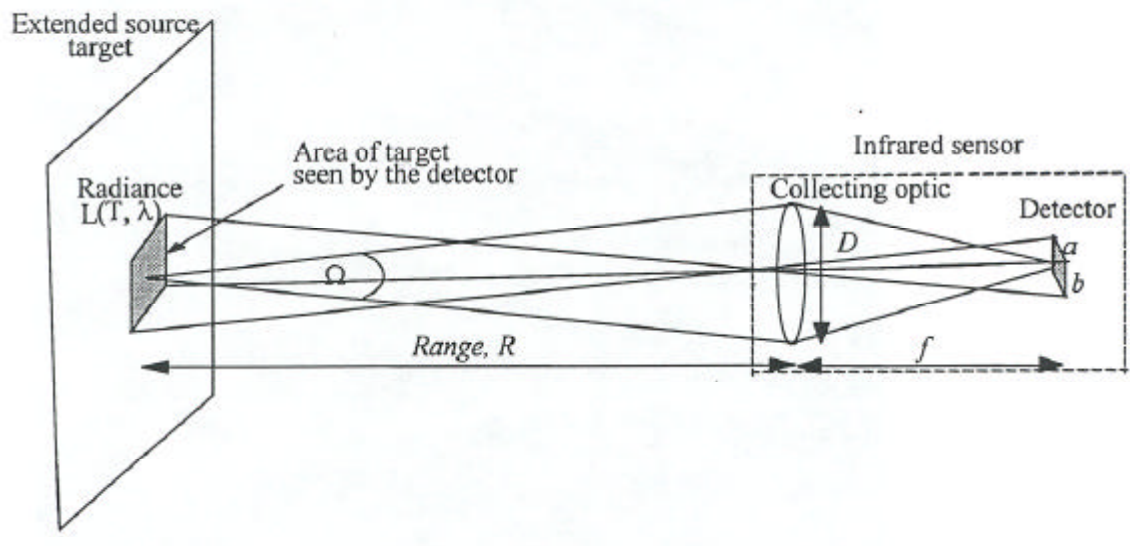


Figure 4.6. Differential Temperature Geometry “From Ref. 21”.

A simple way to describe the apparent delta T is that it produces a differential voltage on the output of a detector corresponding to the difference in flux of the target and the background seen through the atmospheric path [Ref. 21].

It should be remembered that the apparent temperature difference corresponds to the actual target-to-background radiance difference reduced by the atmospheric transmission between the target and the infrared sensor. The real apparent differential temperature is a function of background flux, target flux and atmospheric transmission. Figure 4.7 illustrates the difference between the temperature difference at the target (ΔT_{tgt}) and the temperature difference seen by the sensor through an atmospheric path, apparent delta T (ΔT_{app}).

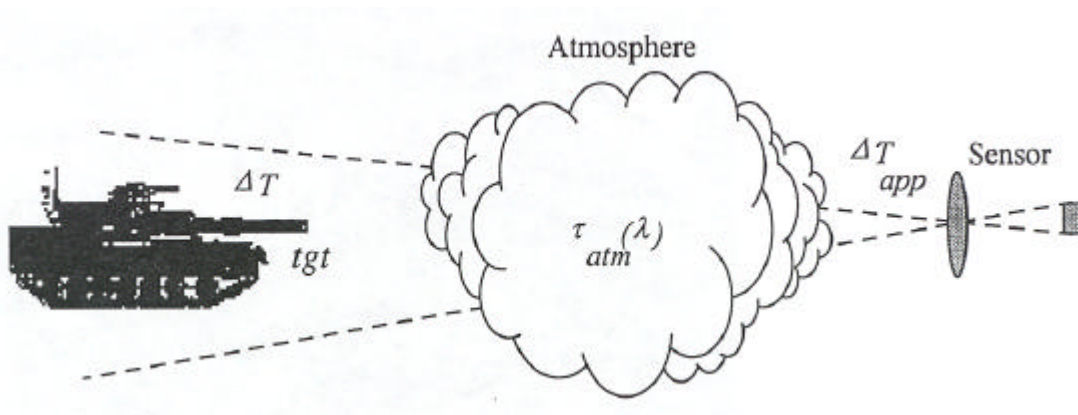


Figure 4.7. Apparent Delta T, ΔT_{app} “From Ref. 21”.

4. Atmospheric Transmission

The thermal signal emitted from an object must pass through the atmosphere before reaching the entrance aperture of a receiver. Earth’s atmosphere is a mixture of various gases with varying characteristics of absorption, emission, and scattering of optical radiation. No matter how strong the target signature is, the thermal signal is always attenuated by the atmosphere it propagates through. Attenuation occurs in the

atmosphere by absorption or/and scattering of radiation. For sensors operating in the infrared, both absorption and scattering are important. The atmospheric attenuation is caused by any combination of the four mechanisms below. These mechanisms are treated as independent and they have to be considered individually.

- Aerosol absorption
- Molecular absorption
- Aerosol scattering
- Molecular scattering

Molecular absorption takes place due to the interaction (vibration and/or rotation) of molecules with infrared radiation. In the process, certain types of molecules go from one vibration-rotation state to another. The most important of these molecules is water vapor. It limits the useful IR wavelengths to 3-5 μm and 8-14 μm bands. Other molecular absorbers, including carbon dioxide, carbon monoxide, ozone, nitrous oxides and methane are of lesser importance.

In addition to the molecular gases, there are many particles of various sizes, densities and chemical compositions in the atmosphere. These particles are produced by natural causes such as volcanic ash, interplanetary dust, etc. and contribute to the attenuation of radiation. These particles are called “aerosol” particles. Aerosols remain suspended in the atmosphere for varying times before settling due to gravity or being washed out by the rain.

Attenuation by scattering is the result of photons colliding with particles in the atmosphere and reradiation of resultant photon energy in all directions. It is a process that changes the direction of motion of the individual photons that results in the divergence of the energy and decrease in the forward radiance. Radiation is redirected from its normal

path by particles in the air. Scattering is a function of relative atmospheric particle size to the incident photon wavelength.

Based on the relationship between the particle size and wavelength, scattering models can be divided into three categories. When the particle radius is approximately less than one-tenth of a wavelength, Rayleigh scattering is dominant. If the wavelength is approximately the same size as the particle radius, then aerosol scattering (or Mie scattering) occurs. The third type of scattering occurs when the wavelength is much smaller than the particles, i.e. raindrops.

The main sources of scattering in the marine atmosphere are the water droplets suspended in the air. Overland, dust and combustion products dominate in populated areas.

Absorption and scattering are grouped together and usually called extinction. Extinction can be defined as the reduction in the flux of radiation caused by the atmosphere and expressed in terms of an exponential coefficient, in Beer's Law:

$$\tau = e^{-\mu R} \quad (4.14)$$

where:

τ = transmittance of a path length R through the atmosphere,

μ = extinction coefficient.

The total extinction coefficient is the sum of the coefficients of total absorption and total non-forward scattering [Ref. 20].

$$\mu = \mu_a + \mu_s \quad (4.15)$$

One further step would be to divide both absorption and scattering coefficients into components caused by the aerosol particles suspended in the air and the molecules of the air. This can be expressed as follows:

$$\mu_a = k_m + k_a \quad (4.16)$$

$$\mu_s = \sigma_m + \sigma_a \quad (4.17)$$

where:

k_m = molecular absorption coefficient,

k_a = aerosol absorption coefficient,

σ_m = molecular scattering,

σ_a = aerosol scattering.

The relative values of the four coefficients depend strongly on the density and molecular composition of the atmosphere and the composition, number density and size distribution of the aerosols [Ref. 20].

A graph of typical atmospheric transmission for 1 km path at sea level is shown in Figure 4.8. It can easily be seen that atmospheric extinction is a strong function of wavelength. Since it severely affects the atmospheric transmission, the 3-5 μm and 8-12 μm spectral bands are commonly used for military applications. The transmission shown is a typical transmission, which will certainly change with climate, temperature, humidity, etc.

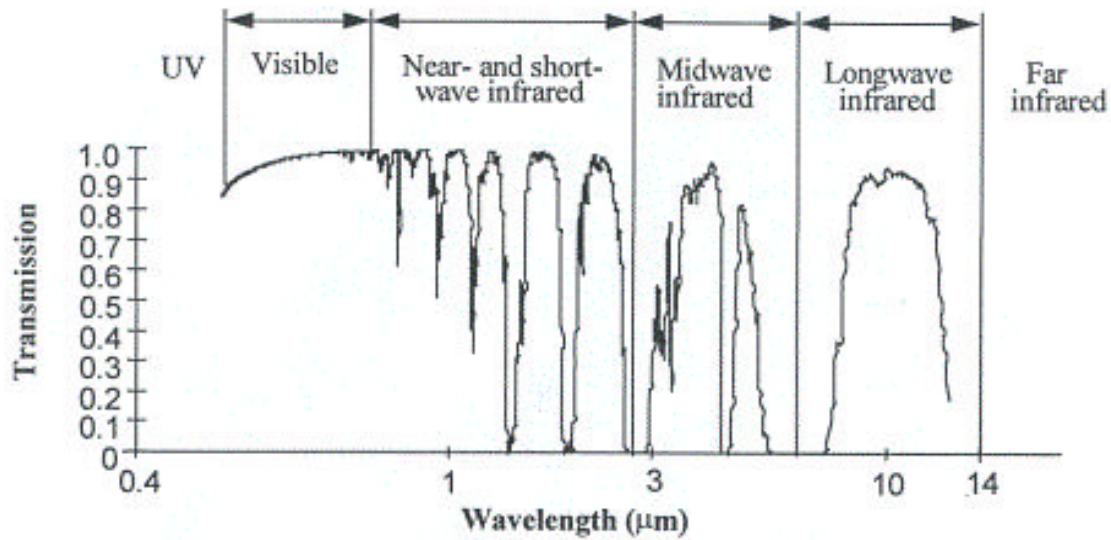


Figure 4.8. Typical Atmospheric Transmission for a 1-km path length “From Ref. 21”.

D. THE CONCEPT OF FLIR

The forward-looking infrared (FLIR) receiver is a military version of an IR² sensor. A FLIR is a device that collects infrared radiation emitted from objects (after that radiation is transmitted to the FLIR) and develops a pseudo-real-time representation of the scene for viewing by a human operator [Ref.27]. This term, FLIR, distinguishes the line scanners, which are intended for surveillance of ground targets, from thermal imagers. Line scanners have a scan frequency that is matched to the aircraft’s forward speed and provides only lateral scanning of the field-of-view (FOV). FLIR devices, on the other hand, do not use aircraft forward speed to provide a continuous raster pattern.

Thermal imager systems operate on extended targets. The function of a thermal imager is to provide a spatially resolved image of flux variations related to temperature and emissivity differences across an extended target. The end product of a thermal imager system is typically an image displayed on a video monitor.

The discussion of performance of a thermal imaging system will be in terms of the detector D^* (pronounced as Dee Star), which is normalized detectivity.

The simple block diagram of FLIR below will be useful in discussion of the operation of the scanning imager.

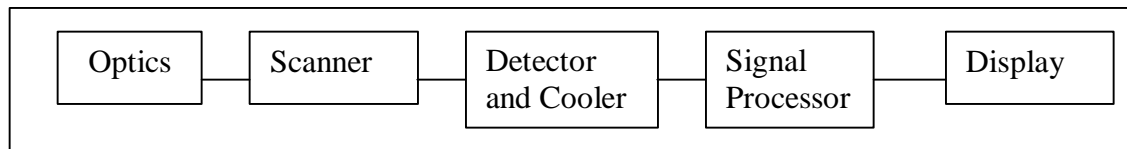


Figure 4.9. Simple FLIR Block Diagram “After Ref. 20”.

The FLIR is capable of detecting infrared radiation that is emitted from target and background objects in the scene. FLIRs are generally used in the 3-5 μm and 8-12 μm wavelength range, because TV techniques are not operable in that region due to detector limitations. The SNR for FLIRs is much lower than that of TV because the sampling time for each pixel is short for FLIRs but long for the TV storage detectors [Ref. 20].

In a detailed design of a FLIR system, many choices are available. Any of the components in the block diagram above might be missing in any system. In other words, the analysis will work well whether there is one scanning detector or a focal plane array and detector, whether the scanner is a serial or a parallel type and so-on. The only element that has to be present in every system is the human observer, because the system performance is based on the signal characteristics of the brain-eye complex.

The optics focuses the infrared radiation, which has been collected from the scene, on to the detector array. The scanner moves the image of the scene over the detectors to be able to make each part of the FOV seen by one or more detectors. The detectors convert the scene radiation to electric signals. If using more than one detector is

desired, then a multiplexer may be added to combine the detector outputs into a single video output.

A generic FLIR uses an opto-mechanical scanning technique, and senses the thermal radiation emitted by the scene viewed. Real time scanning is necessary to avoid flicker. The human eye requires a minimum frame rate of 30 frame/second. Opto-mechanical scanning is accomplished by some moving optical elements, such as a lens, mirror, prism, and etc. To be able to achieve two-dimensional scan, two orthogonal scanning movements are required. In the early generations of FLIR systems, the field was viewed by scanning the small elements of the scene across a single small detector or small number of detectors. For this case, the performance of the imager was limited by the speed of the detector. The scene is then scanned in a sequential array or raster of picture elements, from which a sequential electrical signal carries the picture information [Ref. 20].

FLIR systems detect and display the radiance distribution, typically due to the temperature distribution, of the scene being observed. An object can be detected against its background by temperature difference or emissivity difference from its background. Scene objects are typically at around 300 K or above. Therefore, systems are required to detect very small radiance differences above background. For the detection case, the Minimum Detectable Temperature Difference (MDTD) is a critical performance parameter. But for recognition and identification, the Minimum Resolvable Temperature Difference (MRTD) would be a more appropriate parameter for the performance measure. These performance parameters will be explained in the next section.

The major tasks that the FLIR systems are asked to perform are target detection, classification, identification and tracking. Optimizing the system to perform these tasks might be very difficult. First of all, it has to be considered that the observed scene is imaged as an array of picture elements. Each of these picture elements has a single brightness value. Then the target and the background are considered as a mosaic of white and gray squares. The size of these squares is determined by the resolution of the system. The range to the target is directly related to the size of the image on the screen. Thus the number of the picture elements in the image depends on the range.

The detection criterion requires that at least one picture element has to be significantly brighter than the background. To satisfy this criterion the SNR of the detectors should be optimized, which will lead to the analysis to the optimization of the range for detection. The simplest performance measure for detection is Noise Equivalent Temperature Difference (NETD). This is the Apparent Temperature Difference, which gives an SNR of 1 at the detector electronics output. This SNR does not ensure detection by an operator. Including the eye/brain perception threshold gives the Minimum Detectable Temperature Difference (MDTD), which is defined as the minimum temperature difference required for detection by a human operator for a uniform temperature target in a big uniform background.

Detection by a human operator involves the discrimination of detail on the target. The criterion assigned based on experience is the discrimination of 1.5 pairs of resolution elements (pixels) on the "critical dimension" of the target.

For classification, the criterion is based on the detectable detail in the image of the target. The image must show enough detail to discern the class or type of the target,

which requires a minimum number of resolvable picture elements on the target. Classification depends on the resolution and the sensitivity of the system. The performance parameter for classification is the Minimum Resolvable Temperature Difference (MRTD), a function of the resolvable spatial frequency on the target image.

For identification, a larger number of pixels, which gives a greater level of detail, is required on the image. The identification also depends on the operator. Therefore a number of tests are run, with a large number of operators, to determine the number of picture elements required for an average operator to identify the target. MRTD contains some subjective quantities determined only statistically [Ref. 20].

E. FLIR SYSTEM PERFORMANCE PARAMETERS

The parameters that are used to determine MRTD and MDTT are called physical parameters. They relate to engineering design features of the sensor. The following section describes these physical parameters.

1. Physical Parameters

a. Field of View (FOV)

The FOV of an IR system is one of the most important design parameters, which is defined as the angular space from which the system accepts light. The system FOV (radians²) and the distance (or range) from the sensor to object determine the area that a system will image [Ref. 21].

A large FOV allows the sensor to view a larger area. This results in a lower resolution since the detector elements are spread over a larger area. When the FOV is narrowed, then the resolution increases, but it gets difficult to find objects over a large area. The solution is to have two or more FOVs. Generally military applications have 3

FOVs. Wide Field of View (WFOV) for detection, Medium Field of View (MFOV) for recognition and Narrow Field of View (NFOV) for positive identification are the most common ones. TSS has an additional field of view, Very Narrow Field of View (VNFOV), that increases the probability of positive identification.

b. Detector Angular Subtense (DAS)

DAS is used to describe the resolution limitations of the detector size. There are two DASs: a horizontal DAS (radians), which is the detector width divided by the effective focal length of the optics, and a vertical DAS, the detector height divided by focal length. The DAS describes the very best resolution that can be achieved by an I²R system due to detector size limitations [Ref. 21].

c. Instantaneous Field of View (IFOV)

IFOV can be defined as the angular cone in which the detector senses radiation. It is an optical design parameter and it includes both the DAS and the optical blur diameter. If the optical blur is negligible, very small compared to DAS, then the IFOV and DAS are approximately equal [Ref. 25].

d. Modulation Transfer Function (MTF)

MTF is a primary parameter used for system design, analysis and specifications and describes the imaging resolution of the sensor. It is a primary measure of the overall system resolution. The system MTF is the transfer function of input spatial frequencies and is considered separable in horizontal and vertical directions. MTF is the magnitude of the complex-valued optical transfer function (OTF). Holst [Ref.25] formulates it as the output modulation produced by the system divided by the input modulation at that spatial frequency:

$$\text{MTF} = \frac{\text{OUTPUT MODULATION}}{\text{INPUT MODULATION}} \quad (4.18)$$

2. Noise Equivalent Temperature Difference (NETD)

NETD is a sensitivity parameter for an IR system. Driggers [Ref. 25] defines it as the target-to-background temperature difference in a standard test pattern that produces SNR of unity at the output of a reference filter. It is described as the ability of a system to detect small signals in noise. However, NETD does not account for the spatial and temporal integration effects of the eye. In performance predictions, NETD is used as an intermediate sensitivity parameter for the simplification of formulations of performance parameters such as MRTD and MDTD, which are more directly relatable to FLIR performance [Ref. 23].

Shumaker [Ref. 27] formulates NETD as:

$$\text{NETD} = \frac{20f (\text{FOV}_x \text{FOV}_y F_r N_{os} N_{ss})^{1/2}}{\tau_o (\pi N_D \eta_{sc})^{1/2} D^2 \Delta x \Delta y D^* \delta N / \delta T} \quad (4.19)$$

where:

f is the focal length

FOV_x is the in-scan (horizontal) field-of-view in mRad.

FOV_y is the cross-scan (vertical) field-of-view in mRad.

F_r is the frame rate.

N_{os} is the over scan ratio.

N_{ss} is the serial scan ratio.

N_D is the number of detectors.

η_{sc} is the scan efficiency.

D is the aperture diameter in meters

Δx is the in-scan detector angular subtense in mRad.

Δy is the cross-scan detector angular subtense in mRad.

D^* is the band average detectivity (dee star) in $\text{cm-Hz}^{1/2}/\text{W}$.

$\delta N/\delta T$ is the derivative of Planck's Law (Thermal Gradient) in $\text{W-cm}^{-2}\text{K}^{-1}\text{Sr}^{-1}$

NETD is dependent on focal length, detector size, FOV, etc. None of these parameters can be altered without secondary impact.

3. Minimum Detectable Temperature Difference (MDTD)

MDTD of a FLIR system gives the temperature difference between an isolated uniform square and a uniform background that renders the square just detectable, as a function of the size of the square [Ref. 27]. The measurement of MDTD (often called MDT) is subjective since the judgment of a human observer is involved in the process. MDTD is given by the following equation in Shumaker [Ref. 23]:

$$\text{MDT (v)} = \frac{\text{SNRT (NET)}(\Omega_T + r_s^2)(\Delta x \Delta y)^{1/2}}{\Omega_T [\pi/4(r_s^2 + r_B^2 + \Omega_T) t_e F_r N_{os} N_{ss}]^{1/2}} \quad (4.20)$$

where:

SNRT is the experimentally determined, perceived signal-to-noise ratio threshold for detection.

NET is the noise equivalent temperature difference.

Ω_T is the solid angular subtense of the target (mRad)²

r_s is the resolution of the system that includes the front-end resolution and back-end resolution

Δx is the in-scan detector angular subtense in mRad.

Δy	is the cross-scan detector angular subtense in mRad.
r_B	is the resolution of the back-end that includes the detector electronics resolution, preamp resolution, resolution of the multiplexer, resolution of the display, resolution of the eye, and the resolution due to image motion (mRad).
t_e	is the eye integration time.
F_r	is the system frame rate.
N_{os}	is the over scan ratio.
N_{ss}	is the serial scan ratio.

In the observation process, the observer is assumed to know the target location approximately.

MDT does not have a first-order dependence on MTF, thus it does not show asymptotic behavior, as found in MRTD.

4. Minimum Resolvable Temperature Difference (MRTD)

The final performance parameter of the thermal imager systems is determined by the combination of both spatial resolution and thermal sensitivity. The MRTD (also called MRT) combines spatial resolution and thermal sensitivity. It is the most used and useful FLIR specification parameter. It is useful as a summary measure of performance and a design criterion.

MRTD is defined as the temperature difference required between bars and spaces of a test target, a set of four standard bars with an aspect ratio of 7:1, so that the bars can be discerned by a trained observer with an unlimited viewing time [Ref. 28]. It answers the question “What temperature difference is required for various-sized bar targets to be

visible on the display?” and provides sensor sensitivity as a function of four-bar target frequency. The idea here is that the detection, recognition and identification criteria of a target can be given in terms of a four-bar target spatial frequency. The sensor performance is then determined by the combination of the target characteristics and the sensor response.

The derivation of MRT requires a number of assumptions along with those included in NETD. These are [Ref. 21]:

- The eye integration time can be approximated between 0.1 and 0.2 sec.
- The effects of spatial filtering in the eye for the display of a periodic square bar target of frequency f_T can be approximated by a matched filter for a single bar at $H(\xi) = \text{sinc}(\xi/2f_T)$.
- The electronic processing and monitor are assumed noiseless.
- The system can be considered as an LSI system, where the spatial frequency transfer can be described by the system MTF.

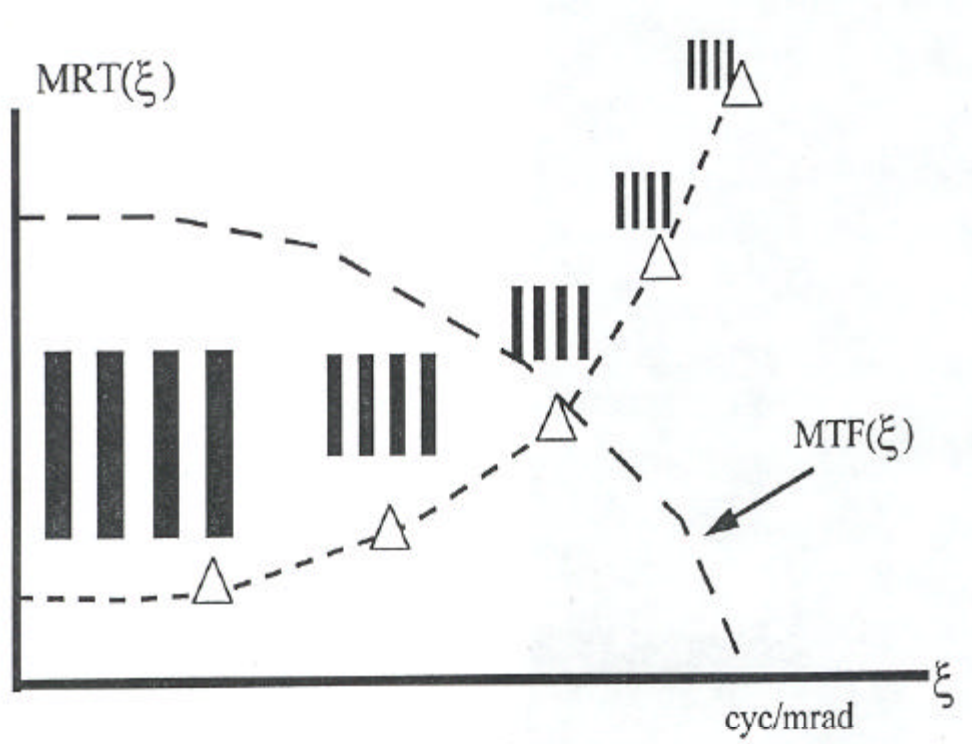


Figure 4.10. Typical MRT Curve “From Ref. 21”.

Since MRT includes the effects of the display and the human observer, it is a good end-to-end system measure, but inconsistencies and variabilities of the human observer make it difficult to get quantitative measurements. Figure 4.10 illustrates an MRT curve. It can easily be seen that the required temperature difference to resolve the four-bar target increases as the size of the bar-target becomes smaller.

There are several alternative expressions for MRTD that have been proposed by different authors. Shumaker [Ref. 23] gives the following equation for the calculation of MRTD:

$$\text{MRT}(\nu) = \frac{2\text{SNRT}(\text{NET}) \nu_x^{1/2} (\nu^2 \Delta x \Delta y)^{1/2}}{\text{MTF}_s(\nu) L^{1/2} (t_e F_r N_{os} N_{ss})^{1/2}} \quad (4.21)$$

where:

$\text{MRT}(\nu)$ is the value of minimum resolvable temperature at spatial frequency ν .

SNRT is the experimentally determined signal-to-noise ratio threshold.

NET is the noise equivalent temperature difference.

ν_x is the noise filter factor

$\text{MTF}_s(\nu)$ is the system MTF at spatial frequency ν .

ν is the spatial frequency.

Δx is the in-scan detector angular subtense in mRad.

Δy is the cross-scan detector angular subtense in mRad.

L is the length-to-width ratio of the MRT bar-always 7.

t_e is the eye integration time

F_r is the system frame rate.

N_{os} is the over scan ratio.

N_{ss} is the serial scan ratio.

F. GENERAL CHARACTERISTICS OF FLIR SYSTEMS

In defining operational performance criteria and parameters for FLIR systems, there are three categories in which we can group a FLIR system. A FLIR system can be categorized in terms of the generation (1st generation, 2nd generation and so on) it represents, or the array type (scanning or staring) it has, or the choice of waveband (3-5 or 8-12 μ m) it uses. In this section, the categorization of the FLIR systems will be explained in detail.

1. Generations of FLIR Systems

In this thesis, we will look into the 2nd generation and the self-styled 3rd generation FLIR systems. The 2nd generation FLIR systems are called Common Module II, based mostly on the Standard Advanced Detector Assembly (SADA) development program. They are well defined and patented. However, U.S. Army definitions differ from the way that some members of industry define them. Especially for the 3rd generation FLIR systems, there is no Common Module nor a global definition. Some members of industry define "3rd generation" FLIR as the technology of staring array detectors that operate in the MWIR spectral region, such as Lockheed Martin's Hawkeye XR Target Sight System. But the U.S. Army, on the other hand, defines a technology as 3rd generation because it provides a significant leap in performance and capability. The technology that the Army defines as 3rd generation is not expected to be patented for another five or ten years. In this thesis the definitions of the Army's Night Vision and

Electronics Directorate (NVESD) will be used for both 2nd generation and 3rd generation FLIR systems. The Army's definition for 2nd generation FLIR is either scanning or staring array that can operate in either 3-5mm (midwave) or 8-12mm (longwave) wavelengths [Ref. 28]. Based on these definitions, the distinction between the 2nd generation and the 3rd generation FLIR systems are presented in Table 4.4 [Ref. 28]. In this thesis current generation scanning and staring systems are compared.

2 nd GEN FLIR	3 rd GEN FLIR
<ul style="list-style-type: none"> • DIGITAL SIGNAL PROCESSING • ON-TURRET PROCESSING • ON-CHIP MULTIPLEXING 	<ul style="list-style-type: none"> • DIGITAL SIGNAL PROCESSING • INCREASED ON-CHIP PROCESSING; FUNCTIONS INCLUDE: <ul style="list-style-type: none"> • Analog/Digital Conversion • Image Processing for ATRs • Initial gain and level correction
<ul style="list-style-type: none"> • EITHER STARING OR SCANNING <ul style="list-style-type: none"> • 3-5 micron InSb or HgCdTe • 8-12 micron HgCdTe • MEDIUM FORMAT FOCAL PLANE ARRAY (480 VERTICAL DETECTORS) 	<ul style="list-style-type: none"> • "MULTICOLOR" - EITHER HYPER-SPECTRAL OR MULTI-SPECTRAL • SINGLE FPA FOR ALL IR REGIONS • VERY LARGE FPA (> or = 1200x1200)
<p><u>SCHEDULE:</u></p> <ul style="list-style-type: none"> • 3-5 micron InSb:EMD for V-22 • SADA II: LRIP • SADA I: Experimental prototype 	<p><u>SCHEDULE:</u></p> <ul style="list-style-type: none"> • Experimental prototype to NVESD for testing in 5-10 years • LRIP: 12 years

Table 4.4. Distinction Between the FLIR Generations "From Ref. 28".

2. Scanning versus Staring Systems

FLIR systems are divided into two broad categories in terms of the array configuration they have: scanning and staring arrays. Scanning systems are further divided into two subcategories of serial and parallel scanning.

a. Staring Systems

A staring array uses a two-dimensional detector configuration. The image plane is filled with detectors. No scanning is required, although some type of periodic shuttering may be used for gain-and-level correction. Staring systems offer much greater potential of having high sensitivity than the scanning systems, because of their longer integration times. Large integration times reduce the NETD values. The trade-off for high sensitivity is low resolution caused by spacing limitation of the detector elements in both vertical and horizontal directions.

b. Scanning Systems

The detector array for a scanning system may be a linear array or a single detector. For a single detector system, a two-dimensional scanner moves the image across the detector in both the vertical and horizontal directions. In a linear array, a scanner moves the image formed by the optics across the detectors. Since the detectors are distributed evenly over the image, the image can be represented spatially. Table 4.5 exhibits the array configurations and scanning types.

Configuration	Single Element	Linear Array	2D Array
Serial Scanning	X	X	
Parallel Scanning		X	X
Staring			X

Table 4.5. Detector Array Configurations “From Ref. 21”.

A serial scan system consists of a linear array of one or more detector elements. “The elements are aligned horizontally and scanned sequentially in a two-dimensional rectilinear raster pattern, from upper left corner to lower right corner, to form an image” [Ref. 21]. A two-axis scanner is required to produce an image. If there is a number of adjacent detectors along the same scan line in any array format, the output of

the adjacent detectors are summed by time-delay-integration (TDI). Because they all lie along the same horizontal line, they all sample the same object point sequentially in time. These images are temporally displaced; to overcome this, time delay integration is used. Each detector output is delayed by one scan time unit from the one before. Then the resulting outputs are added together. While the signal from each element is added linearly, the noise adds as root mean square (rms). This technique improves the SNR by a factor equal to the square root of the number of detectors along the same horizontal line.

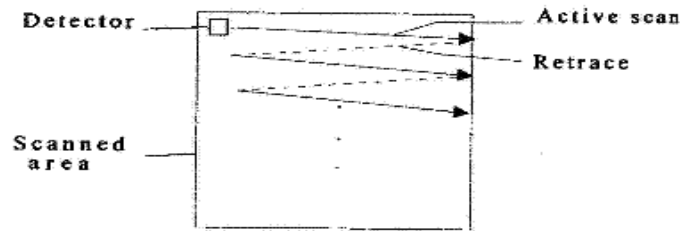


Figure 4.11. Serial Scanning “From Ref. 21”.

A parallel scan system, on the other hand, consists of a linear array of contiguous detectors that are orthogonal to the scan direction. This linear array may have one or more columns in the horizontal direction and has a sufficient number of detectors in the vertical direction to cover the desired FOV entirely. This requires only a one-dimensional scan, which is usually horizontal. There are three primary types of parallel scan configurations. These configurations are shown by Driggers [Ref. 21] as in Figure 4.12.

In Figure 4.12 (a), there is a linear array of N detectors and while the detectors are sampled, the image is scanned horizontally across this array. After the first scan is completed, the scanner is tilted slightly in the vertical direction and the image is scanned across the detector array in the opposite direction. The scan in the opposite

direction provides coverage in the region of the image plane that is not covered in the first scan. The frame formed by the two scans (fields) represents a complete image. The frame rate for this kind of system is 30 Hz. This configuration is used in the first generation Common Module FLIR systems developed by the U.S. military. Figure 4.12 (b), is similar to 4.12 (a) with an addition of TDI. Two or more detectors are sampled in the in-scan direction at the same positions to achieve TDI. The signal adds directly while the noise adds in rms fashion providing a SNR improvement of square root of the number of TDI detectors. Figure 4.12 (c) has a staggered array of detectors together with TDI. With this technique, the entire image plane can be covered with a single scan. Since the number of detector elements in the vertical FOV is increased, there are redundant sample points.

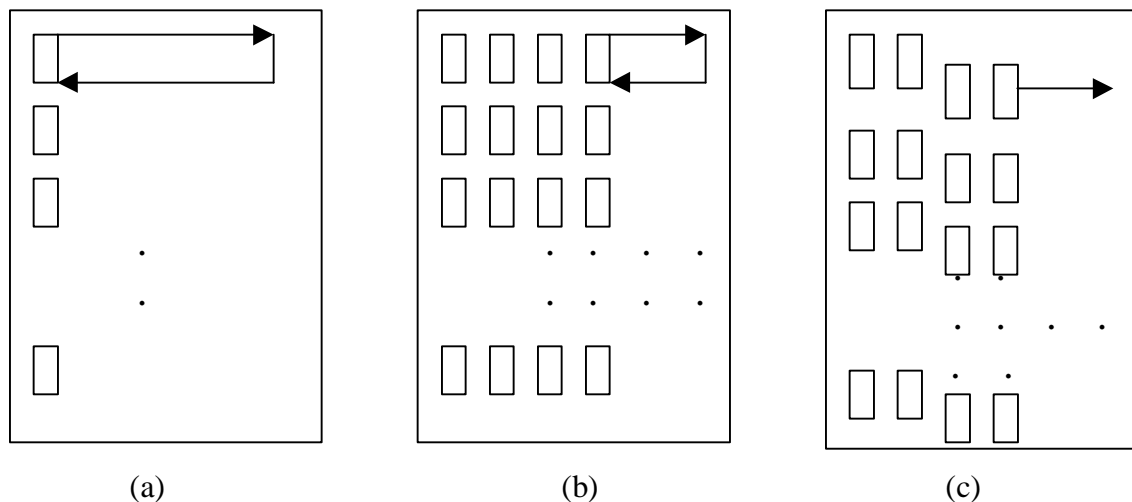


Figure 4.12. Parallel Scan Configurations (a) Bidirectional interlaced scan; (b) bidirectional interlaced scan with TDI; (c) unidirectional scan with TDI “From Ref. 21”.

c. Scanning Versus Staring Performance

There are two major considerations in the evaluation of staring versus scanning systems performance. These considerations are sensitivity and resolution. Staring systems have longer integration times that provide improved sensitivity. Since the

detectors in a staring system can stay at one position, they are not shared with multiple points in the image space and can absorb photons for as long as a frame time. In practice, the detector saturates (fills with electrons) in less than a frame time and sensitivity is limited by pattern noise. A sensor's capacity to reject the background clutter is highly associated with sensitivity. Generally, staring systems are better in detecting dim targets [Ref. 21].

The second major consideration is resolution. Driggers states that: "The sampling frequency of a sensor should be twice that of the sensor cutoff frequency". This can be achieved in scanning systems by sampling at smaller angular intervals than the detector angular subtense. It is not possible in staring systems. Therefore, staring systems are forced to be undersampled. The scanning systems have a resolution capacity higher than the staring systems if their detector angular subtenses are the same. Table 4.6 summarizes the basic differences of staring and scanning systems [Ref. 21].

Scanning Sensors	Staring Sensors
Wide Field of View	Improved sensitivity due to longer integration time
Signal conditioning necessary to process TDI	FOV limited to array size
Optics must accommodate scanner	Simpler optical design
Scanner increases size and reduces reliability	No moving parts, more reliable
Requires line-to-line equalization	Requires individual detector non-uniformity correction
High resolution in scan direction	

Table 4.6. Summary of the Scanning and Staring System Differences "From Ref. 21".

3. Wavelength Issues

The analysis of an imaging system for a given purpose includes performance indicators that are strong functions of wavelength. The transmission of light through an imaging sensor is a function of wavelength. The reflectivity and transmission characteristics of the optical sensor are highly wavelength dependent. Finally, the conversion of photons to electrons by detectors is a strong function of wavelength.

The question of “What is the optimum waveband for an infrared sensor: 3-5 μ m or 8-12 μ m?” has been studied for years and it has been an issue in the community as to whether the midwave (3-5 μ m) or the longwave (8-12 μ m) is a better sensor for a given application. The results of the studies to evaluate the relative performance of 3-5 μ m and 8-12 μ m are often conflicting. The conclusions are highly dependent upon the atmospheric transmission model employed, the target type to be detected, the detector and system technology and the particular path type chosen. In Ref. 30, it is stated that:

On the basis of a modified version of the LOWTRAN6 model, an absolute comparison is made of typical and background limited IR sensors operating in the 3-5 μ m and 8-12 μ m wavebands in a tropical maritime environment. Allowance is made for slant paths and a variety of targets and backgrounds including hot targets and backgrounds spectrally different from the targets. It is found that with current technology the 8-12 μ m waveband is superior for all except very hot targets at long ranges. The validity of various approximations is also investigated, and in particular it is found that the blackbody composite background approximation should not be used for slant paths.

As a general approach, if the FOVs are comparable for the midwave and the longwave sensors, the probability of recognition as a function of range can be used as a measure for comparison. Driggers [Ref. 21] lists the following guidelines for rough comparisons:

a. Target Consideration

The equivalent radiance difference for most terrestrial objects, with a few degrees target to background temperature difference and a 300 K degrees background temperature, can be 20 times greater in the longwave than in the midwave. Sources at 300 K peak around 10 μ m. For the high temperature of an aircraft exhaust, on the other hand, the midwave is superior at all ranges. The radiance difference with a cold sky background is around 4 or 5 times greater in the midwave than in the longwave.

b. Atmospheric Consideration

Atmospherics are extremely complicated and there are several codes used for prediction of atmospherics. Longwave IR propagates through cold, dry air much better than midwave IR; the moisture extinction of the longwave radiation is decreased because of the existing low absolute humidity. Longwave IR may have a factor of three times greater transmission than the midwave for paths of around 10 km. If there is high level of moisture in the air, such as in hot, humid or maritime environments, there is no significant difference between the longwave and the midwave transmission. Some writers state that midwave performs a little better in some maritime conditions, though. Increase in altitude results in decrease in the difference between the longwave and the midwave transmission due to decrease in both aerosol concentration and water vapor content.

As mentioned earlier, the atmospheric transmittance depends upon the amount of the aerosols, water vapor, and the molecular species present in the atmospheric path. Aerosol concentration grows by particle generation; particles may grow due to high relative humidity. MWIR is affected more than LWIR by the growth of the particle concentration. The effect of the water vapor on the LWIR region is greater than on the

MWIR region. The relationship between the visibility (shortwave scattering coefficient) and the water vapor concentration (longwave absorption) is the major factor to determine whether the MWIR transmittance is higher than the LWIR transmittance. When the aerosol concentration is low and the water vapor concentration high, the MWIR transmittance is higher [Ref. 25].

c. Detectivity Considerations

Detectivity is another significant difference in the performance comparison of midwave versus longwave sensors. For InSb detectors, the midwave advantage usually stands with a factor of 3 to 10 over longwave. This factor is not seen in midwave detectors such as PtSi, due to their low quantum efficiency.

d. Integration Time Consideration

There is a large difference in existing midwave and longwave sensor integration times. The reason is that most current midwave sensors use staring arrays and the available advanced longwave sensor includes 2nd generation scanners. Scanners have smaller integration times where staring arrays have much longer integration times. Driggers [Ref.21] states that “With 400 to 600 horizontal samples (with both sensors) and a four-detector TDI, staring array can give a factor of 10 to 13 times the performance as that of the second generation scanner”. This is a rough estimate, but it can be calculated easily. For a scanner with 600 horizontal pixels and four-detector TDI, the integration time is equal to, $\tau_i = (1/30) \times 4/600$. For staring array, if we assume integration time being 1/30 seconds, then the ratio of the integration times becomes 600/4. Since SNR is proportional to the square root of the ratio of the integration times, then the effect of integration time to SNR can be found as a factor of approximately 12. The integration

times of staring arrays is limited by the electron well capacity that reduces the estimate to 5 to 7 times the performance.

THIS PAGE INTENTIONALLY LEFT BLANK

V. PERFORMANCE MODELS

The purpose of this chapter is to present the performance models that will be used in this thesis. Since there is no precise means of characterizing the interaction of the FLIR-observer and the real world targets, the approach of analyzing operational tasks is replaced with the analysis of idealized simple tasks that can be characterized using MRT, also called MRTD and MDT, also called MDTD. The models that are used in the prediction of MRT and MDT will be presented in this chapter. Before moving on to the models, it will be more convenient to start with a general discussion of Tactical Decision Aids (TDAs).

A. TACTICAL DECISION AIDS (TDAS)

TDAs are tools that are used in planning and performing of a task by an operator or a decision maker. They may be in various forms. The form that will be used in this thesis is that of a computer code. TDAs are designed to aid a decision maker by assimilation and convenient presentation of data and analysis of a tactical problem beyond what is feasible by humans in timely fashion [Ref. 26].

The rapid development in the technology of weapon systems makes planning of the deployment and use of these systems on the battlefield more complex. One way of accelerating the planning of the operational process is to use TDA codes that are quick and user-friendly. By doing this the desired impact on the target will be predicted. These TDA codes can also be used in the design and testing phase of a new system, but are usually more simplified and less precise than codes used for design.

These models must be coupled through a relationship between apparent signature of real target and that of a standard target.

The next section will cover the FLIR92 model that will be used in this thesis to design and calculate the performance parameters, such as MRTD and MDTD. It should be noted that, for specifying a detection decision the Johnson criteria will be applied, when necessary, in this thesis. The Johnson Criteria forms the connection between the real target and the sensor MRT performance. They are expressed as the required number of resolvable spatial cycles (pairs of pixels) on the critical dimension of the defined discrimination task.

B. FLIR92 THERMAL IMAGING SYSTEM PERFORMANCE MODEL

FLIR92 is a desktop computer model that runs on MS-DOS compatible PCs and UNIX workstations. It is a system evaluation tool that uses basic sensor parameters to predict overall system performance. The model calculates MTF, NETD, MRTD, and MDTD by using basic system-level parameters. The principal stated function of the model is to predict if a system achieves the required MTF, system noise, MRTD, and MDTD that are necessary to perform a target acquisition and discrimination task [Ref.27]. The application of FLIR92 in this thesis is to define the performance parameters of the generic scanning and staring sensors to be compared.

FLIR92 models parallel scan, serial scan, and staring thermal imagers that operate in the mid-wave and long-wave infrared spectral band. It can only be used for thermal imagers and cannot be used for predicting the performance of any other electro-optical sensor. It does not predict range performance. The two different outputs of FLIR92 are MDTD, which is commonly used for detection, and MRTD, which is commonly used for

identification and also for detection. Based on these outputs, acquisition and discrimination decisions can be made respectively.

FLIR92 calculates an MTF for each system component and then multiplies them together to get the total system MTF. This is achieved by using linear filter theory. It includes generic MTFs for common system components and for additional components it allows the user to specify their MTFs.

"Thermal imaging systems are assumed to be well designed, so those image artifacts due to under-sampling do not significantly degrade the system. For this reason, FLIR92 ignores signal and noise aliasing in the MRTD and MDTD predictions. The model is implemented with enough flexibility to accommodate most system designs through user-determined pre- and post-sampling MTFs. Additionally; MRTD is not predicted at spatial frequencies exceeding the Nyquist frequency" [Ref.27].

FLIR92 defines the system noise in three-dimensional manner (temporal, horizontal spatial, vertical spatial). The model calculates the random spatio-temporal noise. The measuring port where the 3-D noise measurement made is located at a video port prior to the system display. The results of the 3-D noise measurements are inserted to the spatio-temporal noise calculations.

Although FLIR92 is called two-dimensional, it is actually a two-directional model. The threshold is predicted along the two orthogonal axes, taken as the horizontal and vertical directions. FLIR92 calculates MRTD in either direction depending on the orientation of the standard four-bar target. Resolution in any other direction, such as 45 degrees, is not used. If FLIR92 is used with the Johnson criteria, then it is probably better at predicting the range for rectangular objects whose edges are aligned with the thermal imaging system's orthogonal axes. For the case of non-rectangular objects or high aspect ratio targets, such as aircraft, ships, bridges, etc., the model is probably less accurate.

MRTD depends directly on the system transfer function, which is represented by the overall MTF of the system, and the system sensitivity, which is described by NETD. “Currently, MRTD is the best overall performance indicator of the thermal imagers” [Ref.31]. To predict MRTD and MDTD, the spatial integration of the eye/brain system must be modeled. FLIR92 uses a synchronous integrator model to approximate the eye/brain spatial integration. With this method, the eye/brain is assumed to be integrated spatially over the image of a bar. Blurring of the target caused by the finite apertures of the target is ignored. "For periodic targets, the matched filter and the synchronous integrator yield equivalent results" [Ref.27]. For the case of the synchronous method, the algorithm required to implement it is simpler than the matched filter algorithm. With the synchronous model, the eye integrates over an angular region defined by the target edges. However, FLIR92 bases MDTD predictions on the matched filter concept, in which the eye/brain filter is matched to the signal in order to maximize the signal to noise ratio.

Since MDTD is not strongly dependent on the system transfer function, it is not considered as a strong indicator of thermal imager performance. “MDTD is useful for specialized applications where point source detection is required, such as targets against uniform backgrounds, and, in some cases, moving targets” [Ref. 27].

The MRTD and MDTD predictions are made under reasonably controlled laboratory conditions, and they are just an attempt to model subjective human performance. If the sensor is assumed to be properly and accurately characterized, then the modeled MRTD and MDTD can be expected to reasonably represent laboratory measurements made by trained and practiced observers, even though the synchronous integrator and matched filter are rough approximations to the human visual processing

system. “The model’s MRTD prediction is validated for first and second generation scanning systems and for staring systems. The MDTD prediction is not validated for modern systems as of November 1992” [Ref. 27].

C. TARGET ACQUISITION AND WEATHER SOFTWARE (TAWS)

Target Acquisition and Weather Software is a scenario-based field performance tool that runs in Windows compatible environments. It was developed by the Air Force Research Laboratory with the assistance of Naval Research Laboratory, Monterey, SPAWAR System Center, San Diego, and the Army Research Laboratory, Adelphi MD. It can predict the performance of electro-optical weapon systems, such as TV working in the visible (0.4-0.9 micrometer), night vision goggles (NVG) working in the near infrared (0.7-2 micrometers), FLIR devices working in the middle infrared or far infrared (3-5 or 8-12 micrometer), and laser (1.06 micrometer) wavelength regions of the optical spectrum.

Target Acquisition Analysis in TAWS involves the computation of detection or lock-on range for a particular target at a particular location under specified weather conditions. It gives the capability of making either a Single Point-Based or Multiple Map-Based Target Acquisition Analysis.

TAWS program consists of three models:

- Target Model, which converts the radiance difference between the inherent signals emitted from the target and the background into a temperature difference (ΔT , ΔT) at zero range.
- Atmospheric Model, which is the part that calculates the apparent ΔT (ΔT_{app}), by estimating the extinction of the signal in the atmosphere, at the entrance aperture of the sensor.
- Sensor Model, which gives the sensor performance in terms of MRTD and/or MDTD as a function of spatial frequency. This part determines the detection range when applied to apparent target signature.

1. Target Model

Target model consists of tactical and environmental information about the target and the background for the analysis. This information includes the specific target type for both moving and stationary targets, target location, time over target, and background characteristics. It calculates the strength of the thermal signal at zero range using target and background characteristics entered by the user. The radiance difference between the target and background is converted to an equivalent blackbody temperature difference via the thermal models.

TAWS Version 2 supports two IR target contrast models: the new Multi-Service Electro-optics Signature (MuSES) model and the older Target Contrast Model #2 (TCM2). The fundamental difference between TCM2 and MuSES is that the former is a simple 1-D solver (that only allowed conduction through the thickness of the material) while MuSES is a full 3-D solver, which includes lateral heat transfer. Because MuSES is a more sophisticated model than the TCM2 model and performs many more calculations, the time required for a MuSES model run is significantly longer than a TCM2 run. TAWS will determine which model to run based on the target or targets selected for analysis.

TAWS Version 2 includes 20 moving and 23 stationary targets in its target menu, containing rotary and fixed wing aircraft, land vehicles, buildings, radars, and naval ships etc. Heading, operating state, and speed of the target provide the necessary input for the thermal models to calculate the internal heat sources as well as the surface heating and cooling. Target operating state gives information about the heat interaction with the environment, and the surface heating of the target, as the target heading affects the

perceptible solar heating on the target. The movement of the target, represented by its speed and the wind speed, provides a cooling effect on the target.

The backgrounds in the model are grouped under two major categories, as “general backgrounds” and “specific backgrounds”. The general background option offers five subcategories: continental, urban, desert, ocean, and snow. It describes the dominant terrain features of the target area, which gives the information used to calculate the solar reflection by the model. Specific backgrounds, the immediate area surrounding the target, have eight different options: vegetation, soil, snow, water, concrete, asphalt, swamp and rocky field. These immediate backgrounds are further described by the composition, coverage or depth. The background used in this thesis is soil with two different compositions of average and clay. Average represents the urban area and clay represents the desert type area with no dust.

2. Transmittance Model

The transmittance model calculates the degradation of the signal through the atmospheric path from the target to the sensor. TAWS uses a two-layer model, which calculates two extinction coefficients for below and above the boundary layer height. A weighted average of transmission is used for sensors above the boundary layer. TAWS aerosol model includes the LOWTRAN models; rural, urban, maritime, tropospheric, desert, and navy maritime. Desert and urban models, which are used in this thesis, describe aerosols found in the boundary layer of desert and urban environments respectively.

Meteorological data are input by the user. The following parameters of the model are inserted on an hourly basis: temperature, surface dew point temperature, aerosols,

battlefield induced contaminants (BICs), visibility, rain rate, wind speed and direction, boundary layer height, low, middle and high cloud data. The temperature and dew point are used to compute the relative humidity. Then relative humidity, aerosol and visibility parameters are used to calculate the absolute humidity and an extinction coefficient.

3. Sensor Performance Model

The sensor performance model evaluates the range at which the signal received by the sensor equals the threshold value for detection. The target apparent size (angular subtense) as viewed from the sensor determines this threshold value as where the angular subtense is equal to the critical dimension of the target divided by the range to sensor.

TAWS supplies the user with a number of sensor data files identified by the letters SNS followed by a unique 4-digit index, such as SnsXXXX. The user selects the sensor from the sensor list. The program offers two kinds of IDs. There are a number of sensor IDs reserved for the supplied sensors and additional IDs for user-defined sensors. User-defined sensor files used in the program may be generated using an unpublished Microsoft Excel program, provided by Dr. A.Goroch, NRL, Monterey, and copied in Notepad. These files are then saved under the Data folder. Based on the FOVs of the sensors there are at least 2 files under the same sensor name. For a typical sensor 1003 that has wide and narrow FOVs the data files are SNS1003.nam, SNS1003w.dat, and SNS1003n.dat. The identification of these sensors included is not available to the users.

In this thesis two different user-defined sensors are used, one for the Scanning Longwave Sensor and one for the Staring Midwave Sensor. Since the real physical parameters of these sensors are proprietary and are not released, basic sensor parameters found in the literature are used to generate the sensor models. Especially for the scanning

longwave sensor, the available parameters were the FOVs and the array dimensions. The other parameters were taken from the published SADA II scanning focal plane array sensor data. For the staring midwave sensor the only parameter not given was the detector dimension and it is assigned a value using the basic staring sensor parameters.

4. Output Files

TAWS displays the outputs in two different formats that can be selected via the main menu window. Graphic and tabular outputs are created automatically after each run. Graphic output includes the ranges according to different viewing angles, ranges at different times for a fixed viewing angle, target temperatures and delta T values. Tabular outputs are not used in this thesis. TAWS gives maximum range predictions for detection and lock-on, for both Wide and Narrow FOVs. Only detection ranges are useful to this comparison.

THIS PAGE INTENTIONALLY LEFT BLANK

VI. COMPUTATIONS AND RESULTS

A. SCENARIO INPUT PARAMETERS

Two different scenario parameters are chosen to represent a desert environment and an urban area with a high rain rate. These parameters are utilized to reach the ultimate goal of this thesis; that is to make range predictions on a given thermal imaging system or make comparisons between two thermal imaging systems in a given scenario.

The target was chosen to be “T-80 U/B Tank”, which is one of the targets in the TAWS target look-up table, moving at a speed of 20 miles/hour. The atmospheric data were chosen to fit the properties of a typical operational environment of a target in the probable operational area of the AH-1Z KingCobra. An atmospheric data set collected from the Southeast border of Turkey was selected for desert conditions and from Istanbul for urban conditions. The meteorological data is obtained from the following web site:

< http://www.wunderground.com/country/TU_VS.html >

The published parameters of the SADA II Focal Plane Array (FPA) system were used to build a 2nd generation scanning longwave FLIR sensor model, which is assumed to represent the Aselsan ASELFLIR-300T, using the FLIR92 model. For the Lockheed Martin staring midwave FLIR sensor, most of the physical parameters are taken from the USMC’s Light/Attack Helicopter Upgrade Program briefing [Ref.10]. The remaining input data required by the FLIR92 model were gathered from the textbook by Driggers [Ref.21] on 2nd generation scanning sensors and calculated for the staring midwave sensor. The data set was used as input data to the FLIR92 model to obtain NETD, IFOV, MRTD and MDT outputs. These outputs are used as inputs to TAWS user-defined sensor model.

B. FLIR92 MODEL OUTPUTS

The sensor models were formed in Word Perfect using the input parameters included in a data file that was later saved in pure ASCII text mode. The model was run in the DOS environment for prediction of both MRTD and MDTD performance parameters. These parameters form the input for TAWS. There are 7 FLIR92 outputs containing the MRTD, MDTD, NETD and IFOV values, one for each FOV of both sensors. First the outputs of the scanning longwave sensor for Wide, Medium and Narrow FOVs are presented in Appendices A, B, and C, then the outputs of the staring midwave sensor for Wide, Medium, Narrow and Very Narrow FOVs are listed in Appendices D, E, F, and G respectively.

C. TAWS MODEL INPUTS

The TAWS model requires meteorological and tactical inputs before the model can be run. The meteorological data includes target location, surface weather characteristics at a specified time, and information about the boundary layer along with cloud data.

The tactical information includes the inputs for sensor, target and backgrounds. The main screen can be used to enter the input data by selecting and adding the user-defined sensor, target, time over target and background.

1. Target Model

The target model consists of the target and the background information. The target defines the size and the physical characteristics used in TAWS. Background data give information about general background, which is the dominant terrain feature of the target area, and the immediate area of the target.

As given in the Table 6.1, the target type selected was a T-80 U/B Tank. For discrimination of the output ranges for different viewing directions the heading was entered as zero degrees. The operating state that gives the condition of the target at time over target (TOT) was selected “Exercised”, which meant that the target was heated not only by the environment but also by the internal energy (i.e. engine operation). The scenario conditions were described for two different scenarios. The first one is a desert environment without dust. The background for this environment was selected as soil. Since the composition of the background has an effect on its heating and reflective properties, it is described as clay, as most representative of possible operating areas. The second environment is an urban area with a very high rain rate. The background was chosen as soil again and the composition was average. The reason for that, even though Istanbul is a big city, the operating area of the helicopter is not going to be the city. It is going to be the vicinity of the city. Therefore the background is chosen to be soil.

The target location and time data are also used in the target model. For time over target, the time of the day that had the average temperature for that particular day was chosen. The hourly temperatures of the day in the TAWS program are calculated by entering the minimum and maximum temperatures.

2. Transmittance Model

The weather data is entered from the main screen. The entry window offers more options that can be seen after clicking on the individual parameters. The meteorological data used in this thesis is presented in Table 6.1. The parameters that are not listed in the table are left at their default values.

The transmittance model calculates the absolute humidity based on the temperature, the dew point temperature and the relative humidity. Relative humidity can be entered by the user on an hourly basis or the TAWS program will assign the temperature of that particular time as the dew point temperature.

Input Data	Desert	Urban
Target Sensor	T-80 Tank 2 nd generation scanning longwave and staring midwave	T-80 Tank 2 nd generation scanning longwave and staring midwave
Date/time (Local)	15 Aug 2001 1800	15 Dec 2001 2100
Latitude	33 deg 33 min N	41 deg 01 min N
Longitude	44 deg 39 min E	28 deg 57 min E
Temperature (min)	24	5
Temperature (max)	43	11
Temperature (C)	33	8
Dew Point Temperature (C)	10	5-11
Sea Surface Temperature	10	5
Aerosol Model	Desert	Urban
Visibility	10 km	7-10 km
Wind Direction (degrees)	270	270
Wind Speed (KT)	10	10

Table 6.1. Scenario Input Parameters.

The visibility and the rain rate also must be assigned on an hourly basis. In this case visibility and rain rate are kept constant for the whole time period. The program was run for two different rain rates: 1mm/hour and 2mm/hour (light and heavy respectively).

3. Sensor Model

The sensor look-up table offers a numbered sensor list to the user. The user-defined sensors can be added by using the ADD button. The 2nd generation scanning longwave sensor is assigned the ID numbers SNS1500, SNS1501, and SNS1502 for WFOV, MFOV and NFOV respectively. For the staring midwave sensor the ID numbers SNS8500, SNS8501, SNS8502, SNS8503 are assigned to WFOV, MFOV, NFOV, and

VNFOV sensors respectively. Although the sensor model in the TAWS includes two FOVs, for each FOV a sensor model was generated and added to the list.

The other parameters included in the sensor model are the sensor height above the ground, viewing direction, and the scene complexity. The sensor height was entered as 2000 feet for desert conditions and 1000 feet for the urban environment along with a zero degree viewing direction. The scene complexity is described as the number of objects in the immediate vicinity of the target that can be mistaken for the targets. To keep the complexity of this analysis in a certain level this parameter was chosen as “None”.

D. TAWS MODEL OUTPUTS

The simulation was run for two different sensors in two different scenarios. After each successful run, the outputs were automatically generated. These outputs can be seen by clicking on the “View Graph” or “View Table” options. As mentioned earlier, the tabular outputs were not used in this thesis. The graphical outputs can be seen in either by the viewing angle keeping the TOT (time on target) constant or by the TOT keeping the viewing angle constant.

In this thesis, both types of the outputs were taken. First, the time on target was kept constant and the detection ranges were analyzed over view direction for each FOV of both sensors. Then, the viewing angles that provide the maximum and minimum range for each FOV were decided and the ranges are analyzed over time for those viewing angles. Finally the time history of ranges is obtained for a particular viewing angle for each FOV of each sensor.

The results of TAWS in graphical form are presented in terms of the viewing angle for the desert environmental conditions in Appendix H, Figures H.1 through H.7

and for the urban environmental conditions in Appendix I, Figures I.1 through I.4. The time history plots are presented in Appendix J, Figures J.1 through J.4 for Desert conditions and Appendix K, Figures K.1 through K.8 for Urban conditions. These results are summarized in the Table 6.2. Since the TAWS model gives just the detection ranges, the range predictions do not include recognition and identification ranges. The rain rate for the urban conditions is taken as 2mm/hour in Table 6.2 in order to predict the worse case for detection range.

		SCANNING WFOV	STARING WFOV	SCANNING NFOV	STARING NFOV
DESERT	MAX RANGE	4.6 KM	12.2 KM	27.5 KM	31.25 KM
	MIN RANGE	1.1 KM	2.5 KM	14.8 KM	22.1 KM
URBAN- WET	MAX RANGE	2.8 KM	5.6 KM	6.7 KM	9.7 KM
	MIN RANGE	0.9 KM	1.4 KM	1.9 KM	3.6 KM

Table 6.2. Detection Range Comparison Table.

VII. CONCLUSIONS AND RECOMMENDATIONS

A. CONCLUSIONS

This thesis has presented a detection range comparison of two hypothetical FLIR systems. The two systems were modeled after real FLIR systems that will be integrated on the same helicopter airframe by two different Armed Forces. The FLIR sensors that were modeled were Lockheed Martin's midwave staring Target Sight System and Aselsan's longwave scanning ASELFLIR-300T. An important issue that has to be taken into consideration is that the real physical parameters of these systems are proprietary. Because of the lack of real physical parameters, the scope of this thesis was narrowed to the comparison of two generic FLIR sensors that should show performance characteristics similar to the real sensors.

Sensor performance was modeled using the FLIR92 program. The output of the FLIR92 program was used for input into the TAWS field performance model. The TAWS program was used to compare the detection range of the two sensors under two different operational scenarios, a desert scenario and a wet, urban scenario. The scenarios selected were chosen to represent "good" and "bad" conditions in the expected geographical areas of operation. It was not confirmed that this selection did not discriminate against the LWIR (8-12 μ m) band compared to MWIR, or in favor of the staring technology compared with the scanning. The time available for the thesis research did not permit studies of sensitivity to separate parameters.

The scenarios used in this thesis are expected to represent the characteristics of the operating environment of AH-1Z KingCobra. Most of the time the operating

environment of KingCobra will be haze-free. Therefore the selection of the input data to the TAWS program did not include any set of conditions that has a visibility less than 7 km. This visibility range includes light-haze, which is the visibility range from 4-10 km.

In both scenarios the detection range performance of the MWIR staring sensor was better than the LWIR scanning sensor. It is thought that this may be attributed to the effects of humidity. In each case the calculated humidity was very high, which affects the longwave performance more significantly than the midwave performance. MWIR is less sensitive to humidity, but more sensitive to aerosols. If the operating scenarios had included higher aerosol content and lower humidity, the results may have been reversed.

The effects of the rain can be seen from the Appendix J and Appendix K. Compared to the desert conditions the performance of the both sensors is decreased by a factor of 3 or more depending on the TOT. For the scanning longwave FLIR, there is no detection between the 135-225 degrees viewing angle. This is shown in Appendix I, Figure I.1. The change in the detection ranges due to viewing angle can be explained as the apparent delta T changes with the viewing angle. If the target is seen from the back, then the temperature difference required to detect the target is high enough, because of the operating engine and the exhaust. If the target is seen from the front side then there is no significant internal energy to be detected. The only criterion is the target and the background temperature difference. In the case presented in Figure I.1, there is no detection from the front side of the target.

Besides the high humidity, rain has a "cooling effect" on the targets that decreases the temperature difference of the target and the background. If the minimum required MRTD is not present for a particular viewing angle, then no detection is possible.

For desert conditions, the detection ranges with WFOV are 2.5-4.5 km for scanning system and 6-12 km for staring midwave system. If MFOV is used then these ranges increase to 10-15 km for the scanning longwave system and 20-25 km for the staring midwave system. Generally NFOV is used for recognition and identification. The MFOV ranges allow the helicopter to detect the target before entering the battlefield for both systems. This ability decreases the susceptibility of the helicopter to detection by enemy forces. Most of the current attack helicopters carry Hellfire missiles. Maximum range of the Hellfire missile is 8 km. The detection ranges of both sensors are beyond the Hellfire's maximum range. This provides two advantages. First, it allows the pilot to avoid enemy missiles. Second, it assures that the targeting sensor does not limit the range of his missiles.

For urban conditions, even the NFOV ranges are too low to detect the target before entering the battlefield. Figures I.3 and I.4 in Appendix I show these ranges. The staring MWIR sensor gives a detection range of 10 km for a viewing angle of 0 degrees, which is the back of the target. But as mentioned earlier using NFOV for detection is not appropriate since it gets difficult to detect the targets over a larger area.

In the comparison of NFOV and VNFOV of the staring MWIR in figure H.6 and H.7 in Appendix H, NFOV has a slightly higher range than the VNFOV. This is not an intuitive result. It may be attributed to the decrease in the probability of detection with a narrower FOV. Since these ranges are detection ranges, detection with VNFOV is more difficult than detection with NFOV. If these ranges were identification ranges, then these results could be different.

B. RECOMMENDATIONS FOR FURTHER RESEARCH

The readers should not consider this thesis as a comparison of the TSS versus the ASELFLIR-300T. Due to the unavailability of complete data on the actual sensors, the comparison that was performed was one of a generic longwave scanning FLIR versus a generic midwave staring FLIR. If complete data could be obtained for both sensors, further research could make a more direct comparison based on the analysis performed for this thesis. This could be done by simply changing the input parameters to FLIR92 model and using the FLIR92 outputs to run the TAWS program for different sets of conditions. However, even given complete data several precautions should be observed.

These two sensor systems differ from each other in more than one way. The main differences include scanning versus staring array construction and the operational bandwidth, one sensor operating in the longwave infrared band and the other in the midwave. Since there are multiple variables impacting the range performance, it was impossible to determine which variable had the biggest impact on range performance. Future comparisons should examine the sensitivity to various parameters individually. Range performance depends upon many factors such as system design, the target ΔT , target size, and task to be achieved (detection, recognition and identification). Studies must include the specific sensor designs to determine which will perform better in the various scenarios.

Time constraints limited the number of operating scenarios that could be investigated. A more detailed comparison of the two sensors in more scenarios using more target types is recommended for future study.

A desirable extension of the work would be to consider the overall climatology of the area, particularly with respect to the absolute humidity and particulate content. Ranges for detection could then be evaluated in terms of time probability of availability.

In addition to that a cost-effectiveness analysis can be done, since not only the performance of the system but also the cost is a major factor in the selection of it for an aircraft.

Final recommendations concern the field performance models. First, other field performance models can be used to compare the range performance results. The ACQUIRE program is one of the codes that can be used to make comparisons with TAWS outputs. The FLIR92 output can be used to create a sensor data file for both codes. Second, the differences in the predicted ranges as shown in Chapter VI point out the need for field testing of the two sensors to determine the accuracy of the predicted detection ranges. This testing would be used to validate the field performance models and comparisons of sensors that are based on these codes.

THIS PAGE INTENTIONALLY LEFT BLANK

APPENDIX A. FLIR92 MODEL OUTPUTS FOR SCANNING SENSOR (WFOV)

U.S. Army CECOM NVESD FLIR92

Fri Mar 09 10:36:34 2001

output file: 2nd generation scanning sensor short listing for WFOV

data file: scanWFOV

command line arguments: -d scanWFOV -o scanWFOV -p BOTH -a scanWFOV

begin data file listing . . .

gen2: sample data file for 2nd generation FLIR

```

>spectral
  spectral_cut_on           7.6      microns
  spectral_cut_off         10.5      microns
  diffraction_wavelength    0.0      microns
>optics_1
  f_number                  2.0      --
  eff_focal_length          2.2231   cm
  eff_aperture_diameter     00.0     cm
  optics_blur_spot          0.0      mrad
  average_optical_trans      0.75    --
>optics_2
  HFOV:VFOV_aspect_ratio    1.33     --
  Magnification              0.0      --
  frame_rate                 30.0     Hz
  fields_per_frame           2.0      --
>detector
  horz_dimension_(active)    36.0     microns
  vert_dimension_(active)    36.0     microns
  peak_D_star                1.5e10   cm-sqrt(Hz)/W
  integration_time           0.007    microsec
  1/f_knee_frequency         3.0      Hz
>fpa_parallel
  #_detectors_in_TDI         4.0      --
  #_vert_detectors           240.0    --
  #_samples_per_HIFOV        2.0      --
  #_samples_per_VIFOV        2.0      --
  3dB_response_frequency     2032.0   Hz
  scan_efficiency            0.75     --
>electronics
  high_pass_3db_cuton        1.0     Hz
  high_pass_filter_order     0.0      --
  low_pass_3db_cutoff        100000.0 Hz
  low_pass_filter_order      0.0      --
  boost_amplitude            0.0      --

```

boost_frequency	0.0	Hz
sample_and_hold	HORZ	NO_HORZ_VERT
>display		
display_brightness	10.0	milli-Lamberts
display_height	15.24	cm
display_viewing_distance	30.0	cm
>crt_display		
#_active_lines_on_CRT	480.0	--
horz_crt_spot_sigma	0.0	mrاد
vert_crt_spot_sigma	0.0	mrاد
>eye		
threshold_SNR	2.5	--
eye_integration_time	0.1	sec
MTF	EXP	EXP_or_NL
>3d_noise_default		
noise_level	MOD	NO_LO_MOD_or_HI
>random_image_motion		
horz_rms_motion_amplitude	0.02	mrاد
vert_rms_motion_amplitude	0.02	mrاد
>spectral_detectivity		
#_points: 7 microns_____detectivity		
7.6	0.666	
8.0	0.722	
8.5	0.777	
9.0	0.833	
9.5	0.889	
10.0	0.944	
10.5	1.0	
>end		

end data file listing . . .

MESSAGES

diagnostic(): Using default 3D noise components.
diagnostic(): Using _MOD_ level 3D noise defaults.
diagnostic(): Diffraction wavelength set to spectral band midpoint.
diagnostic(): Fields-of-view calculated by model.
diagnostic(): Electronics high pass filter defaulted to order 1.
diagnostic(): Electronics low pass filter defaulted to order 1.

CALCULATED SYSTEM PARAMETERS

field-of-view:	29.252h x 21.994v degrees
	510.54h x 383.86v mrad
magnification:	1.296
optics blur spot:	44.164 microns (diffraction-limited)
	1.987 mrad

detector IFOV: 1.619h x 1.619v mrad

scan velocity: 40340.22 mrad/second

dwell time: 4.014e-005 seconds

TEMPERATURE DEPENDENCE

parameter bandwidth	NETD @ 300 K	NETD @ 0 K	noise
white NETD	0.212 deg C	0.000 deg C	1.957e+004 Hz
classical NETD	0.212 deg C	0.000 deg C	1.961e+004 Hz
sigma_TVH NETD	0.085 deg C	0.000 deg C	3.119e+003 Hz
sigma_TV NETD	0.063 deg C	0.000 deg C	
sigma_V NETD	0.063 deg C	0.000 deg C	
Planck integral	1.565e-004	0.000e+000	W/(cm*cm*K)
. . . w/D-star	1.955e+006	0.000e+000	sqrt(Hz)/(cm*K)

TOTAL HORIZONTAL MTFs

cy/mr	H_SYS	H_PRE	H_TPF	H_SPF
0.000	1.000	1.000	1.000	1.000
0.031	0.798	0.964	0.853	0.971
0.062	0.545	0.921	0.632	0.937
0.093	0.373	0.871	0.477	0.898
0.124	0.263	0.816	0.377	0.855
0.154	0.189	0.756	0.310	0.809
0.185	0.138	0.694	0.262	0.760
0.216	0.101	0.629	0.226	0.709
0.247	0.074	0.564	0.199	0.657
0.278	0.054	0.499	0.177	0.606
0.309	0.038	0.435	0.160	0.554
0.340	0.027	0.373	0.145	0.503
0.371	0.019	0.313	0.133	0.454
0.401	0.013	0.258	0.123	0.407
0.432	0.009	0.206	0.114	0.362
0.463	0.005	0.159	0.106	0.320
0.494	0.003	0.117	0.099	0.280
0.525	0.002	0.080	0.093	0.244
0.556	0.001	0.048	0.088	0.211
0.587	0.000	0.022	0.083	0.181
0.618	0.000	0.000	0.079	0.154

TOTAL VERTICAL MTFs

cy/mr	H_SYS	H_PRE	H_SPF
0.000	1.000	1.000	1.000

0.031	0.937	0.964	0.972
0.062	0.866	0.921	0.941
0.093	0.789	0.871	0.906
0.124	0.709	0.816	0.869
0.154	0.628	0.756	0.830
0.185	0.547	0.694	0.789
0.216	0.470	0.629	0.746
0.247	0.396	0.564	0.703
0.278	0.329	0.499	0.659
0.309	0.267	0.435	0.615
0.340	0.213	0.373	0.572
0.371	0.166	0.313	0.529
0.401	0.126	0.258	0.487
0.432	0.092	0.206	0.447
0.463	0.065	0.159	0.408
0.494	0.043	0.117	0.370
0.525	0.027	0.080	0.335
0.556	0.015	0.048	0.302
0.587	0.006	0.022	0.270
0.618	0.000	0.000	0.241

PREFILTER VALUES AT NYQUIST

horz H_PRE(0.62) = 0.000 vert H_PRE(0.62) = 0.000

SAMPLING RATES

horizontal	1.24 samples/mr
vertical	1.24 samples/mr
effective	1.24 samples/mr

SENSOR LIMITING FREQUENCIES

	spatial	Nyquist
horizontal	0.62	0.62
vertical	0.62	0.62
effective	0.62	0.62

MRTD 3D NOISE CORRECTION (AVERAGE)

	300 K	0 K
horizontal	1.000	0.000
vertical	3.031	0.000

MRTD AT 300 K BACKGROUND TEMPERATURE

	cy/mr	horz		cy/mr	vert	cy/mr	2D
0.05	0.031	0.009	0.05	0.031	0.052	0.056	0.052
0.10	0.062	0.022	0.10	0.062	0.079	0.079	0.069
0.15	0.093	0.044	0.15	0.093	0.103	0.103	0.091
0.20	0.124	0.075	0.20	0.124	0.131	0.132	0.120
0.25	0.154	0.119	0.25	0.154	0.164	0.162	0.158

0.30	0.185	0.182	0.30	0.185	0.203	0.193	0.209
0.35	0.216	0.271	0.35	0.216	0.252	0.223	0.275
0.40	0.247	0.397	0.40	0.247	0.314	0.253	0.363
0.45	0.278	0.582	0.45	0.278	0.394	0.282	0.479
0.50	0.309	0.856	0.50	0.309	0.502	0.309	0.631
0.55	0.340	1.269	0.55	0.340	0.649	0.336	0.832
0.60	0.371	1.907	0.60	0.371	0.855	0.361	1.096
0.65	0.401	2.918	0.65	0.401	1.153	0.384	1.445
0.70	0.432	4.582	0.70	0.432	1.600	0.407	1.905
0.75	0.463	7.325	0.75	0.463	2.306	0.428	2.512
0.80	0.494	12.512	0.80	0.494	3.497	0.448	3.311
0.85	0.525	23.009	0.85	0.525	5.716	0.467	4.365
0.90	0.556	48.102	0.90	0.556	10.628	0.485	5.754
0.95	0.587	99.999	0.95	0.587	26.664	0.501	7.586
1.00	0.618	99.999	1.00	0.618	99.999	0.516	10.000

MDTD AT 300 K BACKGROUND TEMPERATURE

	1/mr	MDTD
0.20	3.088	27.369
0.40	1.544	6.956
0.60	1.029	3.174
0.80	0.772	1.849
1.00	0.618	1.233
1.20	0.515	0.897
1.40	0.441	0.692
1.60	0.386	0.558
1.80	0.343	0.464
2.00	0.309	0.396
2.20	0.281	0.344
2.40	0.257	0.304
2.60	0.238	0.271
2.80	0.221	0.245
3.00	0.206	0.223
3.20	0.193	0.205
3.40	0.182	0.190
3.60	0.172	0.177
3.80	0.163	0.165
4.00	0.154	0.155
4.20	0.147	0.147
4.40	0.140	0.139
4.60	0.134	0.132
4.80	0.129	0.126
5.00	0.124	0.121

FLIR92. . . scanWFOV.1: end of listing

THIS PAGE INTENTIONALLY LEFT BLANK

APPENDIX B. FLIR92 MODEL OUTPUTS FOR SCANNING SENSOR (MFOV)

U.S. Army CECOM NVESD FLIR92

Fri Mar 09 10:32:50 2001

output file: 2nd generation scanning sensor short listing for MFOV

data file: scanMFOV

command line arguments: -d scanMFOV -o scanMFOV -p BOTH -a scanMFOV

begin data file listing . . .

gen2: sample data file for 2nd generation FLIR

```

>spectral
  spectral_cut_on          7.6      microns
  spectral_cut_off        10.5      microns
  diffraction_wavelength   0.0      microns
>optics_1
  f_number                 2.0      --
  eff_focal_length         10.0      cm
  eff_aperture_diameter    00.0      cm
  optics_blur_spot         0.0      mrad
  average_optical_trans     0.75     --
>optics_2
  HFOV:VFOV_aspect_ratio   1.33     --
  magnification            0.0      --
  frame_rate               30.0      Hz
  fields_per_frame         2.0      --
>detector
  horz_dimension_(active)   36.0      microns
  vert_dimension_(active)   36.0      microns
  peak_D_star              1.5e10 cm sqrt(Hz)/W
  integration_time          0.007    microsec
  1/f_knee_frequency        3.0      Hz
>fpa_parallel
  #_detectors_in_TDI        4.0      --
  #_vert_detectors          240.0     --
  #_samples_per_HIFOV       2.0      --
  #_samples_per_VIFOV       2.0      --
  3dB_response_frequency    2032.0   Hz
  scan_efficiency           0.75     --
>electronics
  high_pass_3db_cuton       1.0      Hz
  high_pass_filter_order    0.0      --
  low_pass_3db_cutoff       100000.0 Hz
  low_pass_filter_order     0.0      --

```

boost_amplitude	0.0	--
boost_frequency	0.0	Hz
sample_and_hold	HORZ	NO_HORZ_VERT
>display		
display_brightness	10.0	milli-Lamberts
display_height	15.24	cm
display_viewing_distance	30.0	cm
>crt_display		
#_active_lines_on_CRT	480.0	--
horz_crt_spot_sigma	0.0	mrاد
vert_crt_spot_sigma	0.0	mrاد
>eye		
threshold_SNR	2.5	--
eye_integration_time	0.1	sec
MTF	EXP	EXP_or_NL
>3d_noise_default		
noise_level	MOD	NO_LO_MOD_or_HI
>random_image_motion		
horz_rms_motion_amplitude	0.02	mrاد
vert_rms_motion_amplitude	0.02	mrاد
>spectral_detectivity		
#_points: 7 microns____detectivity		
7.6	0.666	
8.0	0.722	
8.5	0.777	
9.0	0.833	
9.5	0.889	
10.0	0.944	
10.5	1.0	
>end		

end data file listing . . .

MESSAGES

diagnostic(): Using default 3D noise components.
diagnostic(): Using _MOD_ level 3D noise defaults.
diagnostic(): Diffraction wavelength set to spectral band midpoint.
diagnostic(): Fields-of-view calculated by model.
diagnostic(): Electronics high pass filter defaulted to order 1.
diagnostic(): Electronics low pass filter defaulted to order 1.

CALCULATED SYSTEM PARAMETERS

field-of-view:	6.580h x 4.947	v degrees
	114.84h x 86.35	v mrad
magnification:	5.761	
optics blur spot:	44.164	microns (diffraction-limited)

	0.442	mrad
detector IFOV:	0.360h x 0.360	v mrad
scan velocity:	9181.54	mrad/second
dwell time:	3.921e-005	seconds

TEMPERATURE DEPENDENCE

parameter	NETD @ 300 K	NETD @ 0 K	noise bandwidth
-----	-----	-----	
white NETD	0.215 deg C	0.000 deg C	2.003e+004 Hz
classical NETD	0.215 deg C	0.000 deg C	2.008e+004 Hz
sigma_TVH NETD	0.085 deg C	0.000 deg C	3.119e+003 Hz
sigma_TV NETD	0.063 deg C	0.000 deg C	
sigma_V NETD	0.063 deg C	0.000 deg C	
Planck integral	1.565e-004	0.000e+000	W/(cm*cm*K)
. . . w/D-star	1.955e+006	0.000e+000	sqrt(Hz)/(cm*K)

TOTAL HORIZONTAL MTFs

cy/mr	H_SYS	H_PRE	H_TPF	H_SPF
0.000	1.000	1.000	1.000	1.000
0.139	0.792	0.964	0.847	0.971
0.278	0.537	0.920	0.623	0.936
0.417	0.366	0.870	0.469	0.897
0.556	0.257	0.814	0.370	0.853
0.694	0.184	0.754	0.303	0.806
0.833	0.134	0.690	0.256	0.757
0.972	0.098	0.625	0.221	0.706
1.111	0.071	0.559	0.194	0.654
1.250	0.051	0.493	0.173	0.601
1.389	0.037	0.428	0.156	0.549
1.528	0.026	0.366	0.142	0.498
1.667	0.018	0.307	0.130	0.449
1.806	0.012	0.252	0.120	0.402
1.944	0.008	0.200	0.111	0.357
2.083	0.005	0.154	0.104	0.314
2.222	0.003	0.113	0.097	0.275
2.361	0.002	0.077	0.091	0.239
2.500	0.001	0.046	0.086	0.206
2.639	0.000	0.021	0.081	0.176
2.778	0.000	0.000	0.077	0.149

TOTAL VERTICAL MTFs

cy/mr	H_SYS	H_PRE	H_SPF
0.000	1.000	1.000	1.000
0.139	0.937	0.964	0.972
0.278	0.865	0.920	0.940
0.417	0.787	0.870	0.905
0.556	0.706	0.814	0.867
0.694	0.624	0.754	0.827
0.833	0.542	0.690	0.786
0.972	0.464	0.625	0.743
1.111	0.390	0.559	0.699
1.250	0.323	0.493	0.654
1.389	0.261	0.428	0.610
1.528	0.207	0.366	0.566
1.667	0.160	0.307	0.523
1.806	0.121	0.252	0.481
1.944	0.088	0.200	0.440
2.083	0.062	0.154	0.401
2.222	0.041	0.113	0.364
2.361	0.025	0.077	0.328
2.500	0.014	0.046	0.295
2.639	0.005	0.021	0.264
2.778	0.000	0.000	0.235

PREFILTER VALUES AT NYQUIST

horz H_PRE(2.78) = 0.000 vert H_PRE(2.78) = 0.000

SAMPLING RATES

horizontal 5.56 samples/mr
vertical 5.56 samples/mr
effective 5.56 samples/mr

SENSOR LIMITING FREQUENCIES

	spatial	Nyquist
horizontal	2.78	2.78
vertical	2.78	2.78
effective	2.78	2.78

MRTD 3D NOISE CORRECTION (AVERAGE)

	300 K	0 K
horizontal	1.000	0.000
vertical	3.010	0.000

MRTD AT 300 K BACKGROUND TEMPERATURE

	cy/mr	horz		cy/mr	vert		cy/mr	2D
0.05	0.139	0.009	0.05	0.139	0.053	0.252	0.053	
0.10	0.278	0.023	0.10	0.278	0.079	0.351	0.069	
0.15	0.417	0.045	0.15	0.417	0.104	0.461	0.091	
0.20	0.556	0.077	0.20	0.556	0.132	0.588	0.120	
0.25	0.694	0.123	0.25	0.694	0.165	0.722	0.159	
0.30	0.833	0.188	0.30	0.833	0.205	0.858	0.209	
0.35	0.972	0.281	0.35	0.972	0.254	0.993	0.275	
0.40	1.111	0.413	0.40	1.111	0.318	1.126	0.363	
0.45	1.250	0.608	0.45	1.250	0.401	1.254	0.479	
0.50	1.389	0.898	0.50	1.389	0.513	1.376	0.631	
0.55	1.528	1.337	0.55	1.528	0.665	1.494	0.832	
0.60	1.667	2.018	0.60	1.667	0.881	1.605	1.097	
0.65	1.806	3.106	0.65	1.806	1.194	1.712	1.446	
0.70	1.944	4.904	0.70	1.944	1.666	1.813	1.906	
0.75	2.083	7.890	0.75	2.083	2.416	1.908	2.512	
0.80	2.222	13.565	0.80	2.222	3.686	1.998	3.312	
0.85	2.361	25.118	0.85	2.361	6.066	2.081	4.365	
0.90	2.500	52.898	0.90	2.500	11.359	2.162	5.755	
0.95	2.639	99.999	0.95	2.639	28.712	2.235	7.586	
1.00	2.778	99.999	1.00	2.778	99.999	2.302	10.000	

MDTD AT 300 K BACKGROUND TEMPERATURE

	1/mr	MDTD
0.20	13.889	28.031
0.40	6.944	7.122
0.60	4.630	3.248
0.80	3.472	1.890
1.00	2.778	1.260
1.20	2.315	0.916
1.40	1.984	0.706
1.60	1.736	0.568
1.80	1.543	0.472
2.00	1.389	0.403
2.20	1.263	0.350
2.40	1.157	0.309
2.60	1.068	0.275
2.80	0.992	0.249
3.00	0.926	0.227
3.20	0.868	0.208
3.40	0.817	0.193
3.60	0.772	0.179
3.80	0.731	0.168
4.00	0.694	0.157
4.20	0.661	0.148

4.40	0.631	0.141
4.60	0.604	0.134
4.80	0.579	0.127
5.00	0.556	0.122

FLIR92. . . scanMFOV.1: end of listing

APPENDIX C. FLIR92 MODEL OUTPUTS FOR SCANNING SENSOR (NFOV)

U.S. Army CECOM NVESD FLIR92

Fri Mar 09 10:40:23 2001

output file: scannFOV.1 short listing

data file: scannFOV

command line arguments: -d scannFOV -o scannFOV -p BOTH -a scannFOV

begin data file listing . . .

gen2: sample data file for 2nd generation FLIR

>spectral

spectral_cut_on	7.6	microns
spectral_cut_off	10.5	microns
diffraction_wavelength	0.0	microns

>optics_1

f_number	2.0	--
eff_focal_length	40.0	cm
eff_aperture_diameter	00.0	cm
optics_blur_spot	0.0	mrاد
average_optical_trans	0.75	--

>optics_2

HFOV:VFOV_aspect_ratio	1.33	--
Magnification	0.0	--
frame_rate	30.0	Hz
fields_per_frame	2.0	--

>detector

horz_dimension_(active)	36.0	microns
vert_dimension_(active)	6.0	microns
peak_D_star	1.5e10	cm-sqrt(Hz)/W
integration_time	0.007	microsec
1/f_knee_frequency	3.0	Hz

>fpa_parallel

#_detectors_in_TDI	4.0	--
#_vert_detectors	240.0	--
#_samples_per_HIFOV	2.0	--
#_samples_per_VIFOV	2.0	--
3dB_response_frequency	2032.0	Hz
scan_efficiency	0.75	--

>electronics

high_pass_3db_cuton	1.0	Hz
high_pass_filter_order	0.0	--
low_pass_3db_cutoff	100000.0	Hz
low_pass_filter_order	0.0	--
boost_amplitude	0.0	--
boost_frequency	0.0	Hz

sample_and_hold	HORZ	NO_HORZ_VERT
>display		
display_brightness	10.0	milli-Lamberts
display_height	15.24	cm
display_viewing_distance	30.0	cm
>crt_display		
#_active_lines_on_CRT	480.0	--
horz_crt_spot_sigma	0.0	mrاد
vert_crt_spot_sigma	0.0	mrاد
>eye		
threshold_SNR	2.5	--
eye_integration_time	0.1	sec
MTF	EXP	EXP_or_NL
>3d_noise_default		
noise_level	MOD	NO_LO_MOD_or_HI
>random_image_motion		
horz_rms_motion_amplitude	0.02	mrاد
vert_rms_motion_amplitude	0.02	mrاد
>spectral_detectivity		
#_points: 7 microns_____detectivity		
7.6	0.666	
8.0	0.722	
8.5	0.777	
9.0	0.833	
9.5	0.889	
10.0	0.944	
10.5	1.0	
>end		

end data file listing . . .

MESSAGES

diagnostic(): Using default 3D noise components.
diagnostic(): Using _MOD_ level 3D noise defaults.
diagnostic(): Diffraction wavelength set to spectral band midpoint.
diagnostic(): Fields-of-view calculated by model.
diagnostic(): Electronics high pass filter defaulted to order 1.
diagnostic(): Electronics low pass filter defaulted to order 1.

CALCULATED SYSTEM PARAMETERS

field-of-view:	1.646h x 1.238	v degrees
	28.73h x 21.60	v mrاد
magnification:	23.032	
optics blur spot:	44.164	microns (diffraction-limited)
	0.110	mrاد

detector IFOV:	0.090h x 0.090	v mrad
scan velocity:	2298.06	mmrad/second
dwell time:	3.916e-005	seconds

TEMPERATURE DEPENDENCE

parameter	NETD @ 300 K	NETD @ 0 K	noise bandwidth
-----	-----	-----	
white NETD	0.215 deg C	0.000 deg C	2.005e+004 Hz
classical NETD	0.215 deg C	0.000 deg C	2.010e+004 Hz
sigma_TVH NETD	0.085 deg C	0.000 deg C	3.119e+003 Hz
sigma_TV NETD	0.063 deg C	0.000 deg C	
sigma_V NETD	0.063 deg C	0.000 deg C	
Planck integral	1.565e-004	0.000e+000	W/(cm*cm*K)
. . . w/D-star	1.955e+006	0.000e+000	sqrt(Hz)/(cm*K)

TOTAL HORIZONTAL MTFs

cy/mr	H_SYS	H_PRE	H_TPF	H_SPF
0.000	1.000	1.000	1.000	1.000
0.556	0.790	0.962	0.847	0.971
1.111	0.531	0.912	0.622	0.936
1.667	0.358	0.852	0.468	0.897
2.222	0.247	0.785	0.369	0.853
2.778	0.174	0.712	0.303	0.806
3.333	0.123	0.636	0.256	0.757
3.889	0.087	0.559	0.221	0.706
4.444	0.061	0.483	0.194	0.653
5.000	0.043	0.410	0.173	0.601
5.556	0.029	0.341	0.156	0.549
6.111	0.020	0.278	0.142	0.498
6.667	0.013	0.221	0.130	0.449
7.222	0.008	0.171	0.120	0.401
7.778	0.005	0.128	0.111	0.356
8.333	0.003	0.092	0.104	0.314
8.889	0.002	0.063	0.097	0.275
9.444	0.001	0.040	0.091	0.239
10.000	0.000	0.022	0.086	0.206
10.556	0.000	0.009	0.081	0.176
11.111	0.000	0.000	0.077	0.149

TOTAL VERTICAL MTFs

cy/mr	H_SYS	H_PRE	H_SPF
0.000	1.000	1.000	1.000
0.556	0.934	0.962	0.972
1.111	0.857	0.912	0.940
1.667	0.771	0.852	0.905
2.222	0.680	0.785	0.867
2.778	0.589	0.712	0.827
3.333	0.499	0.636	0.785
3.889	0.415	0.559	0.742
4.444	0.337	0.483	0.698
5.000	0.268	0.410	0.654
5.556	0.208	0.341	0.610
6.111	0.157	0.278	0.566
6.667	0.115	0.221	0.523
7.222	0.082	0.171	0.480
7.778	0.056	0.128	0.440
8.333	0.037	0.092	0.401
8.889	0.023	0.063	0.363
9.444	0.013	0.040	0.328
10.000	0.006	0.022	0.295
10.556	0.002	0.009	0.263
11.111	0.000	0.000	0.234

PREFILTER VALUES AT NYQUIST

horz H_PRE(11.11) = 0.000 vert H_PRE(11.11) = 0.000

SAMPLING RATES

horizontal	22.22 samples/mr
vertical	22.22 samples/mr
effective	22.22 samples/mr

SENSOR LIMITING FREQUENCIES

	spatial	Nyquist
horizontal	11.11	11.11
vertical	11.11	11.11
effective	11.11	11.11

MRTD 3D NOISE CORRECTION (AVERAGE)

	300 K	0 K
horizontal	1.000	0.000
vertical	3.009	0.000

MRTD AT 300 K BACKGROUND TEMPERATURE

	cy/mr	horz		cy/mr	vert		cy/mr	2D
0.05	0.556	0.009	0.05	0.556	0.053	1.002	0.053	
0.10	1.111	0.023	0.10	1.111	0.080	1.387	0.069	
0.15	1.667	0.046	0.15	1.667	0.106	1.810	0.091	
0.20	2.222	0.080	0.20	2.222	0.137	2.289	0.120	
0.25	2.778	0.130	0.25	2.778	0.175	2.783	0.159	
0.30	3.333	0.204	0.30	3.333	0.222	3.278	0.209	
0.35	3.889	0.315	0.35	3.889	0.285	3.769	0.276	
0.40	4.444	0.479	0.40	4.444	0.368	4.246	0.364	
0.45	5.000	0.733	0.45	5.000	0.483	4.708	0.479	
0.50	5.556	1.131	0.50	5.556	0.644	5.150	0.632	
0.55	6.111	1.766	0.55	6.111	0.878	5.574	0.833	
0.60	6.667	2.810	0.60	6.667	1.224	5.982	1.098	
0.65	7.222	4.578	0.65	7.222	1.757	6.371	1.447	
0.70	7.778	7.690	0.70	7.778	2.609	6.746	1.907	
0.75	8.333	13.220	0.75	8.333	4.042	7.105	2.514	
0.80	8.889	24.399	0.80	8.889	6.621	7.442	3.313	
0.85	9.444	48.722	0.85	9.444	11.749	7.769	4.367	
0.90	10.000	99.999	0.90	10.000	23.837	8.075	5.756	
0.95	10.556	99.999	0.95	10.556	65.572	8.368	7.587	
1.00	11.111	99.999	1.00	11.111	99.999	8.645	10.000	

MDTD AT 300 K BACKGROUND TEMPERATURE

	1/mr	MDTD
0.20	55.556	30.061
0.40	27.778	7.618
0.60	18.519	3.461
0.80	13.889	2.004
1.00	11.111	1.329
1.20	9.259	0.960
1.40	7.937	0.737
1.60	6.944	0.590
1.80	6.173	0.489
2.00	5.556	0.415
2.20	5.051	0.359
2.40	4.630	0.316
2.60	4.274	0.282
2.80	3.968	0.254
3.00	3.704	0.231
3.20	3.472	0.212
3.40	3.268	0.196
3.60	3.086	0.182
3.80	2.924	0.170
4.00	2.778	0.160
4.20	2.646	0.151

4.40	2.525	0.142
4.60	2.415	0.135
4.80	2.315	0.129
5.00	2.222	0.124

FLIR92. . . scannFOV.1: end of listing

APPENDIX D. FLIR92 MODEL OUTPUTS FOR STARING SENSOR (WFOV)

U.S. Army CECOM NVESD FLIR92

Thu Mar 15 13:50:35 2001

output file: stawfov.1 short listing

data file: stawfov

command line arguments: -d stawfov -o stawfov -p BOTH -a stawfov

begin data file listing . . .

sniper: thermal imaging system

>spectral

spectral_cut_on	3.0	microns
spectral_cut_off	5.0	microns
diffraction_wavelength	0.0	microns

>optics_1

f_number	4.6	--
eff_focal_length	4.0	cm
eff_aperture_diameter	0.0	cm
geometric_blur_spot	0.0	mrad
average_optical_trans	0.78	--

>optics_2

HFOV:WFOV_aspect_ratio	1.323	--
magnification	0.0	--
frame_rate	60.0	Hz
fields_per_frame	1.0	--

>detector

horz_detector_size	22.56	microns
vert_detector_size	22.56	microns
peak_D_star	5.97e11	cm-sqrt(Hz)/W
integration_time	16666.667	microsec
1/f_knee_frequency	0.0	Hz

>fpa_stare

#_horz_detectors	640.0	--
#_vert_detectors	480.0	--
horz_unit_cell_dimension	24.0	microns
vert_unit_cell_dimension	24.0	microns

>electronics

high_pass_3db_cuton	0.0	Hz
high_pass_filter_order	0.0	--
low_pass_3db_cutoff	0.0	Hz
low_pass_filter_order	0.0	--
boost_amplitude	0.0	--
boost_frequency	0.0	Hz

sample_and_hold	HORZ	HORZ_or_VERT_or_NO
>display		
display_brightness	10.0	milli-Lamberts
display_height	15.24	cm
display_viewing_distance	30.0	cm
>crt_display		
#_active_lines_on_CRT	480.0	--
horz_crt_spot_sigma	0.0	mrاد
vert_crt_spot_sigma	0.0	mrاد
>eye		
threshold_SNR	2.5	--
eye_integration_time	0.1	sec
MTF	EXP	EXP_or_NL
>3d_noise_default		
noise_level	MOD	NO_LO_MOD_or_HI
>spectral_detectivity		
#_points: 5 microns_____detectivity		
3.0	0.666	
3.5	0.7495	
4.0	0.833	
4.5	0.9165	
5.0	1.0	
>end		

end data file listing . . .

MESSAGES

diagnostic(): Using default 3D noise components.
diagnostic(): Using _LO_ level 3D noise defaults.
diagnostic(): Diffraction wavelength set to spectral band midpoint.
diagnostic(): Fields-of-view calculated by model.

CALCULATED SYSTEM PARAMETERS

field-of-view:	21.737h x 16.389	v degrees
	379.38h x 286.03	v mrاد
magnification:	1.739	
optics blur spot:	44.896	microns (diffraction-limited)
	1.122	mrاد
detector IFOV:	0.564h x 0.564	v mrاد
FPA fill factor:	0.884	
FPA duty cycle:	1.000	

TEMPERATURE DEPENDENCE

parameter	NETD @ 300 K	NETD @ 0 K	noise bandwidth
white NETD	0.029 deg C	0.000 deg C	4.712e+001 Hz
classical NETD	0.029 deg C	0.000 deg C	4.714e+001 Hz
sigma_TVH NETD	0.023 deg C	0.000 deg C	3.004e+001 Hz
sigma_VH NETD	0.009 deg C	0.000 deg C	
Planck integral	2.127e-005	0.000e+000	W/(cm*cm*K)
. . . w/D-star	1.144e+007	0.000e+000	sqrt(Hz)/(cm*K)

TOTAL HORIZONTAL MTFs

cy/mr	H_SYS	H_PRE	H_TPF	H_SPF
0.000	1.000	1.000	1.000	1.000
0.089	0.880	0.944	1.000	0.932
0.177	0.743	0.882	1.000	0.842
0.266	0.601	0.814	1.000	0.739
0.355	0.467	0.742	1.000	0.629
0.443	0.347	0.668	1.000	0.519
0.532	0.246	0.594	1.000	0.415
0.621	0.167	0.520	1.000	0.322
0.709	0.108	0.448	1.000	0.241
0.798	0.066	0.380	1.000	0.174
0.887	0.038	0.315	1.000	0.122
0.975	0.021	0.256	1.000	0.082
1.064	0.011	0.203	1.000	0.053
1.152	0.005	0.156	1.000	0.032
1.241	0.002	0.116	1.000	0.019
1.330	0.001	0.082	1.000	0.010
1.418	0.000	0.054	1.000	0.005
1.507	0.000	0.033	1.000	0.002
1.596	0.000	0.017	1.000	0.001
1.684	0.000	0.006	1.000	-0.000
1.773	0.000	0.000	1.000	0.000

TOTAL VERTICAL MTFs

cy/mr	H_SYS	H_PRE	H_SPF
0.000	1.000	1.000	1.000
0.089	0.884	0.944	0.936
0.177	0.757	0.882	0.858
0.266	0.627	0.814	0.771
0.355	0.503	0.742	0.678
0.443	0.391	0.668	0.585

0.532	0.293	0.594	0.494
0.621	0.212	0.520	0.409
0.709	0.148	0.448	0.331
0.798	0.100	0.380	0.263
0.887	0.064	0.315	0.204
0.975	0.040	0.256	0.156
1.064	0.024	0.203	0.116
1.152	0.013	0.156	0.085
1.241	0.007	0.116	0.061
1.330	0.003	0.082	0.043
1.418	0.002	0.054	0.029
1.507	0.001	0.033	0.020
1.596	0.000	0.017	0.013
1.684	0.000	0.006	0.008
1.773	0.000	0.000	0.000

PREFILTER VALUES AT NYQUIST

horz H_PRE(0.83) = 0.354 vert H_PRE(0.83) = 0.354

SAMPLING RATES

horizontal	1.67	samples/mr
vertical	1.67	samples/mr
effective	1.67	samples/mr

SENSOR LIMITING FREQUENCIES

	spatial	Nyquist
horizontal	1.77	0.83
vertical	1.77	0.83
effective	1.77	0.83

MRTD 3D NOISE CORRECTION (AVERAGE)

	300 K	0 K
horizontal	1.400	0.000
vertical	1.400	0.000

MRTD AT 300 K BACKGROUND TEMPERATURE

	cy/mr	horz		cy/mr	vert		cy/mr	2D
0.05	0.089	0.002	0.05	0.089	0.002	0.089	0.002	
0.10	0.177	0.004	0.10	0.177	0.004	0.114	0.002	
0.15	0.266	0.007	0.15	0.266	0.006	0.139	0.003	
0.20	0.355	0.010	0.20	0.355	0.010	0.164	0.003	
0.25	0.443	0.016	0.25	0.443	0.015	0.194	0.004	
0.30	0.532	0.026	0.30	0.532	0.023	0.231	0.005	
0.35	0.621	0.042	0.35	0.621	0.034	0.268	0.006	
0.40	0.709	0.070	0.40	0.709	0.053	0.312	0.008	
0.45	0.798	0.122	0.45	0.798	0.084	0.355	0.010	

0.50	0.887	99.999	0.50	0.887	99.999	0.401	0.013
0.55	0.975	99.999	0.55	0.975	99.999	0.447	0.016
0.60	1.064	99.999	0.60	1.064	99.999	0.492	0.020
0.65	1.152	99.999	0.65	1.152	99.999	0.538	0.025
0.70	1.241	99.999	0.70	1.241	99.999	0.584	0.031
0.75	1.330	99.999	0.75	1.330	99.999	0.629	0.039
0.80	1.418	99.999	0.80	1.418	99.999	0.672	0.049
0.85	1.507	99.999	0.85	1.507	99.999	0.713	0.062
0.90	1.596	99.999	0.90	1.596	99.999	0.753	0.078
0.95	1.684	99.999	0.95	1.684	99.999	0.780	0.097
1.00	1.773	99.999	1.00	1.773	99.999	0.800	0.122

MDTD AT 300 K BACKGROUND TEMPERATURE

	1/mr	MDTD
0.20	8.865	2.314
0.40	4.433	0.585
0.60	2.955	0.264
0.80	2.216	0.152
1.00	1.773	0.100
1.20	1.478	0.072
1.40	1.266	0.055
1.60	1.108	0.044
1.80	0.985	0.036
2.00	0.887	0.031
2.20	0.806	0.026
2.40	0.739	0.023
2.60	0.682	0.021
2.80	0.633	0.019
3.00	0.591	0.017
3.20	0.554	0.016
3.40	0.521	0.014
3.60	0.493	0.013
3.80	0.467	0.012
4.00	0.443	0.012
4.20	0.422	0.011
4.40	0.403	0.010
4.60	0.385	0.010
4.80	0.369	0.009
5.00	0.355	0.009

FLIR92. . . stawfov.1: end of listing

THIS PAGE INTENTIONLLY LEFT BLANK

APPENDIX E. FLIR92 MODEL OUTPUTS FOR STARING SENSOR (MFOV)

U.S. Army CECOM NVESD FLIR92

Wed Mar 07 13:39:34 2001

output file: sniperm.1 short listing

data file: sniperm

command line arguments: -d sniperm -o sniperm -p BOTH -a sniperm

begin data file listing . . .

sniper: thermal imaging system

>spectral

spectral_cut_on	3.0	microns
spectral_cut_off	5.0	microns
diffraction_wavelength	0.0	microns

>optics_1

f_number	4.6	--
eff_focal_length	20.0	cm
eff_aperture_diameter	0.0	cm
geometric_blur_spot	0.0	mrad
average_optical_trans	0.80	--

>optics_2

HFOV:WFOV_aspect_ratio	1.323	--
Magnification	0.0	--
frame_rate	60.0	Hz
fields_per_frame	1.0	--

>detector

horz_detector_size	22.56	microns
vert_detector_size	22.56	microns
peak_D_star	5.97e11	cm-sqrt(Hz)/W
integration_time	16666.667	microsec
1/f_knee_frequency	0.0	Hz

>fpa_stare

#_horz_detectors	640.0	--
#_vert_detectors	480.0	--
horz_unit_cell_dimension	24.0	microns
vert_unit_cell_dimension	24.0	microns

>electronics

high_pass_3db_cuton	0.0	Hz
high_pass_filter_order	0.0	--
low_pass_3db_cutoff	0.0	Hz
low_pass_filter_order	0.0	--
boost_amplitude	0.0	--
boost_frequency	0.0	Hz

sample_and_hold	HORZ	HORZ_or_VERT_or_NO
>display		
display_brightness	10.0	milli-Lamberts
display_height	15.24	cm
display_viewing_distance	30.0	cm
>crt_display		
#_active_lines_on_CRT	480.0	--
horz_crt_spot_sigma	0.0	mrاد
vert_crt_spot_sigma	0.0	mrاد
>eye		
threshold_SNR	2.5	--
eye_integration_time	0.1	sec
MTF	EXP	EXP_or_NL
>3d_noise_default		
noise_level	MOD	NO_LO_MOD_or_HI
>spectral_detectivity		
#_points: 5 microns_____detectivity		
3.0	0.666	
3.5	0.7495	
4.0	0.833	
4.5	0.9165	
5.0	1.0	
>end		

end data file listing . . .

MESSAGES

diagnostic(): Using default 3D noise components.
diagnostic(): Using _LO_ level 3D noise defaults.
diagnostic(): Diffraction wavelength set to spectral band midpoint.
diagnostic(): Fields-of-view calculated by model.

CALCULATED SYSTEM PARAMETERS

field-of-view:	4.398h x 3.299	v degrees
	76.76h x 57.58	v mrad
magnification:	8.639	
optics blur spot:	44.896	microns (diffraction-limited)
	0.224	mrاد
detector IFOV:	0.113h x 0.113	v mrad
FPA fill factor:	0.884	
FPA duty cycle:	1.000	

TEMPERATURE DEPENDENCE

parameter	NETD @ 300 K	NETD @ 0 K	noise bandwidth
-----------	--------------	------------	-----------------

white NETD	0.028 deg C	0.000 deg C	4.712e+001 Hz
classical NETD	0.028 deg C	0.000 deg C	4.714e+001 Hz
sigma_TVH NETD	0.022 deg C	0.000 deg C	3.004e+001 Hz
sigma_VH NETD	0.009 deg C	0.000 deg C	
Planck integral	2.127e-005	0.000e+000	W/(cm*cm*K)
. . . w/D-star	1.144e+007	0.000e+000	sqrt(Hz)/(cm*K)

TOTAL HORIZONTAL MTFs

cy/mr	H_SYS	H_PRE	H_TPF	H_SPF
0.000	1.000	1.000	1.000	1.000
0.443	0.879	0.944	1.000	0.931
0.887	0.742	0.882	1.000	0.841
1.330	0.600	0.814	1.000	0.737
1.773	0.465	0.742	1.000	0.627
2.216	0.345	0.668	1.000	0.516
2.660	0.245	0.594	1.000	0.412
3.103	0.166	0.520	1.000	0.319
3.546	0.107	0.448	1.000	0.238
3.989	0.065	0.380	1.000	0.172
4.433	0.038	0.315	1.000	0.120
4.876	0.021	0.256	1.000	0.080
5.319	0.010	0.203	1.000	0.051
5.762	0.005	0.156	1.000	0.031
6.206	0.002	0.116	1.000	0.018
6.649	0.001	0.082	1.000	0.010
7.092	0.000	0.054	1.000	0.005
7.535	0.000	0.033	1.000	0.002
7.979	0.000	0.017	1.000	0.001
8.422	0.000	0.006	1.000	-0.000
8.865	0.000	0.000	1.000	0.000

TOTAL VERTICAL MTFs

cy/mr	H_SYS	H_PRE	H_SPF
0.000	1.000	1.000	1.000
0.443	0.883	0.944	0.936
0.887	0.756	0.882	0.857
1.330	0.626	0.814	0.769
1.773	0.502	0.742	0.676
2.216	0.389	0.668	0.582
2.660	0.291	0.594	0.490
3.103	0.210	0.520	0.405
3.546	0.147	0.448	0.327

3.989	0.098	0.380	0.259
4.433	0.063	0.315	0.201
4.876	0.039	0.256	0.153
5.319	0.023	0.203	0.113
5.762	0.013	0.156	0.083
6.206	0.007	0.116	0.059
6.649	0.003	0.082	0.041
7.092	0.002	0.054	0.028
7.535	0.001	0.033	0.019
7.979	0.000	0.017	0.012
8.422	0.000	0.006	0.008
8.865	0.000	0.000	0.000

PREFILTER VALUES AT NYQUIST

horz H_PRE(4.17) = 0.354 vert H_PRE(4.17) = 0.354

SAMPLING RATES

horizontal	8.33	samples/mr
vertical	8.33	samples/mr
effective	8.33	samples/mr

SENSOR LIMITING FREQUENCIES

	spatial	Nyquist
horizontal	8.87	4.17
vertical	8.87	4.17
effective	8.87	4.17

MRTD 3D NOISE CORRECTION (AVERAGE)

	300 K	0 K
horizontal	1.400	0.000
vertical	1.400	0.000

MRTD AT 300 K BACKGROUND TEMPERATURE

	cy/mr	horz		cy/mr	vert	cy/mr	2D
0.05	0.443	0.002	0.05	0.443	0.002	0.444	0.002
0.10	0.887	0.004	0.10	0.887	0.004	0.569	0.002
0.15	1.330	0.006	0.15	1.330	0.006	0.695	0.003
0.20	1.773	0.010	0.20	1.773	0.010	0.820	0.003
0.25	2.216	0.016	0.25	2.216	0.015	0.973	0.004
0.30	2.660	0.026	0.30	2.660	0.022	1.157	0.005
0.35	3.103	0.041	0.35	3.103	0.034	1.343	0.006
0.40	3.546	0.069	0.40	3.546	0.052	1.561	0.008
0.45	3.989	0.120	0.45	3.989	0.083	1.780	0.010
0.50	4.433	99.999	0.50	4.433	99.999	2.008	0.012
0.55	4.876	99.999	0.55	4.876	99.999	2.236	0.016
0.60	5.319	99.999	0.60	5.319	99.999	2.465	0.020

0.65	5.762	99.999	0.65	5.762	99.999	2.694	0.025
0.70	6.206	99.999	0.70	6.206	99.999	2.924	0.031
0.75	6.649	99.999	0.75	6.649	99.999	3.148	0.039
0.80	7.092	99.999	0.80	7.092	99.999	3.360	0.049
0.85	7.535	99.999	0.85	7.535	99.999	3.565	0.061
0.90	7.979	99.999	0.90	7.979	99.999	3.766	0.076
0.95	8.422	99.999	0.95	8.422	99.999	3.903	0.096
1.00	8.865	99.999	1.00	8.865	99.999	4.001	0.120

MDTD AT 300 K BACKGROUND TEMPERATURE

	1/mr	MDTD
0.20	44.326	2.262
0.40	22.163	0.571
0.60	14.775	0.258
0.80	11.082	0.149
1.00	8.865	0.098
1.20	7.388	0.070
1.40	6.332	0.054
1.60	5.541	0.043
1.80	4.925	0.035
2.00	4.433	0.030
2.20	4.030	0.026
2.40	3.694	0.023
2.60	3.410	0.020
2.80	3.166	0.018
3.00	2.955	0.017
3.20	2.770	0.015
3.40	2.607	0.014
3.60	2.463	0.013
3.80	2.333	0.012
4.00	2.216	0.011
4.20	2.111	0.011
4.40	2.015	0.010
4.60	1.927	0.010
4.80	1.847	0.009
5.00	1.773	0.009

FLIR92. . . sniperm.1: end of listing

THIS PAGE INTENTIONALLY LEFT BLANK

APPENDIX F. FLIR92 MODEL OUTPUTS FOR STARING SENSOR (NFOV)

U.S. Army CECOM NVESD FLIR92

Wed Mar 07 13:39:34 2001

output file: sniperm.1 short listing

data file: sniperm

command line arguments: -d sniperm -o sniperm -p BOTH -a sniperm

begin data file listing . . .

sniper: thermal imaging system

>spectral

spectral_cut_on	3.0	microns
spectral_cut_off	5.0	microns
diffraction_wavelength	0.0	microns

>optics_1

f_number	4.6	--
eff_focal_length	20.0	cm
eff_aperture_diameter	0.0	cm
geometric_blur_spot	0.0	mrاد
average_optical_trans	0.80	--

>optics_2

HFOV:WFOV_aspect_ratio	1.323	--
Magnification	0.0	--
frame_rate	60.0	Hz
fields_per_frame	1.0	--

>detector

horz_detector_size	22.56	microns
vert_detector_size	22.56	microns
peak_D_star	5.97e11	cm-sqrt(Hz)/W
integration_time	16666.667	microsec
1/f_knee_frequency	0.0	Hz

>fpa_stare

#_horz_detectors	640.0	--
#_vert_detectors	480.0	--
horz_unit_cell_dimension	24.0	microns
vert_unit_cell_dimension	24.0	microns

>electronics

high_pass_3db_cuton	0.0	Hz
high_pass_filter_order	0.0	--
low_pass_3db_cutoff	0.0	Hz
low_pass_filter_order	0.0	--
boost_amplitude	0.0	--
boost_frequency	0.0	Hz
sample_and_hold	HORZ	HORZ_or_VERT_or_NO

```

>display
  display_brightness      10.0      milli-Lamberts
  display_height          15.24     cm
  display_viewing_distance 30.0     cm
>crt_display
  #_active_lines_on_CRT   480.0     --
  horz_crt_spot_sigma     0.0       mrad
  vert_crt_spot_sigma     0.0       mrad
>eye
  threshold_SNR           2.5       --
  eye_integration_time     0.1       sec
  MTF                     EXP       EXP_or_NL
>3d_noise_default
  noise_level             MOD       NO_LO_MOD_or_HI
>spectral_detectivity
#_points:  5 microns_____detectivity
           3.0           0.666
           3.5           0.7495
           4.0           0.833
           4.5           0.9165
           5.0           1.0
>end
end data file listing . . .

```

MESSAGES

```

diagnostic(): Using default 3D noise components.
diagnostic(): Using _LO_ level 3D noise defaults.
diagnostic(): Diffraction wavelength set to spectral band midpoint.
diagnostic(): Fields-of-view calculated by model.

```

CALCULATED SYSTEM PARAMETERS

```

field-of-view:      4.398h x 3.299      v degrees
                   76.76h x 57.58      v mrad

magnification:      8.639

optics blur spot:   44.896              microns (diffraction-limited)
                   0.224              mrad

detector IFOV:      0.113h x 0.113      v mrad
FPA fill factor:    0.884
FPA duty cycle:     1.000

```

TEMPERATURE DEPENDENCE

```

parameter    NETD @ 300 K    NETD @ 0 K    noise bandwidth
-----

```


white NETD	0.028 deg C	0.000 deg C	4.712e+001 Hz
classical NETD	0.028 deg C	0.000 deg C	4.714e+001 Hz
sigma_TVH NETD	0.022 deg C	0.000 deg C	3.004e+001 Hz
sigma_VH NETD	0.009 deg C	0.000 deg C	
Planck integral	2.127e-005	0.000e+000	W/(cm*cm*K)
. . . w/D-star	1.144e+007	0.000e+000	sqrt(Hz)/(cm*K)

TOTAL HORIZONTAL MTFs

cy/mr	H_SYS	H_PRE	H_TPF	H_SPF
0.000	1.000	1.000	1.000	1.000
0.443	0.879	0.944	1.000	0.931
0.887	0.742	0.882	1.000	0.841
1.330	0.600	0.814	1.000	0.737
1.773	0.465	0.742	1.000	0.627
2.216	0.345	0.668	1.000	0.516
2.660	0.245	0.594	1.000	0.412
3.103	0.166	0.520	1.000	0.319
3.546	0.107	0.448	1.000	0.238
3.989	0.065	0.380	1.000	0.172
4.433	0.038	0.315	1.000	0.120
4.876	0.021	0.256	1.000	0.080
5.319	0.010	0.203	1.000	0.051
5.762	0.005	0.156	1.000	0.031
6.206	0.002	0.116	1.000	0.018
6.649	0.001	0.082	1.000	0.010
7.092	0.000	0.054	1.000	0.005
7.535	0.000	0.033	1.000	0.002
7.979	0.000	0.017	1.000	0.001
8.422	0.000	0.006	1.000	-0.000
8.865	0.000	0.000	1.000	0.000

TOTAL VERTICAL MTFs

cy/mr	H_SYS	H_PRE	H_SPF
0.000	1.000	1.000	1.000
0.443	0.883	0.944	0.936
0.887	0.756	0.882	0.857
1.330	0.626	0.814	0.769
1.773	0.502	0.742	0.676
2.216	0.389	0.668	0.582
2.660	0.291	0.594	0.490
3.103	0.210	0.520	0.405
3.546	0.147	0.448	0.327
3.989	0.098	0.380	0.259

4.433	0.063	0.315	0.201
4.876	0.039	0.256	0.153
5.319	0.023	0.203	0.113
5.762	0.013	0.156	0.083
6.206	0.007	0.116	0.059
6.649	0.003	0.082	0.041
7.092	0.002	0.054	0.028
7.535	0.001	0.033	0.019
7.979	0.000	0.017	0.012
8.422	0.000	0.006	0.008
8.865	0.000	0.000	0.000

PREFILTER VALUES AT NYQUIST

horz H_PRE(4.17) = 0.354 vert H_PRE(4.17) = 0.354

SAMPLING RATES

horizontal	8.33 samples/mr
vertical	8.33 samples/mr
effective	8.33 samples/mr

SENSOR LIMITING FREQUENCIES

	spatial	Nyquist
horizontal	8.87	4.17
vertical	8.87	4.17
effective	8.87	4.17

MRTD 3D NOISE CORRECTION (AVERAGE)

	300 K	0 K
horizontal	1.400	0.000
vertical	1.400	0.000

MRTD AT 300 K BACKGROUND TEMPERATURE

	cy/mr	horz		cy/mr	vert	cy/mr	2D
0.05	0.443	0.002	0.05	0.443	0.002	0.444	0.002
0.10	0.887	0.004	0.10	0.887	0.004	0.569	0.002
0.15	1.330	0.006	0.15	1.330	0.006	0.695	0.003
0.20	1.773	0.010	0.20	1.773	0.010	0.820	0.003
0.25	2.216	0.016	0.25	2.216	0.015	0.973	0.004
0.30	2.660	0.026	0.30	2.660	0.022	1.157	0.005
0.35	3.103	0.041	0.35	3.103	0.034	1.343	0.006
0.40	3.546	0.069	0.40	3.546	0.052	1.561	0.008
0.45	3.989	0.120	0.45	3.989	0.083	1.780	0.010
0.50	4.433	99.999	0.50	4.433	99.999	2.008	0.012
0.55	4.876	99.999	0.55	4.876	99.999	2.236	0.016
0.60	5.319	99.999	0.60	5.319	99.999	2.465	0.020
0.65	5.762	99.999	0.65	5.762	99.999	2.694	0.025

0.70	6.206	99.999	0.70	6.206	99.999	2.924	0.031
0.75	6.649	99.999	0.75	6.649	99.999	3.148	0.039
0.80	7.092	99.999	0.80	7.092	99.999	3.360	0.049
0.85	7.535	99.999	0.85	7.535	99.999	3.565	0.061
0.90	7.979	99.999	0.90	7.979	99.999	3.766	0.076
0.95	8.422	99.999	0.95	8.422	99.999	3.903	0.096
1.00	8.865	99.999	1.00	8.865	99.999	4.001	0.120

MDTD AT 300 K BACKGROUND TEMPERATURE

	1/mr	MDTD
0.20	44.326	2.262
0.40	22.163	0.571
0.60	14.775	0.258
0.80	11.082	0.149
1.00	8.865	0.098
1.20	7.388	0.070
1.40	6.332	0.054
1.60	5.541	0.043
1.80	4.925	0.035
2.00	4.433	0.030
2.20	4.030	0.026
2.40	3.694	0.023
2.60	3.410	0.020
2.80	3.166	0.018
3.00	2.955	0.017
3.20	2.770	0.015
3.40	2.607	0.014
3.60	2.463	0.013
3.80	2.333	0.012
4.00	2.216	0.011
4.20	2.111	0.011
4.40	2.015	0.010
4.60	1.927	0.010
4.80	1.847	0.009
5.00	1.773	0.009

FLIR92. . . sniperm.1: end of listing

THIS PAGE INTENTIONALLY LEFT BLANK

APPENDIX G. FLIR92 MODEL OUTPUTS FOR STARING SENSOR (VNFOV)

U.S. Army CECOM NVESD FLIR92

Wed Mar 07 13:59:13 2001

output file: snipervn.1 short listing

data file: snipervn

command line arguments: -d snipervn -o snipervn -p BOTH -a snipervn

begin data file listing . . .

sniper: thermal imaging system

>spectral

spectral_cut_on	3.0	microns
spectral_cut_off	5.0	microns
diffraction_wavelength	0.0	microns

>optics_1

f_number	6.9	--
eff_focal_length	150.0	cm
eff_aperture_diameter	0.0	cm
geometric_blur_spot	0.0	mrاد
average_optical_trans	0.77	--

>optics_2

HFOV:WFOV_aspect_ratio	1.323	--
Magnification	0.0	--
frame_rate	60.0	Hz
fields_per_frame	1.0	--

>detector

horz_detector_size	22.56	microns
vert_detector_size	22.56	microns
peak_D_star	5.97e11	cm-sqrt(Hz)/W
integration_time	16666.667	microsec
1/f_knee_frequency	0.0	Hz

>fpa_stare

#_horz_detectors	640.0	--
#_vert_detectors	480.0	--
horz_unit_cell_dimension	24.0	microns
vert_unit_cell_dimension	24.0	microns

>electronics

high_pass_3db_cuton	0.0	Hz
high_pass_filter_order	0.0	--
low_pass_3db_cutoff	0.0	Hz
low_pass_filter_order	0.0	--

```

    boost_amplitude      0.0      --
    boost_frequency      0.0      Hz
    sample_and_hold      HORZ     HORZ_or_VERT_or_NO
>display
    display_brightness   10.0     milli-Lamberts
    display_height       15.24    cm
    display_viewing_distance 30.0    cm
>crt_display
    #_active_lines_on_CRT 480.0    --
    horz_crt_spot_sigma  0.0      mrad
    vert_crt_spot_sigma  0.0      mrad
>eye
    threshold_SNR        2.5      --
    eye_integration_time  0.1      sec
    MTF                  EXP       EXP_or_NL
>3d_noise_default
    noise_level          MOD       NO_LO_MOD_or_HI
>spectral_detectivity
#_points: 5 microns_____detectivity
          3.0           0.666
          3.5           0.7495
          4.0           0.833
          4.5           0.9165
          5.0           1.0
>end
end data file listing . . .

```

MESSAGES

```

diagnostic(): Using default 3D noise components.
diagnostic(): Using _LO_ level 3D noise defaults.
diagnostic(): Diffraction wavelength set to spectral band midpoint.
diagnostic(): Fields-of-view calculated by model.

```

CALCULATED SYSTEM PARAMETERS

```

    field-of-view:      0.587h x 0.440  v degrees
                      10.24h x 7.68    v mrad
    magnification:      64.776
    optics blur spot:   67.344          microns (diffraction-limited)
                      0.045            mrad

    detector IFOV:      0.015h x 0.015  v mrad
    FPA fill factor:     0.884
    FPA duty cycle:      1.000

```

TEMPERATURE DEPENDENCE

parameter	NETD @ 300 K	NETD @ 0 K	noise bandwidth
white NETD	0.066 deg C	0.000 deg C	4.712e+001 Hz
classical NETD	0.066 deg C	0.000 deg C	4.714e+001 Hz
sigma_TVH NETD	0.053 deg C	0.000 deg C	3.004e+001 Hz
sigma_VH NETD	0.021 deg C	0.000 deg C	
Planck integral	2.127e-005	0.000e+000	W/(cm*cm*K)
. . . w/D-star	1.144e+007	0.000e+000	sqrt(Hz)/(cm*K)

TOTAL HORIZONTAL MTFs

cy/mr	H_SYS	H_PRE	H_TPF	H_SPF
0.000	1.000	1.000	1.000	1.000
3.324	0.855	0.918	1.000	0.931
6.649	0.699	0.831	1.000	0.841
9.973	0.545	0.740	1.000	0.737
13.298	0.405	0.647	1.000	0.627
16.622	0.287	0.555	1.000	0.516
19.947	0.192	0.466	1.000	0.412
23.271	0.122	0.382	1.000	0.318
26.596	0.073	0.305	1.000	0.238
29.920	0.040	0.235	1.000	0.172
33.245	0.021	0.174	1.000	0.120
36.569	0.010	0.122	1.000	0.080
39.894	0.004	0.080	1.000	0.051
43.218	0.001	0.047	1.000	0.031
46.543	0.000	0.024	1.000	0.018
49.867	0.000	0.008	1.000	0.010
53.191	0.000	0.001	1.000	0.005
56.516	0.000	0.000	1.000	0.002
59.840	0.000	0.000	1.000	0.001
63.165	0.000	0.000	1.000	-0.000
66.489	0.000	0.000	1.000	0.000

TOTAL VERTICAL MTFs

cy/mr	H_SYS	H_PRE	H_SPF
0.000	1.000	1.000	1.000
3.324	0.859	0.918	0.936
6.649	0.712	0.831	0.857
9.973	0.569	0.740	0.769
13.298	0.437	0.647	0.676
16.622	0.323	0.555	0.582
19.947	0.229	0.466	0.490

23.271	0.155	0.382	0.405
26.596	0.100	0.305	0.327
29.920	0.061	0.235	0.259
33.245	0.035	0.174	0.201
36.569	0.019	0.122	0.152
39.894	0.009	0.080	0.113
43.218	0.004	0.047	0.083
46.543	0.001	0.024	0.059
49.867	0.000	0.008	0.041
53.191	0.000	0.001	0.028
56.516	0.000	0.000	0.019
59.840	0.000	0.000	0.012
63.165	0.000	0.000	0.008
66.489	0.000	0.000	0.000

PREFILTER VALUES AT NYQUIST

horz H_PRE(31.25) = 0.210 vert H_PRE(31.25) = 0.210

SAMPLING RATES

horizontal 62.50 samples/mr
vertical 62.50 samples/mr
effective 62.50 samples/mr

SENSOR LIMITING FREQUENCIES

	spatial	Nyquist
horizontal	66.49	31.25
vertical	66.49	31.25
effective	66.49	31.25

MRTD 3D NOISE CORRECTION (AVERAGE)

	300 K	0 K
horizontal	1.400	0.000
vertical	1.400	0.000

MRTD AT 300 K BACKGROUND TEMPERATURE

	cy/mr	horz		cy/mr	vert	cy/mr	2D
0.05	3.324	0.004	0.05	3.324	0.004	3.330	0.004
0.10	6.649	0.009	0.10	6.649	0.009	4.329	0.005
0.15	9.973	0.016	0.15	9.973	0.016	5.329	0.006
0.20	13.298	0.027	0.20	13.298	0.026	6.328	0.008
0.25	16.622	0.045	0.25	16.622	0.041	7.620	0.011
0.30	19.947	0.076	0.30	19.947	0.066	9.049	0.014
0.35	23.271	0.130	0.35	23.271	0.106	10.560	0.018
0.40	26.596	0.237	0.40	26.596	0.179	12.217	0.023
0.45	29.920	0.454	0.45	29.920	0.315	13.893	0.029
0.50	33.245	99.999	0.50	33.245	99.999	15.598	0.037

0.55	36.569	99.999	0.55	36.569	99.999	17.297	0.048
0.60	39.894	99.999	0.60	39.894	99.999	18.976	0.061
0.65	43.218	99.999	0.65	43.218	99.999	20.650	0.079
0.70	46.543	99.999	0.70	46.543	99.999	22.302	0.101
0.75	49.867	99.999	0.75	49.867	99.999	23.893	0.130
0.80	53.191	99.999	0.80	53.191	99.999	25.385	0.167
0.85	56.516	99.999	0.85	56.516	99.999	26.837	0.214
0.90	59.840	99.999	0.90	59.840	99.999	28.235	0.275
0.95	63.165	99.999	0.95	63.165	99.999	29.309	0.354
1.00	66.489	99.999	1.00	66.489	99.999	30.026	0.454

MDTD AT 300 K BACKGROUND TEMPERATURE

	1/mr	MDTD
0.20	332.447	6.261
0.40	166.223	1.578
0.60	110.816	0.711
0.80	83.112	0.407
1.00	66.489	0.267
1.20	55.408	0.190
1.40	47.492	0.144
1.60	41.556	0.114
1.80	36.939	0.093
2.00	33.245	0.079
2.20	30.222	0.067
2.40	27.704	0.059
2.60	25.573	0.052
2.80	23.746	0.047
3.00	22.163	0.042
3.20	20.778	0.039
3.40	19.556	0.036
3.60	18.469	0.033
3.80	17.497	0.031
4.00	16.622	0.029
4.20	15.831	0.027
4.40	15.111	0.025
4.60	14.454	0.024
4.80	13.852	0.023
5.00	13.298	0.021

FLIR92. . . snipervn.1: end of listing

THIS PAGE INTENTIONALLY LEFT BLANK

APPENDIX H. TAWS OUTPUTS FOR DESERT ENVIRONMENTAL CONDITIONS WITH CONSTANT TOT (1800) FOR DIFFERENT VIEWING ANGLES

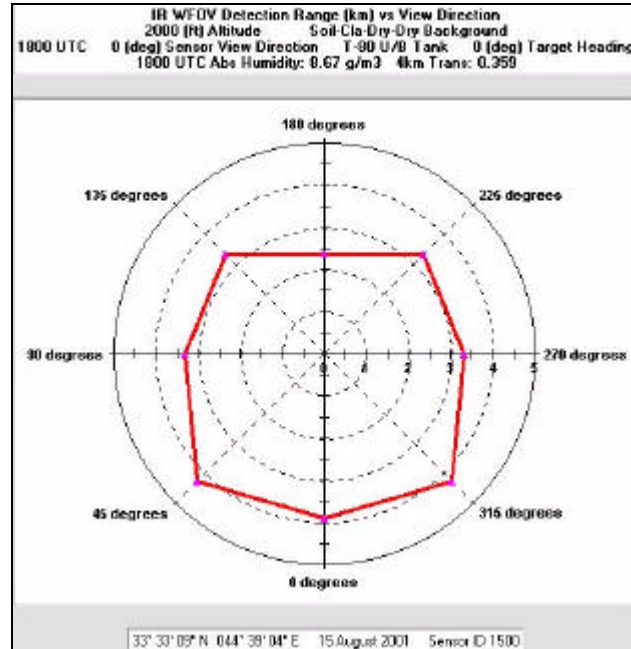


Figure H.1. Scanning Sensor WFOV.

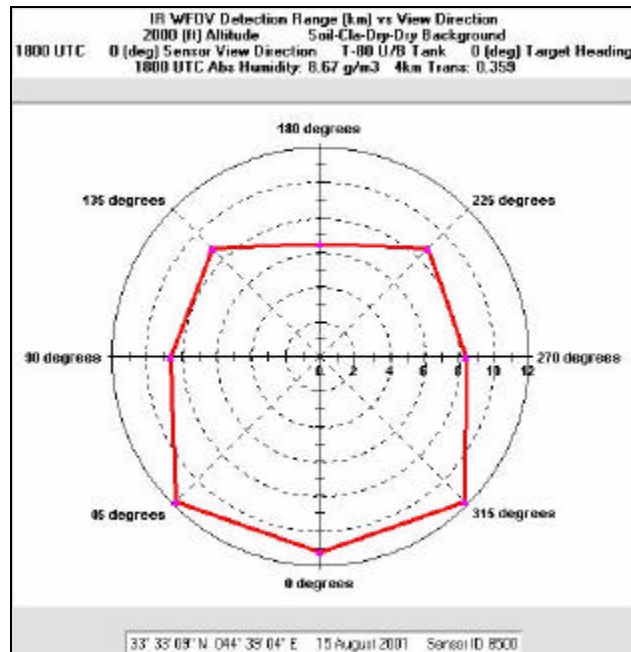


Figure H.2. Staring Sensor WFOV.

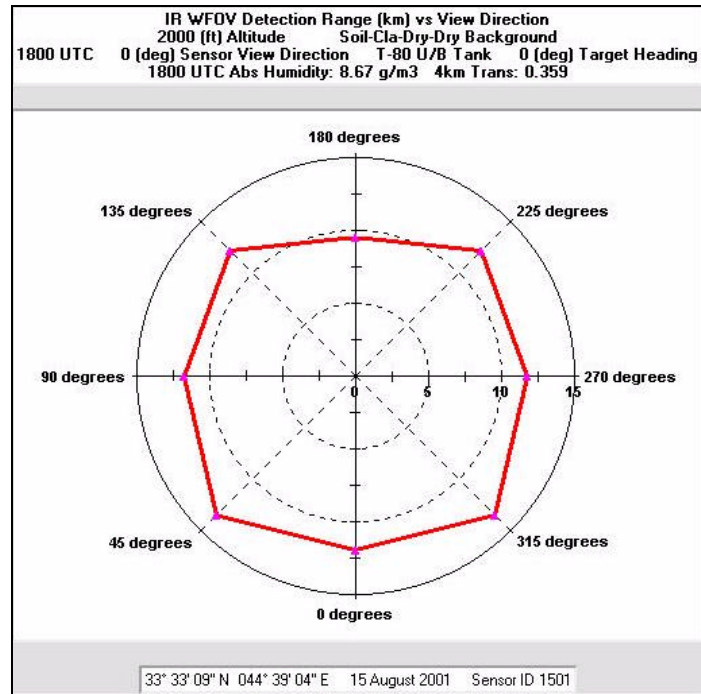


Figure H.3. Scanning Sensor MFOV

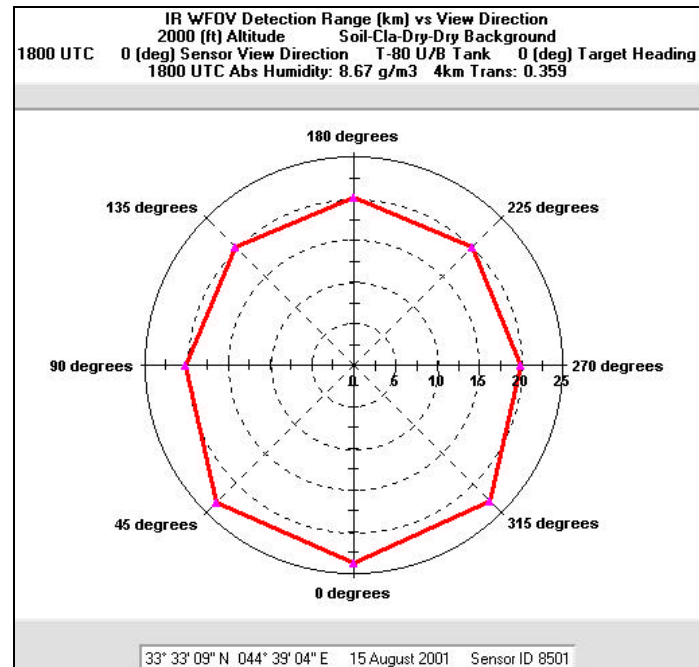


Figure H.4. Staring Sensor MFOV.

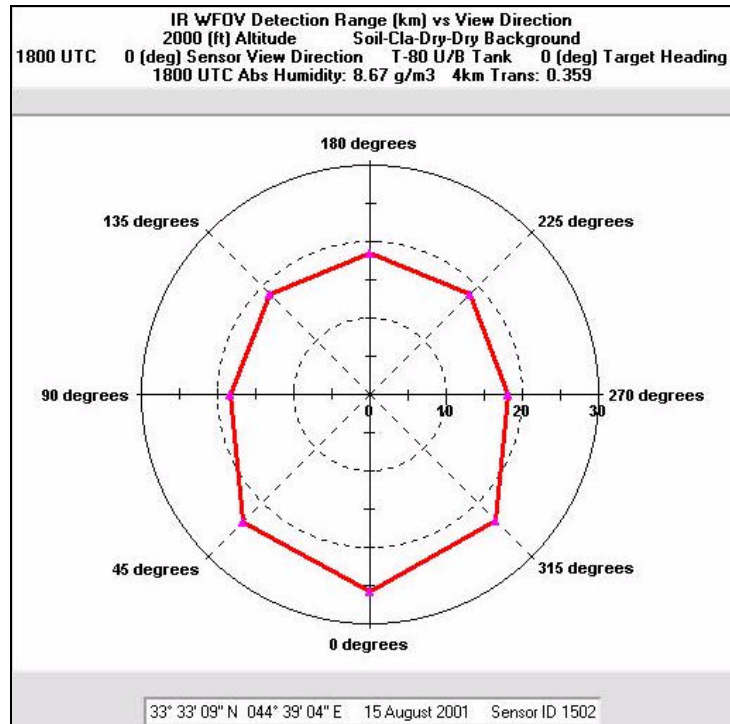


Figure H.5. Scanning Sensor NFOV.

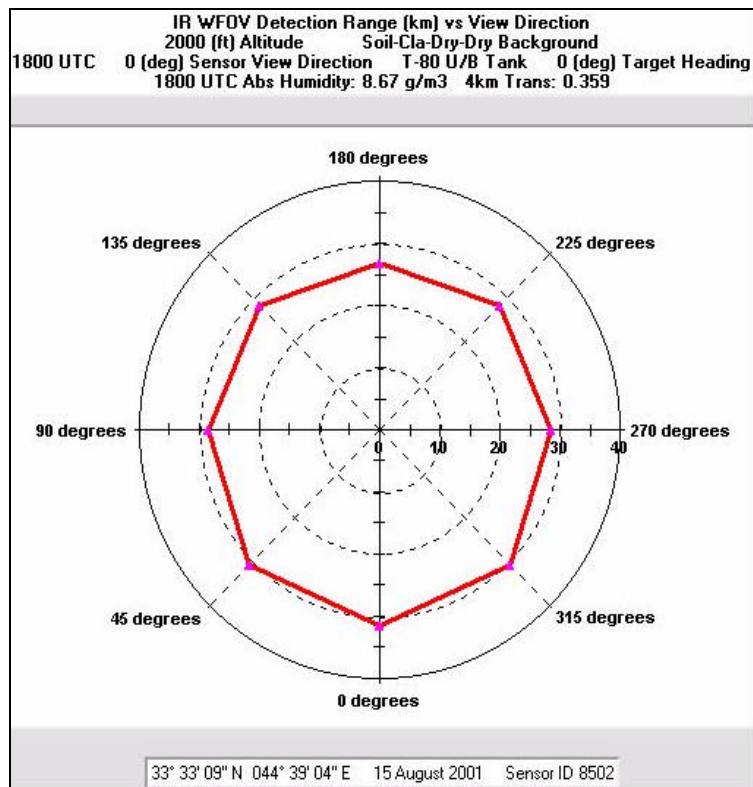


Figure H.6. Staring Sensor NFOV

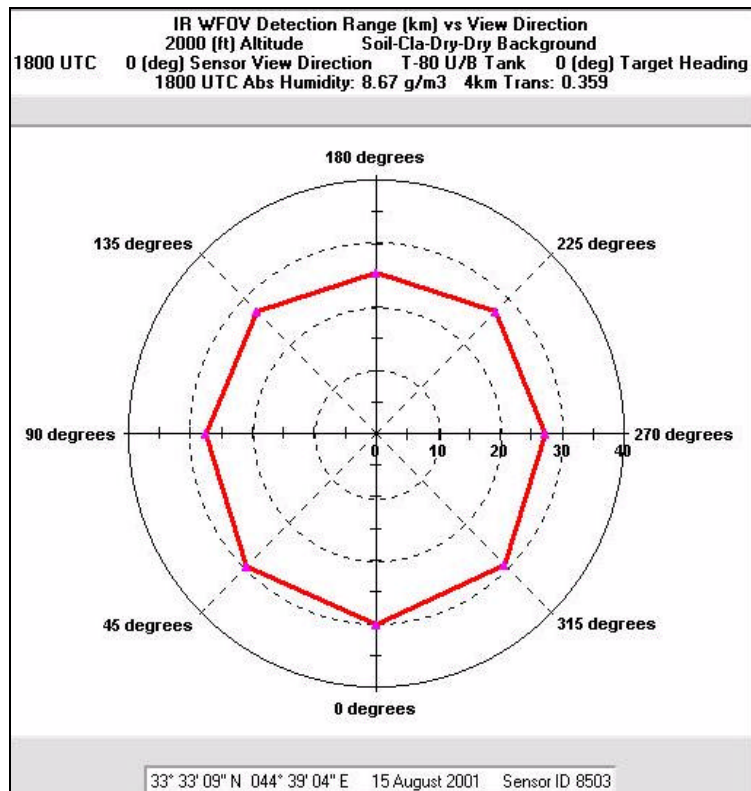


Figure H.7. Staring Sensor VNFOV.

APPENDIX I. TAWS OUTPUTS FOR URBAN ENVIRONMENTAL CONDITIONS WITH CONSTANT TOT (2100) FOR DIFFERENT VIEWING ANGLES

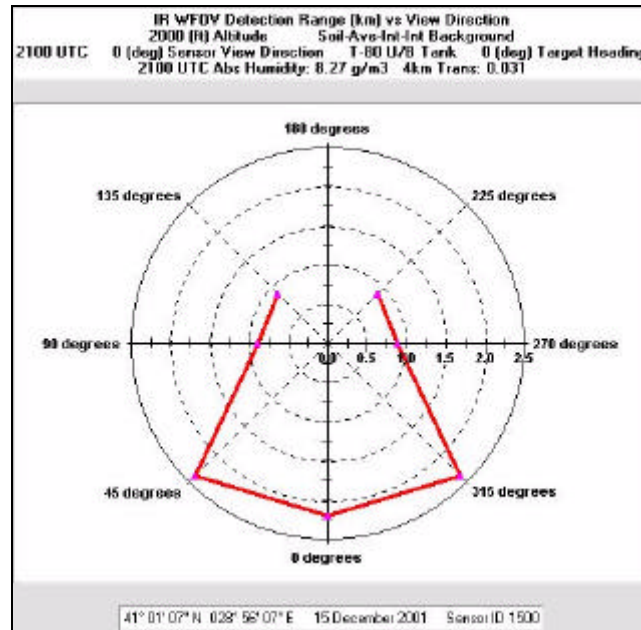


Figure I.1. Scanning Sensor WFOV.

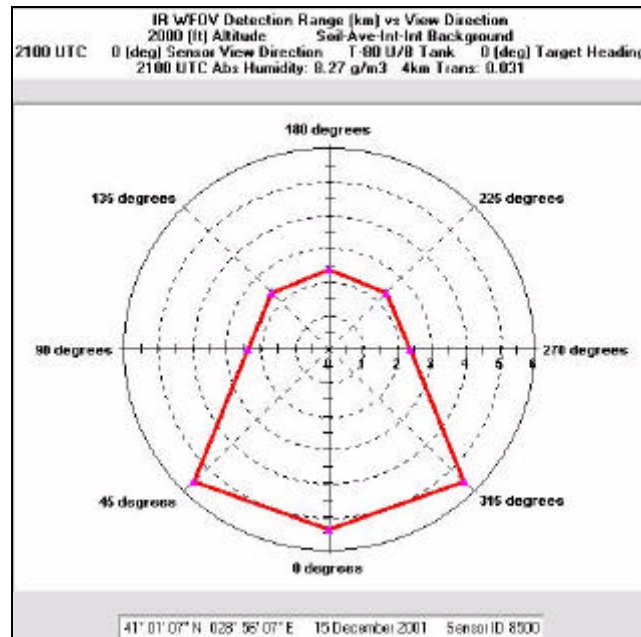


Figure I.2. Staring Sensor WFOV.

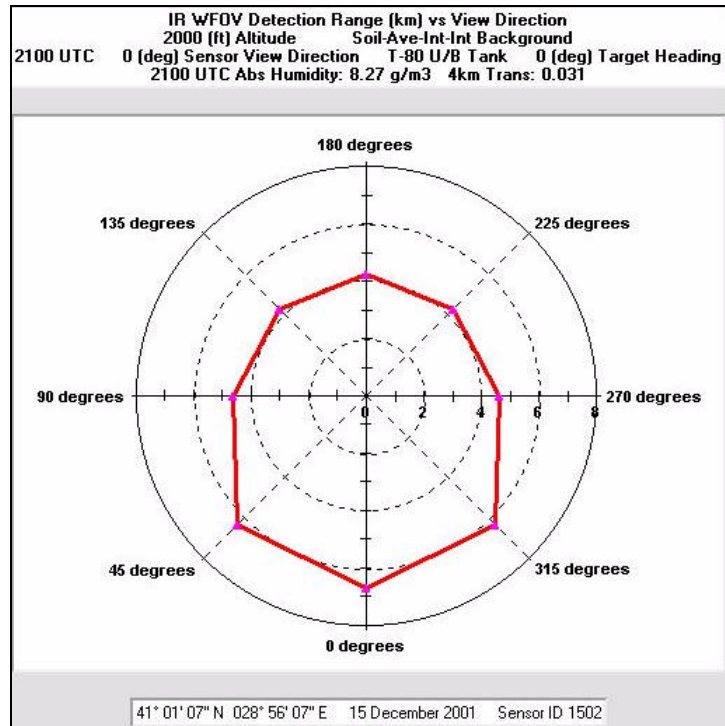


Figure I.3. Scanning Sensor NFOV.

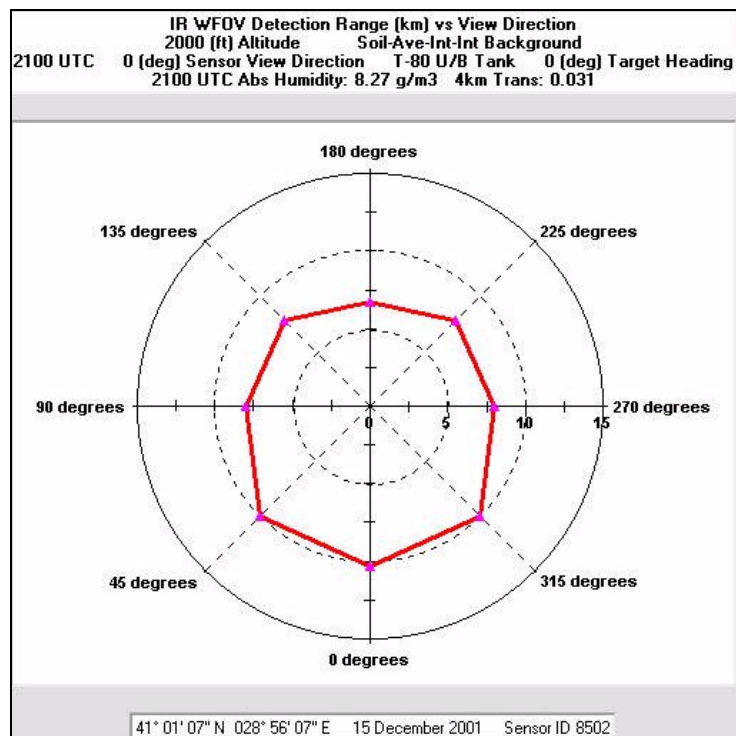


Figure I.4. Staring Array NFOV.

APPENDIX J. TAWS TIME HISTORY PLOTS FOR DESERT ENVIRONMENTAL CONDITIONS

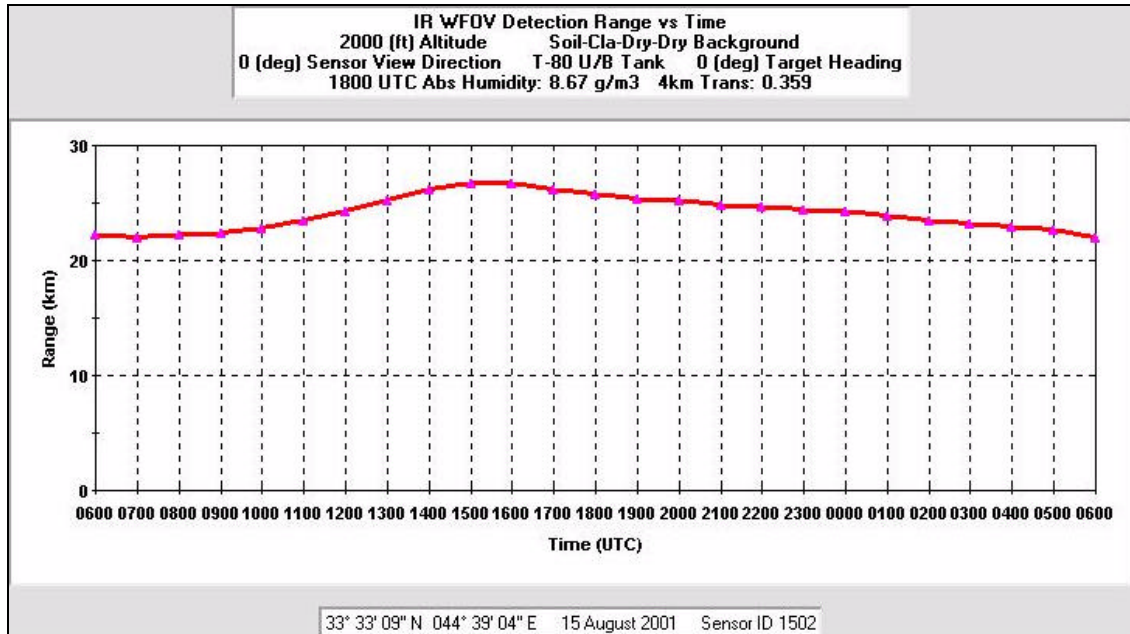


Figure J.1. Scanning Sensor NFOV Max. Range Time History Plot at 0 Degrees.

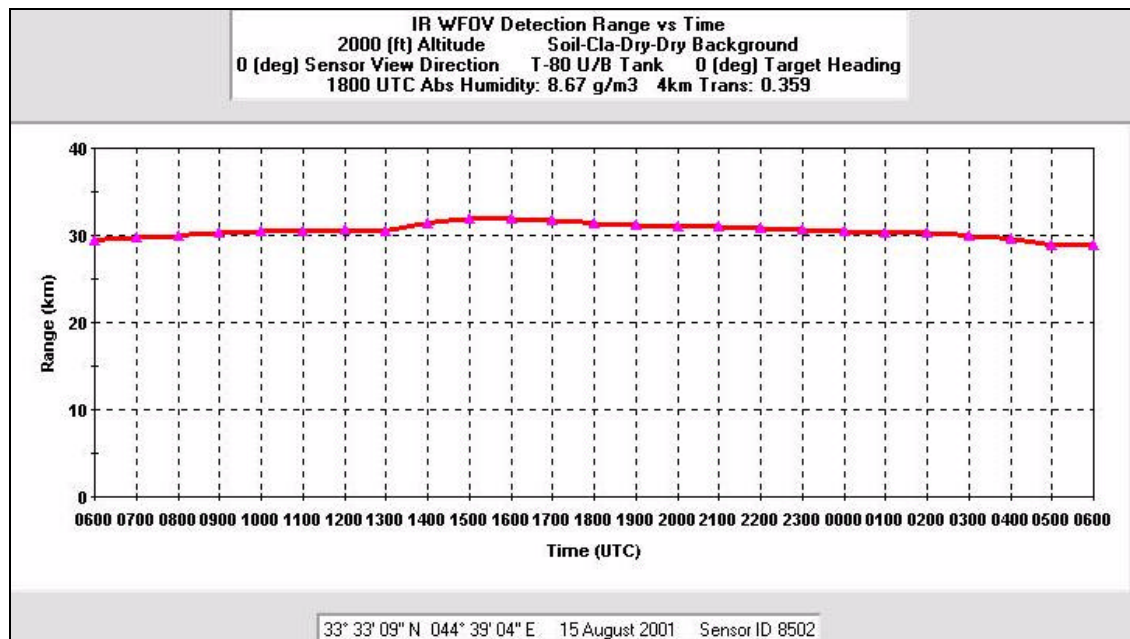


Figure J.2. Staring Sensor NFOV Max. Range Time History Plot at 0 Degrees.

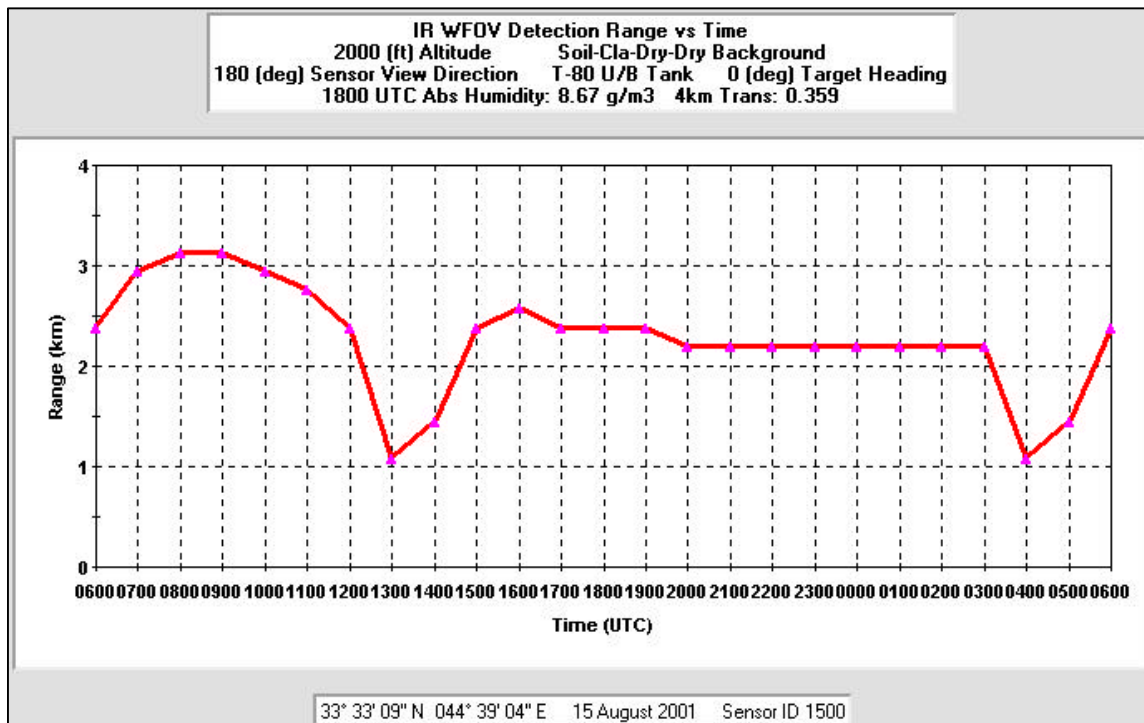


Figure J.3 Staring Sensor WFOV Min Range Time History Plot at 180 Degrees.

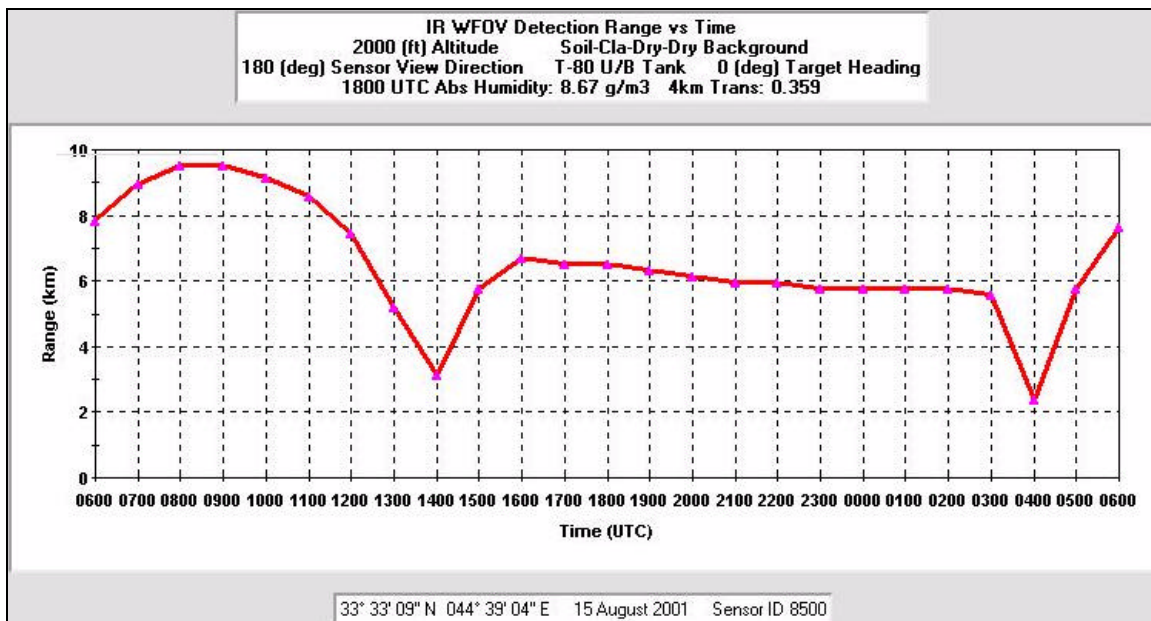


Figure J.4. Staring Sensor WFOV Min Range Time History Plot at 180 Degrees.

APPENDIX K. TAWS TIME HISTORY PLOTS FOR URBAN ENVIRONMENTAL CONDITIONS

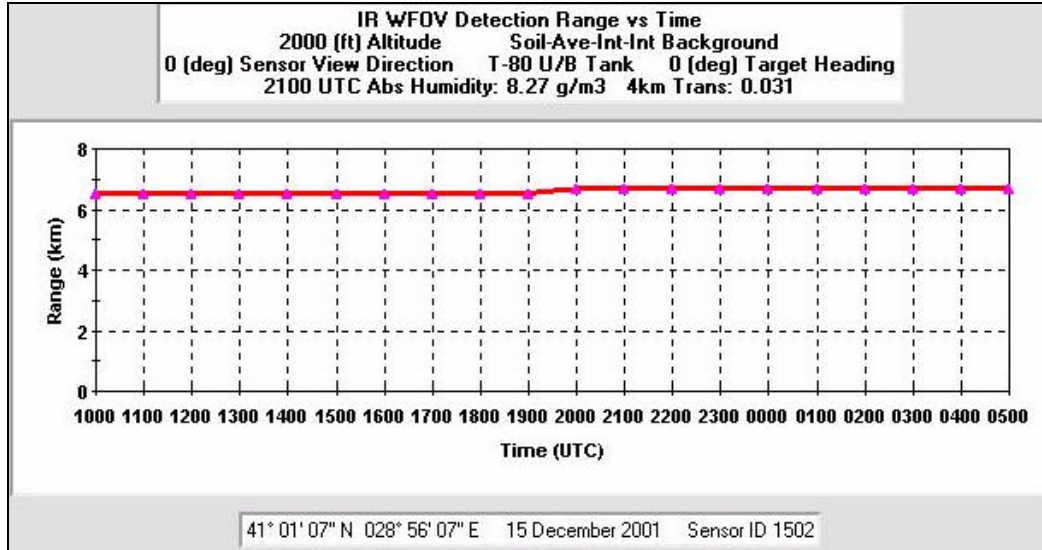


Figure K.1. Scanning Sensor NFOV Max. Range Time History Plot at 0 degrees with 2mm/hour Rain Rate.

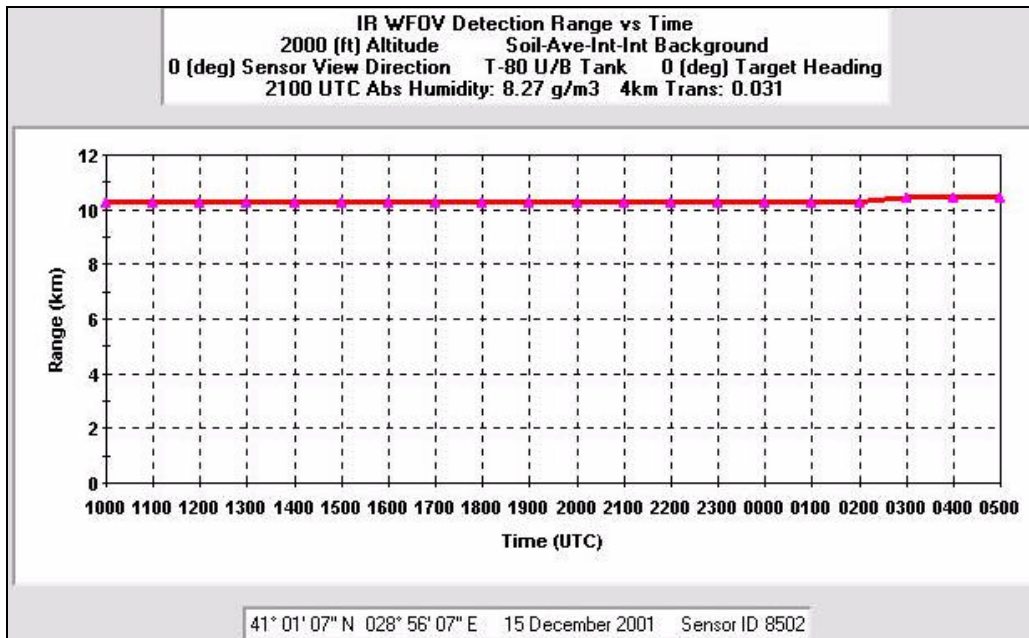


Figure K.2 Staring Sensor NFOV Max. Range Time History Plot at 0 degrees with 2mm/hour Rain Rate.

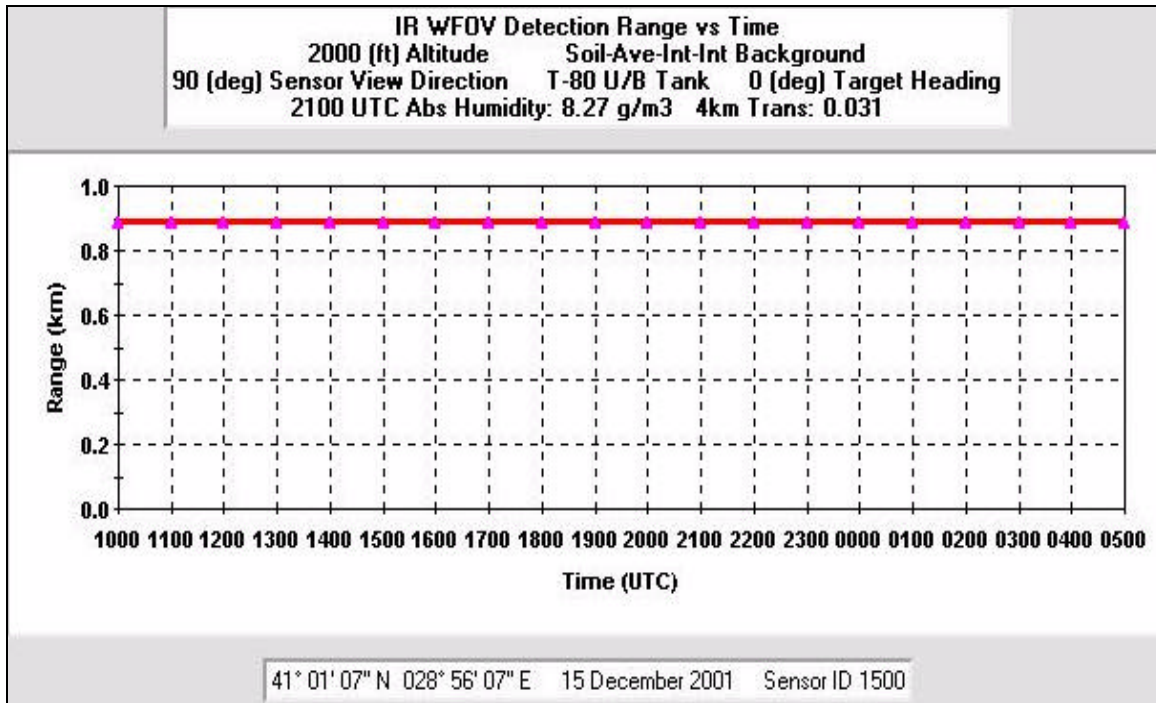


Figure K.3. Scanning Sensor WFOV Min Range Time History Plot at 90 degrees with 2mm/hour Rain Rate.

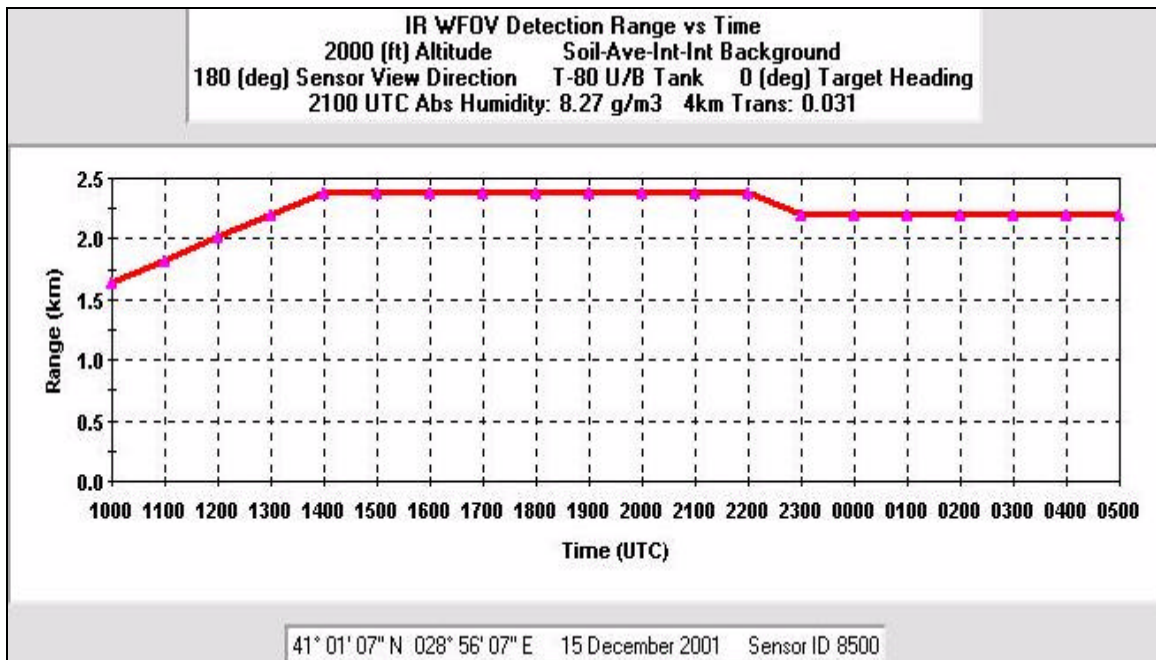


Figure K.4 Staring Sensor WFOV Min Range Time History Plot at 180 degrees with 2mm/hour Rain Rate.

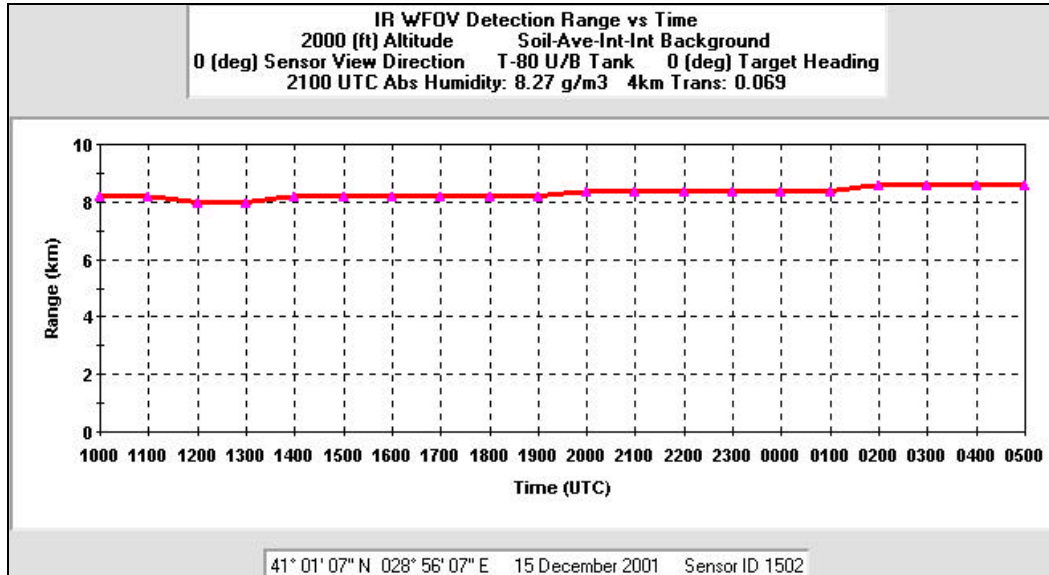


Figure K.5. Scanning Sensor NFOV Max. Range Time History Plot at 0 degrees with 1mm/hour Rain Rate.

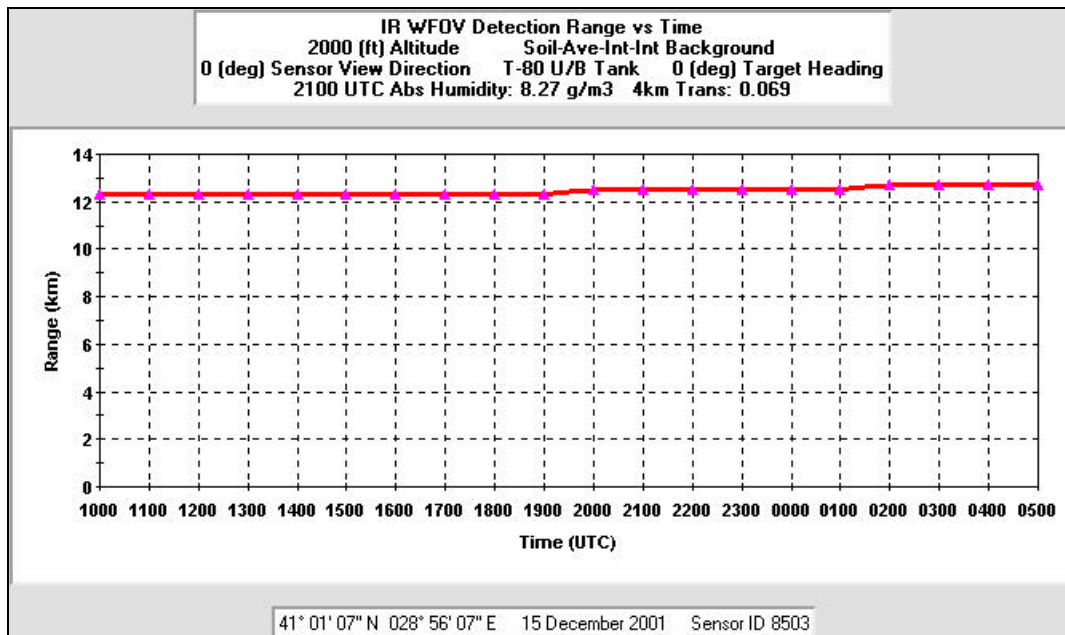


Figure K.6. Staring Sensor NFOV Max. Range Time History Plot at 0 degrees with 1mm/hour Rain Rate.

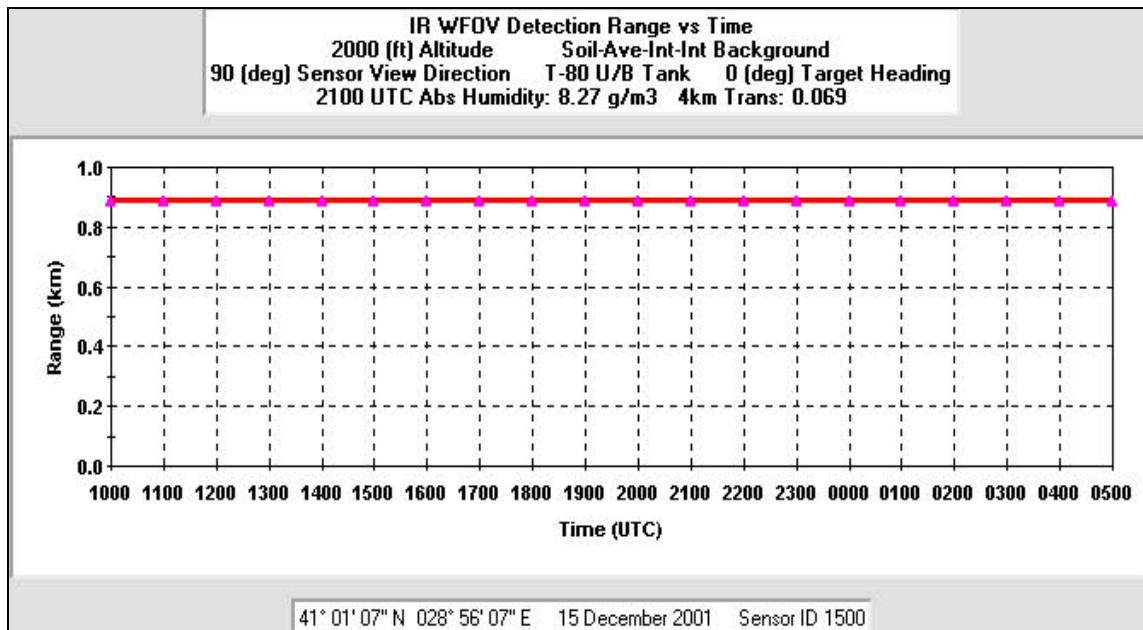


Figure K.7. Scanning Sensor WFOV Min. Range Time History Plot at 90 degrees with 1mm/hour Rain Rate.

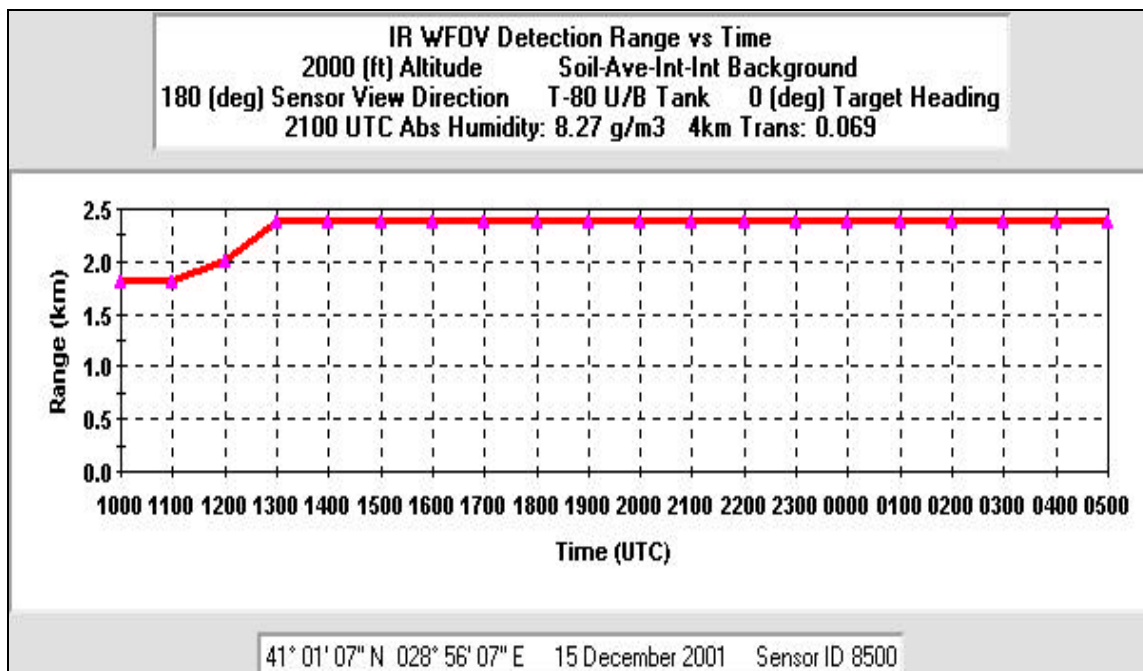


Figure K.8. Staring Sensor WFOV Min. Range Time History Plot at 180 degrees with 1mm/hour Rain Rate.

LIST OF REFERENCES

1. Undersecretariat for Defense Industries, Republic of Turkey, *RFP for the Turkish Attack and Reconnaissance Helicopter (Volume V)*, Revision-A6, 20 July 1999.
2. Perry, Hank, Bell Helicopter-Textron, *KingCobra Configuration vs. USMC AH-1Z*, Information Brochure on KingCobra "Personal Communication".
3. Kett F., Kevin., Bell Helicopter-Textron, *What You Should Know About the KingCobra and its Competition*, Sales Brochure, "Personal Communication".
4. Dowell John, Lockheed Martin Electronics, *Hawkeye Target Sight System*, Program Brief "Personal Communication".
5. Dowell John, Lockheed Martin Electronics, *TSS Receives a New Name, Hawkeye XR*, Program Update Briefing "Personal Communication"
6. Elmer Joe, Litton Guidance & Control Systems, *H-1 Platforms Upgrade (The Next Generation Helicopter Fleet)*, Personal Essay, "Personal Communication"
7. ORUC, Hezarfen, Program Manager, Aselsan Military Electronics, *ASELFLIR-200 2nd Generation Gyro-Stabilized Airborne FLIR*, Program Briefing, "Personal Communication".
8. Gibson, Mark J., *The Marine Corps' New AH-1Z Attack Helicopter Excels in Comparison with the Army's AH-64D*, Personal Essay, "Personal Communication"
9. Wade, R.C. and Dowell J.A., *A Modern Integrated Avionics System for the Next Generation USMC AH-1Z and UH-1Y*, Presentation on integrated Avionics Systems of AH-1Z and UH-1Y, "Personal Communication".
10. Col. Conant, Tom. "Stash", *USMC's Light/Attack Helicopter Upgrade Program*, USMC Upgrade Program Briefing, Presented in NPS by Capt. Tom Curtis, USN, Program Manager, USMC Light/Attack Helicopters, in May 1999.
11. Johnston, S.L., *Millimeter Wave Radar*, Artech House, Inc. MA, 1980.
12. Currie N.C. and Brown, C.E., *Principles and Applications of Millimeter Wave Radar*, Artech House, Inc. MA, 1987.
13. "BELL HELICOPTER AH-1Z FACT SHEET"
[<http://www.bellhelicopter.com/products/MilitaryHelicopters/h1upgrade/>]

14. Pike, John, "AH-64D Apache",
[<http://www.fas.org/man/dod-101/sys/ac/ah-64.htm>], May 2000.
15. "Bell Helicopter Chosen to Partner with Turkish Industry For Helicopter Production"
[http://www.defence-discovery.com/cgi-bin/htm_hl?DB=industry&STEMMER=en&WORDS=kingcobra+&COLOUR=Red&STYLE=ues&URL=http://www.bellhelicopter.texttron.com/content/companyInfo/pressReleases/PR_000721_1358.html#muscat_highlighter_first_match]. July 2000.
16. "AH-64D, Longbow Apache"
[<http://www.jolly-rogers.com/airpower/ah-64d/64d-av.htm>]
17. "The AGM-114L Longbow Hellfire"
[<http://ah-64d.freewebtools.com/AGM-114L%20Longbow%20Hellfire.htm>]
18. Kopp, Carlo, "AH-64D Longbow Flight Report"
[<http://www.csse.monash.edu.au/carlo/archive/MILITARY/AA/longbow-aa.html>].
19. Lange, A.W., ARMOR, *HELLFIRE-Getting the Most from a Lethal Missile System*, pp. 25-30, January-February 1998.
20. Cooper, A. W. and E. C. Crittenden, Jr, *Electro-Optic Sensors and Systems*, Naval Postgraduate School, Monterey, CA, 1998.
21. Driggers, R. G., Cox, P. and Edwards, T, *Introduction to Infrared and Electro-Optical Systems*, Artech House, Inc. MA, 1999.
22. Khalil Seyrafi and S. A. Hovanessian, *Introduction to Electro-Optical Imaging and Tracking Systems*, Artech House, Inc. MA, 1993.
23. Shumaker, David L., J. T. Wood and C. R. Thacker, *Infrared Imaging Systems Analysis*, The Environmental Research Institute of Michigan, 1993.
24. Dereniak, E.L. and Boreman G. D., *Infrared Detectors and Systems*, John Wiley & Sons Inc., NY, 1996.
25. Holst, Gerald C., *Electro-Optical Imaging System Performance*, JCD Publishing, FL, 1995.
26. Wagner, H. Daniel, *Naval Tactical Decision Aids, Lecture Notes*, Naval Postgraduate School, 1989.

27. U.S. Army Night Vision and Electronic Sensors Directorate, *FLIR92 Thermal Imaging Systems Performance Model, Analyst's Reference Guide*, 1993.
28. Chase, Deborah., *Definition of 2nd generation and 3rd generation FLIRs*, US Army Night Vision and Electronic Sensors Directorate.
29. Accetta, Joseph S., Schumaker, David L., *The Infrared and Electro-Optical Systems Handbook, Volume 5*, SPIE Optical Engineering Press, Bellingham, Washington, 1996.
30. Findlay, Geoffrey A. and Cutten, Dean R., "Applied Optics", *Comparison of Performance of 3-5 and 8-12 μ m Infrared Systems*, Vol. 28, No. 23, pp. 5029-5037, 1 December 1989.
31. Target Acquisition and Weather Software (TAWS), Software Available from Navy Research Lab Marine Meteorology Division, Monterey, CA, 93943

THIS PAGE INTENTIONALLY LEFT BLANK

INITIAL DISTRIBUTION LIST

1. Defense Technical Information Center..... 2
8725 John J. Kingman Rd., STE 0944
Ft. Belvoir, VA 22060-6218
2. Dudley Knox Library..... 2
Naval Postgraduate School
411 Dyer Rd.
Monterey, CA 93943-5101
3. Dr. Russ Duren..... 3
Code AA/Dr
Naval Postgraduate School
Monterey, CA 93940
4. Professor Alfred W. Cooper 2
Code PH/Cr
Naval Postgraduate School
Monterey, CA 93943-5101
5. Gokhan Lutfu REYHAN 2
2nci Ordu Hava Alayi
2nci Helicopter Tabur Komutanligi
Malatya, TURKEY
6. Kara Harp Okulu Kutuphanesi..... 1
Bakanliklar
Ankara, Turkey 06200
7. Kara Kuvvetleri K.ligi Kutuphanesi..... 1
Bakanliklar
Ankara, Turkey 06200
8. Dr. Andreas Goroch..... 1
Naval Research Laboratory
Marine Meteorology Division
Monterey, CA, 93943